5-2014

Development of Optical Sensors for Chemical Detection

Jonathan Kelly Fong
University of Tennessee - Knoxville, jfong@utk.edu

To the Graduate Council:

I am submitting herewith a dissertation written by Jonathan Kelly Fong entitled "Development of Optical Sensors for Chemical Detection." I have examined the final electronic copy of this dissertation for form and content and recommend that it be accepted in partial fulfillment of the requirements for the degree of Doctor of Philosophy, with a major in Chemistry.

Zi-ling Xue, Major Professor

We have read this dissertation and recommend its acceptance:

Jon P. Camden, Robert J. Hinde, James Drake

Accepted for the Council:

Carolyn R. Hodges

Vice Provost and Dean of the Graduate School

(Original signatures are on file with official student records.)

Development of Optical Sensors for Chemical Detection

A Dissertation Presented for the

Doctor of Philosophy

Degree

The University of Tennessee, Knoxville

Jonathan Kelly Fong

May 2014

DEDICATION

This dissertation is dedicated to my friends and family, who have supported me emotionally and financially throughout my years at the University of Tennessee, Knoxville. I am indebted to all of them for the encouragement and support that they have given me in this long journey.

ACKNOWLEDGEMENTS

As my time at the University of Tennessee, Knoxville comes to a close, there are several people who I would like to thank for assisting and guiding me through this process. The first person I would like to thank is my research advisor, Dr. Zi-Ling Xue, whose broad knowledge of science continues to impress and astound me. I believe he is one of the best research advisors in the chemistry department at the University of Tennessee, Knoxville and I am extremely grateful for all the guidance, support, and advice that he has provided throughout my years in his research group. I would also like to thank my other committee members, Drs. Jon Camden, Robert Hinde, and James Drake. I had the pleasure to be in Dr. Camden's class where I learned so much on electronics. I enjoyed being able to do computational research chemistry as an undergraduate in Dr. Hinde's group which gave me my first experience in a research setting. I would also like to thank Dr. Drake's biology class where I learned to think about some topics outside of the box. It was truly an honor to be a student to each one of these professors.

During my time in Dr. Xue's research group, I had the enjoyment of working with some very impressive people. When I first joined the group, I was assigned to learn under one of the best graduate students in the department, Dr. Royce Dansby-Sparks. I am truly thankful for being able to learn so much under Royce's tutelage even for just one semester. His guidance, advice, and work ethic continued to inspire me throughout my years as a graduate student. Dr. Ruizhuo Ouyang has also been an amazing colleague and friend who was always helpful to talk to about research, Chinese culture,

or just life in general. I would also like to thank Drs. Adam Lamb and Bhavna Sharma for all their help and assistance in Dr. Xue's inorganic lab. I am truly grateful for them sharing all their experiences and their stimulating conversations during slow times of the days. I would also like to acknowledge Dr. Mathew Urffer for helping me in the computational aspect of one my projects and for introducing and teaching me to use Matlab and Origin software programs. I had the great pleasure to work with Dr. Clarissa Tatum who was one of the senior members of Dr. Xue's research lab at the time. I owe her a great deal in learning about how Dr. Xue's analytical lab worked and as an example of how to be a graduate student. This leaves me with Dr. Stefanie Bragg who was the last senior member of the group to leave the analytical group before me. After enduring the majority of our years in graduate school in the same lab together, I consider her a great friend and an excellent scientist who always had suggestions to help me in my research. I also enjoyed all of the conversations that we had and the food that she made for the lab from time to time.

I will greatly miss the people that I am leaving behind in Dr. Xue's lab including Seth Hunter, Tabi Callaway, Sam Rosolina, Thomas Carpenter, Kendhl Witt, Roberto Alan Federico Perez, and Shelby Stavretis. I wish the best of luck to Seth, Tabi, and Shelby in all their future endeavors in Dr. Xue's inorganic lab. I will miss being able to talk sports from time to time with Thomas. I believe the future is bright for Dr. Xue's analytical lab with the recent additions of Kendhl and Roberto. I think they are great fits for the analytical lab and their hard work is already showing through in just one semester of research. I believe they will go on to do amazing things in the future. Last but not least, I would like to mention Sam Rosolina. His work ethic, advice, and unique

perspective were very refreshing and made me strive to always be a better researcher in the lab. Additionally, I enjoyed all of his stories and the interesting conversations we had throughout my time here. These are the people that will make moving on from graduate school bittersweet.

Most of this work would not have been possible without the help from collaborators and other researchers, staff, and facilities. I would like to thank the research staff at InnoSense, LLC for providing countless hours of guidance and effort writing proposals for research projects. More specifically, I would like to thank Drs. Maksudul Alam, Uma Sampathkumaran, and Kisholoy Goswami. Also, I would like to thank the dedicated staff in the chemistry department. I appreciate all the things that they do so that the chemistry department can function and work smoothly. I would like to acknowledge Bill Gurley for his assistance with any computer related issues or electronic problems that arose in the lab and Gary Wynn for his expertise in designing custom electronics and building machines such as spin coaters that have been immensely helpful for my research. Gail Cox in the business office was instrumental in assisting me with any problems I had with orders and the department glass blower Art Pratt for making me a custom glass gas bubbler.

One of the last organizations I would like to acknowledge would be the Tennessee Ultimate and Knoxville Ultimate community. I am so grateful for the Ultimate community welcoming me with such open arms and becoming such a large part of my life in Knoxville. I firmly believe that being able to play frisbee kept me sane during my time at Knoxville. Having something to do and look forward to outside of the lab was immensely comforting after working in the lab. I am also forever grateful for meeting

such wonderful people in the Ultimate community and hope someday to play with them again. I truly believe that there are only two things that people can improve and that is their mind through education and their body through exercise. I want to thank everyone who came to the TRECS with me to work out with me over the last two years. It helped fuel not only a physical change but a change to a much healthier lifestyle.

Funding for my Ph.D. research was provided by the National Aeronautics and Space Administration, Department of Energy, and the University of Tennessee Research Foundation. I would also like to thank Dr. Nghia Chiem for all his support and knowledge regarding patent applications.

ABSTRACT

Detection of biodiesel at low and high concentrations in diesel is highly desired in the aviation and fuel industries. Cross contamination of jet fuel with biodiesel may impact the thermal stability and freezing point which can cause deposits in the fuel system or cause the fuel to gel, leading to jet engine operability problems and possible engine flameout. A dye doped optical sensor utilizing the dye Nile Blue Chloride has been developed for quick and direct detection of biodiesel which mainly contains fatty acid methyl esters (FAME). The sensing mechanism relies on the solvatochromatic properties of the dye which undergoes a color change from blue to pink. A detection limit of 0.250 ppm (parts per million) and quantification limit of 0.750 ppm is obtained with a dynamic range from 0.5–200,000 ppm (20% v/v) FAME. This sensor is a viable alternative to compliment more sophisticated and expensive bench top techniques in current use.

The detection of chloroform in aqueous and non-aqueous has direct environmental and pharmaceutical applications, due to its well documented toxicity. A sensor has been developed based on a modified Fujiwara reaction for detecting chloroform, a halogenated hydrocarbon, in the visible spectrum. 2,2’-dipyridyl and tetra-n-butyl ammonium hydroxide are the modified Fujiwara reagents encapsulated within a sensing film. Upon exposure to chloroform in non-aqueous solution, a colored product is produced within the film which can be analyzed spectroscopically yielding a detection limit of 0.830 ppm (v/v) and quantification limit of 2.77 ppm.

Monitoring and detection of gas plume constituents is a useful diagnostic tool in evaluating combustion efficiency, ensuring safe testing conditions, and in quantifying greenhouse gas emissions. Rocket engine ground tests are vital to ensure the performance of the rocket engines during critical space missions. Optical sensors were developed for remote sensing applications to detect isopropyl alcohol utilizing the dye Chromoionophore IX. This sensor gave a detection limit of 9, 13, 21 ppm and quantification limits of 32, 43, and 70 ppm for methanol, ethanol, and isopropyl alcohol respectively. Also a fingerprinting method was developed utilizing several indicator dyes in order to detect kerosene vapor.

TABLE OF CONTENTS

LIST OF TABLES

LIST OF FIGURES

NOMENCALTURE AND ABBREVIATIONS

A	absorbance
ATMOS	bis[3-trimethoxysilylpropyl]amine
b	pathlength
B20	20% biodiesel
c	concentration
^{o}C	degrees Celcius
CHC	chlorinated hydrocarbon
CIX	Chromoionophore IX
DI	deionized
DOS	dioctyl sebacate
EC	ethyl cellulose
EPA	Environmental Protection Agency
EtOH	ethanol
FAME	fatty acid methyl esters
ε	molar absorptivity
g	gram
GPTMS	3-glycidoxypropyltrimethoxysilane
h	hour
H_2O_2	hydrogen peroxide
λ	wavelength of visible light
L	liter

LOX	liquid oxygen
m	meter
MeOH	methanol
mM	milli molar
M	Molar
mol	mole
MOSRT	Multi-Analyte Optical Sensor for Rocket Engine Testing
MΩ	megaohm
min	minutes
mg	milligram
mL	milliliter
MTEOS	methyltriethoxysilane
MTMOS	methyltrimethoxysilane
NBC	Nile Blue Chloride
nm	nanometer
ORMOSIL	Organically Modified Silica
ppb/µg L^{-1}	parts per billion
ppm/mg L^{-1}	parts per million
ppt/ng L^{-1}	parts per trillion
$Pr^{i}OH$	isopropyl alcohol
PS	polystyrene
PVC	polyvinyl chloride
R^2	square of correlation coefficient

rpm	rotations per minute
s	second
SEM	scanning electron microscopy
t	time
TBAH	tetra-n-butylammonium hydroxide
TDMACl	tridodecylmethylammonium chloride
TFPTMOS	3,3,3-trifluoropropyltrimethoxysilane
THF	tetrahydrofuran
TMOS	trimethoxysilane
UV-Vis	ultraviolet-visible
µg	microgram
µL	microliter
µm	micrometer
wt	weight

Part 1

Introduction and Background

1.1. Foreword

With the increasing capabilities of chemical sensors, it is no surprise that they have been established as an important component in a wide variety of studies and applications. Sensors rely on an array of different methods such as optical, electrochemical, or mass-sensitive techniques and are highly sought after for their ability to easily detect a range of concentrations. The focus of the research presented primarily covers the development of chemical sensors as analytical detection tools for environmental, aviation, and pharmaceutical industries. Optical thin film sensors have been developed to detect fatty acid methyl esters (FAME) in diesel, testing for trace halogenated organic contaminants, and monitoring of gaseous analytes in test plumes for rocket engine analysis.

Spectroscopic methods are an ideal technique in coupling optical sensors for monitoring a variety of gas and liquid analyte constituents. The monitoring of biodiesel or FAME in petroleum based diesel fuel is a serious concern in industry. FAME is a highly surface active material as it can adhere to pipelines and distribution tank walls and desorb into other transportation fuels causing future issues with cross fuel contamination.[2,3] This raises a difficult problem for the aviation industry where FAME contamination can impact the thermal stability and freezing point of jet fuel leading to jet engine operability problems and possible engine flameout.[3-5] Therefore, the ability to rapidly detect FAME at low concentrations in a simple user-friendly and easy fashion would be highly valuable in evaluating fuel safety integrity. Another significant concern is the detection and quantification of chlorinated hydrocarbon (CHC) pollution in groundwater and sediments, as well as, quality control of residual CHCs in

pharmaceutical products.[6-10] CHCs in low concentrations can cause a variety of health problems.[11-13] Therefore, detection of CHCs would enhance environmental monitoring as well as industries where CHCs occur such as the pharmaceutical industry. There is also a critical need for miniaturized and remote near real-time monitoring of exhaust plumes from chemical steam generators placed in rocket test stands for the development of space engines as well as for health monitoring and failure detection systems.[1] The ability to characterize plume constituents provides important information about test stand performance as well as address any safety concerns that ground personnel may have. This dissertation involves the development of optical sensors using polymer films or sol-gel chemistry to encapsulate sensing materials for the detection of FAME, chloroform, isopropyl alcohol vapor, and kerosene vapor.

1.2. Analysis Techniques Used in the Research

1.2.1. Ultraviolet and Visible Spectroscopy

The research performed in this dissertation utilized a specific type of absorption spectroscopy called molecular absorption. In experiments using UV-Vis spectroscopy, incident light is absorbed by molecules in the path of the light. When a molecule absorbs the energy from this photon, an electron transition follows in which outer electrons are promoted from their ground state to a higher energy excited state. Using a radiationless transition, the absorbed energy is then transferred to nearby solvent molecules or through vibrational relaxation.[14] According to Beer's law (Eq. 1.1), the concentration of the absorbing species is directly proportional to the absorbance

$$A = \varepsilon b c \qquad \text{Eq. 1.1}$$

where A is the absorbance, ε is the molar absorptivity constant ($M^{-1}cm^{-1}$), b is the pathlength (cm), and c is the concentration (M) of the analyte.[14] UV-Vis spectroscopy was coupled to different optical sensors to monitor various concentrations of FAME in diesel as well as halogenated organic contaminants in aqueous and non-aqueous solutions.

1.2.2. Fluorescence Spectroscopy

Fluorescence spectroscopy is a technique that primarily focuses on the relationship between a molecule's various energy levels. Fluorescence examines a molecule's ground electronic state or low energy state, and a high energy excited electronic state. Within each of these electronic states are various vibrational states. When a molecule absorbs a photon, it becomes excited and proceeds to go from a ground electronic state to one of the various vibrational states in the excited electronic state. The excited molecule's energy will then decay and go to lower vibrational energy states until it reaches the lowest vibrational state of the excited electronic state. The molecule will then drops down to the ground electronic state and emit a photon in the process.[14] This process is illustrated by the Jablonski diagram (Figure 1.1).[15] Molecules are able to emit photons at wavelengths longer than that of the excitation source in all directions. In order to detect the emission from a compound, fluorescence spectroscopy utilizes a monochromator which holds the excitation light at a constant wavelength. Then, an emission spectrum is generated by scanning along the emission

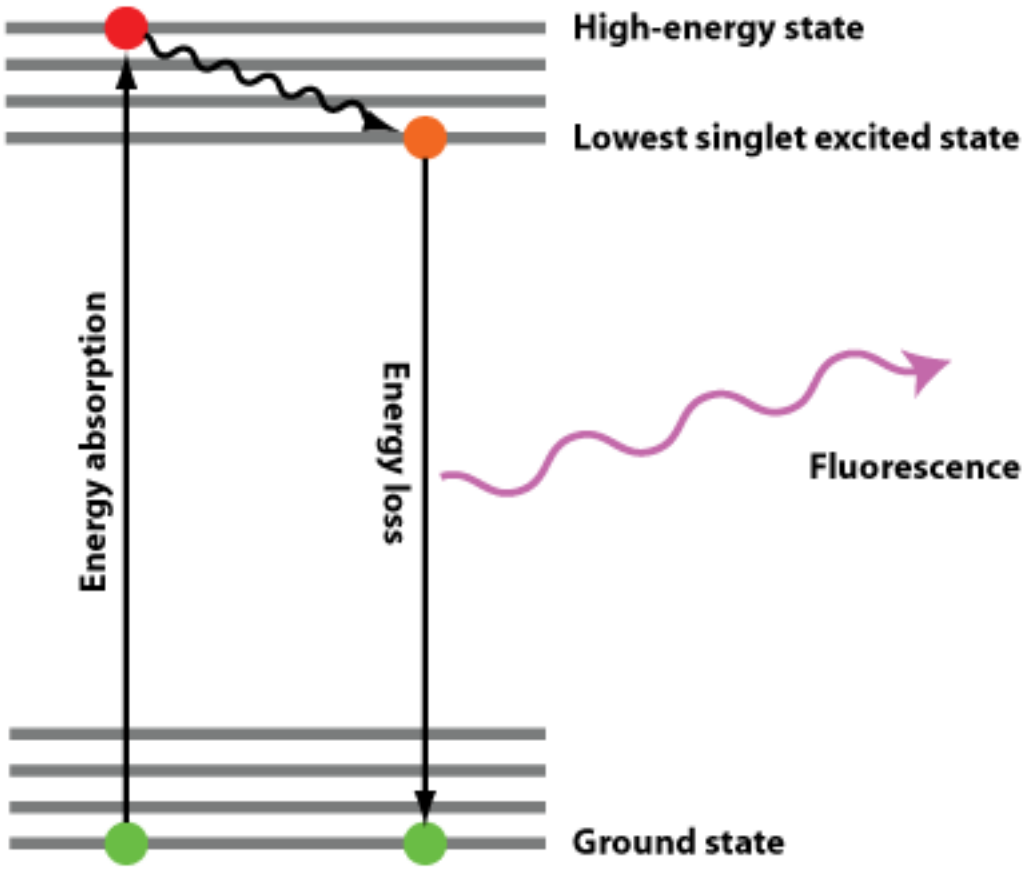

Figure 1.1. Jablonski diagram illustrating the process of fluorescence.[15]

wavelength. Luminescence is measured at another monochromator placed at a 90^{o} angle from the incident light to avoid any impact from the excitation source. An excitation spectrum is collected using the reverse process by holding the emission wavelength at a certain wavelength and scanning along the excitation wavelength.[15] The emission or excitation intensity at a single wavelength is then proportional to the concentration of the analyte being examined.

1.2.3. Immobilization Methods

In general, a good immobilization technique should be simple and fast, be nonspecific to the type of reagent being immobilized, produce a stable product, and allow the immobilized reagents to retain their initial chemical activities.[16,17] One of the most common techniques used for immobilization of sensing agents onto solid substrates to produce optical sensors is encapsulation. Encapsulation involves the physical entrapment of reagents such as indicator dyes or organic reagents inside a polymer or silica substrate.

1.3. Overview of Sol-gel Chemistry

Sol-gel chemistry refers to reactions incorporating alkoxide precursors to prepare solid glass and ceramic oxide materials. This started as early as the mid-1800s by Ebelman and Graham's study on silica glass. However, little interest was generated from sol-gels because there was a lack of understanding on preventing the sol-gel process from cracking and fracturing.[18] By the 1950s, there was a resurgence in sol-gel chemistry when Roy and coworkers were able to synthesize various novel homogenous

ceramic oxide composites involving Al, Si, Ti, Zr, and other metals using what is now a standard sol-gel method.[19] The ceramic industry began to realize the enormous amount of potential in sol-gel chemistry in the 1970s when Yoldas, Yamane, and coworkers were able to create sol-gel monoliths by carefully drying the gels forming solid structures at room temperature.[20] Only recently have researchers begun to fully understand the chemistry derived from alkoxide precursors.[20]

1.3.1. Sol-gel Processing

Sol-gels offer many advantages over traditional glass and ceramic methods such as their homogeneity, lower processing temperatures, and compatibility with many chemical reagents.[21] The sol-gel process generally involves an alkoxide precursor such as $Si(OR)_4$ or $R'Si(OR'')_3$ (R = alkyl) becoming hydrolyzed followed by a condensation reaction which generates an inorganic cross-linked polymer with a three dimensional porous structure. This reaction is summarized in Figure. 1.2. However, the sol-gel reaction is strongly influenced by a multitude of factors such as the size of the alkoxide ligand, solution pH, solvents, temperature, and catalyst selection.[21-28] By utilizing these factors, the physical properties of the resulting sol-gel structure can be tailored and adjusted to give different products to meet the specific needs of a particular study. A brief example is through the use of catalysts. Sol-gels reactions that utilize an acid catalyst result in thick, dense gels while base catalyzed reactions give a less dense structure with greater porosity throughout the gel.[20,29-31] The versatility of sol-gels allows it to be used in a variety of different applications including electronics, optics, separations, catalysis, and sensing.[22,29-32]

Hydrolysis

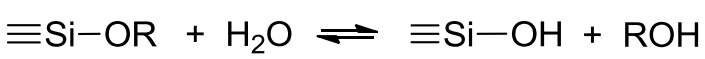

Alcohol Condensation

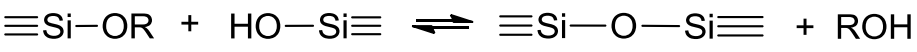

Water Condensation

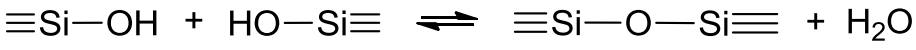

Figure 1.2. The basic reactions in the sol-gel process.

1.3.2. Development and Applications of Sol-gel Sensors

The area of chemical sensing utilizing sol-gels has been a focus in our research group.[33-35] Sol-gels possess a variety of unique physical properties that make them attractive for sensing applications. Since sol-gels are extremely inert and compatible with many chemical agents, they are good candidates to be used for sensor matrix supports. Sol-gels are able to produce glass-like properties with little to no heating. This permits temperature sensitive organic molecules such as chemical sensing agents to be easily incorporated within the sol-gel without the fear of decomposition.[16] Generally, sensing materials are encapsulated by doping them inside the sol-gel or grafting them to the backbone of the sol-gel matrix. Although doping sol-gels is a much easier process and includes the physical entrapment of the sensing agent, the major drawback is that the sensing agent can be leached from the matrix. Grafting reagents to produce organofunctionalized sol-gel materials offers a more rigid and stable product but the process is far more tedious and limited to the number of materials available that contain necessary $–Si(OR)_3$ groups.[16,17,36,37] Also, the porous nature of sol-gels easily allows the analyte of interest to be transported to the encapsulated sensing agents. Another important feature of sol-gels is that they are transparent in the visible region which allows their use in optical sensing.[38] Sensors are now being produced that utilize sol-gels towards applications in monitoring pH,[17,22,24,27,28,36,39-45] metal ions,[46-49] and various other analytes.[50-52] Sol-gels have also found use in electrochemical[53-60] and spectroelectrochemical[61] sensing applications.

1.4. Preparation of the Sensor Substrate and Coating Techniques

To prepare sol-gel films, microscope slides (Fischer Scientific) were cut into the appropriate glass substrate size depending on placement in either a cuvette or sensor platform. The cut glass slides were washed in piranha solution (concentrated H_2SO_4 and 30% H_2O_2 in 3:1 ratio) for 30 min, followed by rinses with deionized water, acetone, methanol, and ethanol. The use of piranha solution ensures the maximum formation of Si-OH groups on the surface of the slide. These slides were then allowed to dry in an oven up to two days before use. All other glass substrates that did not need Si-OH groups were cleaned using deionized water, acetone, and ethanol rinses.

Once the glass slides were prepared, they were fastened onto a custom built spin coater using double sided tape. Solution was pipetted onto the slide and drawn to the edges of the glass substrate with a plastic pipette tip. The slide was then spun at a set revolutions per minute (RPM) and for a specific amount of time. Another coating method used was drop coating a solution onto the glass slide and drawing the solution to the edges to ensure full coverage. This method is helpful if organic precursor reagents need to be retained in the film. Both of the resulting films were subsequently cured and conditioned before use.

1.4.1. Scanning Electron Microscopy

Scanning electron microscopy (SEM) is an imaging technique that provides information to characterize a sample's composition and topography. Typically, SEM utilizes electrons accelerated between a cathode and anode to produce an electron beam as a probe. The electron beam is focused by one or more condenser lenses to

increase or decrease the diameter and current of the probe. The beam then passes through scanning coils or deflection plates located in the final lens. Afterwards, the beam scans over the surface of a sample in a raster fashion, where the beam sweeps the surface in a straight line and returns to the starting position and then shifts downward.[62] This sequence is repeated until the entire area is scanned and converted into an image. SEM is capable of producing high resolution images down to the nanometer scale with magnification ranging from 10 to 100,000x.[63] The straightforward sample preparation, excellent contrast, and large depth of focus have helped contribute to the widespread use of SEM and its success.

1.5. Summary of Dissertation Parts

1.5.1. Part Two

In Part two, studies are performed to detect biodiesel at low and high concentrations in diesel. The current techniques for the detection of biodiesel, which generally consists of fatty acid methyl esters (FAME), rely on chromatography, infrared spectroscopy, or nuclear magnetic resonance. We have found that solvatochromism can be used to detect FAME/biodiesel in diesel. Here, we present a simple, optical sensor containing the dye, Nile Blue Chloride (NBC), in an ethyl cellulose film for quick and direct biodiesel detection. Based on the solvatochromatic properties of the dye, the sensor undergoes a color change from blue to pink in the presence of FAME. The highly sensitive and disposable sensor in this study detects 0.5-200,000 ppm (20% v/v) FAME (or biodiesel) in diesel. It may be used for both low, ppm-level detection of

FAME in diesel or jet fuels and high-level measurement of biodiesel in biodiesel-diesel blends.

1.5.2. Part Three

Part three describes the use of optical thin film sensors for the detection of trace amounts of chloroform in aqueous and nonaqueous solutions. The sensors utilize a modified Fujiwara reaction, one of the only known methods for detecting halogenated hydrocarbons by the visible spectroscopy. The modified Fujiwara reagents, 2,2'-dipyridyl and tetra-n-butyl ammonium hydroxide (Bu^n_4NOH or TBAH), are encapsulated in an ethyl cellulose (EC) or sol-gel film. Upon exposure of the EC sensor film to $HCCl_3$ in petroleum ether, a colored product is produced within the film, which is analyzed spectroscopically, yielding a detection limit of 0.830 ppm (v/v) and quantification limit of 2.77 ppm. In aqueous solution of $HCCl_3$, reaction in the sol-gel sensor film turns the sensor from colorless to dark yellow/brown with a detection limit of 500 ppm. To our knowledge, these are the first optical quality thin film sensors using Fujiwara reactions for halogenated hydrocarbon detection. The sensors are easy to fabricate and inexpensive, The EC sensor may be coupled to visible spectroscopy and/or with a fiber optic bundle for direct measurement studies in the field.

1.5.3. Part Four

Part four of this dissertation describes the use of optical sensors utilizing the fluorescent dye 4-dibutylamino-4′-(trifluoroacetyl)stilbene (Chromoionophore IX or CIX) as the sensing agent. The dye is dissolved in an ethyl cellulose solution and spin-

coated onto glass substrates to form thin films for the detection of alcohol vapors. When the sensor is exposed to alcohol vapors, the trifluoroacetyl group of the dye reacts with alcohol to form a hemiacetal which quenches the luminescence intensity of the sensor. Results are shown using these sensors in a custom-designed multichannel portable sensing device for remote simultaneous multi-analyte sensing of test plume constituents.

1.5.4. Part Five

Initial studies to evaluate optical sensing strategies for gas phase kerosene detection are discussed in Part 5. Kerosene is mainly composed of long chain saturated hydrocarbons. Therefore, it is difficult to employ a sensing agent that will respond to kerosene vapor because no appropriate functional group is available. Thus, a fingerprinting-type method has been closely looked into using up to 4 different sensing materials in hopes to produce a unique response to kerosene or constituents of kerosene such as hydrocarbons. Optical detection will be achieved by using indicators and monitoring either absorbance or fluorescence emission characteristics in the presence of kerosene vapor.

1.5.5. Part Six

A summary of each part of this dissertation is discussed in Part 6. Highlights for important findings as well as concluding remarks are given for each work. The significance of each research project and how they relate to each other are also

discussed. Lastly, a central theme is provided that helps to unify all parts of this dissertation.

References

1. Tejwani, G. D.; Bircher, F. E.; Van Dyke, D. B.; McVay, G. P.; Stewart, C. D.; Langford, L. A.; Thurman, C. C. *Spectroscopy* **1996**, *11*, 31-43.
2. Nygren, E.; Aleklett, K.; Höök, M. *Energ. Policy* **2009**, *37*, 4003–4010.
3. Froment, M. *FAST* **2010**, *46*, 8–13. (http://www.airbus.com/fileadmin/media_gallery/files/brochures_publications/FAST_magazine/fast46-5-jet-fuel.pdf, accessed on 20 February 2013).
4. FAME: Fuelling the Safety Debate, *Aerospace Technology*, 16 February 2012 (http://www.aerospace-technology.com/features/featurefame-fuelling-the-safety-debate, accessed on 20 February 2013)
5. Zeman, N. *Biodiesel Magazine*, 19 January 2010.
6. K. Broholm, S. Feenstra, *Environ. Toxicol. Chem.* **1995**, *14*, 9-15.
7. Vali, S.J.; Garg, L.K.; Sait. S.S. *J. Chem. Pharm. Res*. **2012**, *4*, 4312–4218.
8. Grodowska, K.; Parczewski, A. *Acta Pol. Pharm*. **2010**, *67*, 3–12.
9. Jacobs, P.; Dewé, W.; Flament, A.; Gibella, M.; Ceccato, A. *J. Pharmaceut Biomed.* **2006**, *40*, 294–304.
10. Klick, S.; Sköld, A.*J. Pharmaceut Biomed.* **2004**, 36, 401–409.
11. *U.S. Code of Federal Regulations, Occupational Safety and Health Standards on Toxic and Hazardous Substances,* 29 CFR 1910.1000, Tables Z-1, Z-2, and Z-3.
12. US EPA Seminar Publication. Chapter 3. EPA/625/R-93/002.
13. Ferguson, J.F.; Pietary, J.M.H. *Environ. Pollut.* **2000**, *107*, 209–215.
14. Harris, D. C. *Quantitative Chemical Analysis, Sixth Edition*; Sixth Edition; W. H. Freeman, 2002.

15. Fluorescence microscopy – a brief explanation. (http://www.scienceinyoureyes.com/index.php?id=79, accessed on 3 March 2014).

16. Lin, J.; Brown, C.W. *Anal*. *Chem*. **1997**, 16, 200-211.

17. Lobnik, A.; Oehme, I.; Murkovic, I.; Wolfbeis, O.S.; *Anal. Chim. Acta.* **1998**, *367*, 159-165.

18. Ebelman, M. *Ann. Chimie Phys.* **1846**, *16*, 129.

19. Roy, R. *J. Am. Ceram. Soc.* **1969**, *52*, 344.

20. Brinker, C.J.; Scherer, G.W. *Sol-Gel Science*; Academic Press, Inc.: Boston, 1990, pp 541-546.

21. Hench, L. L.; West, J. K. *Chem. Rev.* **1990**, *90*, 33-72.

22. Allain, L. R.; Sorasaenee, K.; Xue, Z. *Anal. Chem.* **1997**, *69*, 3076-3080.

23. Lev, O.; Tsionsky, M.; Rabinovich, L.; Glezer, V.; Sampath, S.; Pankratov, I.; Gun, J. *Anal. Chem.* **1995**, *67*, 22A-30A.

24. Allain, L. R.; Canada, T. A.; Xue, Z. *Anal. Chem.* **2001**, *73*, 4592-4598.

25. Brinker, C.; Hurd, A.; Schunk, P.; Frye, G.; Ashley, C. *J. Non-Cryst. Solids* **1992**, *147-148*, 424-436.

26. Schubert, U.; Huesing, N.; Lorenz, A. *Chem. Mater.* **1995**, *7*, 2010-2027.

27. Carey, W. P.; DeGrandpre, M. D.; Jorgensen, B. S. *Anal. Chem.* **1989**, *61*, 1674-1678.

28. Carey, W. P.; Jorgensen, B. S. *Appl. Spectrosc.* **1991**, *45*, 834-838.

29. Klein, L. C.; *Solgel Coatings* in *Coatings Technology Handbook*, 3rd ed.; Tracton, A. A. Ed.; CRC Press: Boca Raton, Florida 2006, pp. 96/1-96/4.

30. Sanchez, C.; Julian, B.; Belleville, P.; Popall, M. *J. Mater. Chem.* **2005**, *15*, 3559-3592.

31. McDonagh, C.; MacCraith, B. D.; McEvoy, A. K. *Anal. Chem.* **1998**, *70*, 45-50.

32. Yost; Fagan, B. C.; Allain, L. R.; Barnes, C. E.; Dai, S.; Sepaniak, M. J.; Xue, Z. *Anal. Chem.* **2000**, *72*, 5516-5519.

33. Dansby-Sparks, R. N.; Jin, J.; Mechery, S. J.; Sampathkumaran, U.; Owen, T. W.; Yu, B. D.; Goswami, K.; Hong, K.; Grant, J.; Xue, Z. *Anal. Chem.* **2010**, *82*, 593-600.

34. Dansby-Sparks, R.; Ouyang, R.; Xue, Z. *Sci. China Ser. B Chem.* **2009**, *52*, 1777-1788.

35. Carrington, N. A.; Xue, Z. *Acc. Chem. Res.* **2007**, *40*, 343-350.

36. MacCraith, B. D.; Ruddy, V.; Potter, C.; O'Kelly, B.; McGilp, J. F. *Electron. Lett.* **1991**, *27*, 1247-1248.

37. Avnir, D. *Acc. Chem. Res.* **1995**, *28*, 328-334.

38. Dunn, B.; Zink, J. I. *J. Mater. Chem.* **1991**, *1*, 903-913.

39. Allain, L. R.; Xue, Z. *Anal. Chem.* **2000**, *72*, 1078-1083.

40. Shamsipur, M.; Azimi, G. *Anal. Lett.* **2001**, *34*, 1603-1616.

41. Wang, E.; Chow, K.; Wang, W.; Wong, C.; Yee, C.; Persad, A.; Mann, J.; Bocarsly, A. *Anal. Chim. Acta* **2005**, *534*, 301-306.

42. Canada, T.; Allain, L.; Beach, D.; Xue, Z. *Anal. Chem.* **2002**, *74*, 2535-2540.

43. Canada, T. A.; Xue, Z. *Ana.l Chem.* **2002**, *74*, 6073-6079.

44. Canada, T. A.; Beach, D. B.; Xue, Z. *Anal. Chem.* **2005**, *77*, 2842-2851.

45. Allain, L. R.; Xue, Z. *Anal. Chim. Acta* **2001**, *433*, 97-102.

46. Carrington, N. A.; Thomas, G. H.; Rodman, D. L.; Beach, D. B.; Xue, Z. *Anal. Chim. Acta* **2007**, *581*, 232-240.

47. Clavier, C. W.; Rodman, D. L.; Sinski, J. F.; Allain, L. R.; Im, H.; Yang, Y.; Clark, J. C.; Xue, Z. *J. Mater. Chem.* **2005**, *15*, 2356-2361.

48. Rodman, D. L.; Pan, H.; Clavier, C. W.; Feng, X.; Xue, Z. *Anal. Chem.* **2005**, *77*, 3231-3237.

49. Zevin, M.; Reisfeld, R.; Oehme, I.; Wolfbeis, O. S. *Sensor. Actuat. B- Chem.* **1997,** *39*, 235-238.

50. Lan, E. H.; Dave, B. C.; Fukuto, J. M.; Dunn, B.; Zink, J. I.; Valentine, J. S. *J. Mater. Chem.* **1999**, *9*, 45-53.

51. Narang, U.; Prasad, P. N.; Bright, F. V.; Ramanathan, K.; Kumar, N. D.; Malhotra, B. D.; Kamalasanan, M. N.; Chandra, S. *Anal. Chem.* **1994**, *66*, 3139-3144.

52. Rao, M.; B. C. Dave *Adv. Mater.* **2002**, *14*, 443-447.

53. Carrington, N. A.; Yong, L.; Xue, Z. *Anal. Chim. Acta* **2006**, *572*, 17-24.

54. Jena, B. K.; Raj, C. R. *Talanta* **2008**, *76*, 161-165.

55. Walcarius, A.; Mandler, D.; Cox, J. A.; Collinson, M.; Lev, O. *J. Mater. Chem.* **2005**, *15*, 3663-3689.

56. Lev, O.; Wu, Z.; Bharathi, S.; Glezer, V.; Modestov, A.; Gun, J.; Rabinovich, L.; Sampath, S. *Chem. Mater.* **1997**, *9*, 2354-2375.

57. Alber, K. S.; Cox, J. A. *Microchim. Acta* **1997**, *127*, 131-147.

58. Deepa, P. N.; Kanungo, M.; Claycomb, G.; Sherwood, P. M. A.; Collinson, M. M. *Anal. Chem.* **2003**, *75*, 5399-5405.

59. Walcarius, A.; Sibottier, E. *Electroanal.* **2005**, *17*, 1716-1726.

60. Shacham, R.; David Avnir; Daniel Mandler *Adv. Mater.* **1999**, *11*, 384-388.

61. Shi, Y.; Slaterbeck, A. F.; Seliskar, C. J.; Heineman, W. R. *Anal. Chem.* **1997**, *69*, 3679-3686.

62. Skoog, D. A.; Holler, F. J.; Nieman, T. A. *Principles of Instrumental Analysis*, 5th ed.; Brooks Cole, 1998.

63. Whan, R. E. *Metals Handbook – Materials Characterization*, 9th ed.; American Society for Metals: Ohio, 1986, Vol. 10.

Part 2

A Dye-Doped Optical Sensor for the Detection of Biodiesel in Diesel

This chapter is revised based on a paper by Jonathan K. Fong, and Zi-Ling Xue. Only minor revisions were made.

J.K. Fong and Z.-L. Xue. A Dye-Doped Optical Sensor for the Detection of Biodiesel in Diesel. *Chemical Communications*, **2013**, *49*, 9015-9017.

Abstract

The ability to detect biodiesel at low and high concentrations in diesel is an important goal in several industrial sectors. The current techniques for the detection of biodiesel, which generally consists of fatty acid methyl esters (FAME), rely on chromatography, infrared spectroscopy, or nuclear magnetic resonance. We have found that solvatochromism can be used to detect FAME/biodiesel in diesel. Here, we present a simple, optical sensor containing the dye, Nile Blue Chloride, in an ethyl cellulose film for quick and direct biodiesel detection. Based on the solvatochromatic properties of the dye, the sensor undergoes a color change from blue to pink in the presence of FAME. The highly sensitive and disposable sensor in this study detects 0.5-200,000 ppm (20% v/v) FAME (or biodiesel) in diesel. It may be used for both low, ppm-level detection of FAME in diesel and high-level measurement of biodiesel in biodiesel-diesel blends.

2.1. Introduction

Biofuels and biodiesel are an area of intense interest. With the rapid depletion of non-renewable fossil fuels, there is an increasing demand for alternative energy sources. Thus, a greater emphasis has been put on developing and producing renewable forms of energy such as biofuels and biodiesel.[1] Several key advantages of biodiesel usage are the decrease in hydrocarbon emission, carbon monoxide, and sulfur dioxide as well as being carbon neutral.[2-4] FAME in biodiesel is usually produced by a transesterification process from vegetable oil, animal fat, or cooking grease where triglycerides are cleaved and reacted with methanol to produce glycerol and FAME. Because biodiesel generally consists of FAME, both terms are used interchangeably here. With the recent passage of ASTM D975 and EN 590 biodiesel regulations, the U.S allows on-and-off-road diesel to contain up to 5% v/v biodiesel while European countries permit up to 7% v/v biodiesel in automotive diesel without specific labeling.[5-7] In most cases, its distribution and supply systems use the same refineries, storage tank facilities, and pipelines as the majority of other transportation fuels. This practice raises a difficult problem regarding cross fuel contamination because FAME is a highly surface active material, adhering to pipelines and distribution tank walls during its transportation.[7-8] Therefore, FAME can potentially desorb into other transportation fuels that use the same pipelines or storage tanks.

In the aviation industry, there is a particular concern over FAME contamination in jet fuel because at higher levels it can impact the thermal stability and freezing point of jet fuel leading to deposits in the fuel system or cause the fuel to gel.[8-10] These issues can result in jet engine operability problems and possible engine flameout. An aviation

catastrophe was avoided when fuel contamination caused the throttles of two engines on a Cathay Pacific flight to stick while in flight. It was only because the skill of the pilots and a long runway at the landing airport that the 322 passengers and crew were not injured.[11-12] Currently, the aviation industry allows up to 5 ppm FAME in its jet fuel before it is off specification.[13] While protective measures and strict regulations are in place to prevent cross contamination, the permitted threshold of FAME in jet fuel makes it difficult to completely prevent FAME contamination in a shared fuel system.[13] Since 5 ppm FAME in jet fuel has proved to be difficult to detect, very sophisticated instrumentation is needed in order to determine FAME contamination. In addition to the highly sensitive, ppm-level detection of FAME in the aviation industry, there is also a need for quick, easy, and direct detection of biodiesel in biodiesel-diesel blends for the verification of the blend accuracy.[14-15] Such blends (e.g., 20% v/v biodiesel known as B20) are commercially available in gas stations. Therefore, a quick verification check of the biodiesel blend accuracy would be an indispensable tool before a delivery of the blend is made. As discussed below, current biodiesel detection methods are more amenable to laboratory testing where waiting for an off-site test may take several hours to days.[14-15]

Some of the most common standard techniques applied for FAME detection include specialised gas chromatography (GC) usually in tandem with supplementary methods,[16-19] Fourier transform infrared spectroscopy (FT-IR),[15,20] high-performance liquid chromatography (HPLC),[21,22] and nuclear magnetic resonance (NMR).[23,24] Despite the regular use of these standard techniques, there are a few noticeable drawbacks such as bulky and expensive instrumentation, and portability issues. A

variety of other specialized and specific methods have been developed for FAME detection which utilize electrospray ionization with chemometrics, x-ray fluorescence spectrometry (EDXRF), several spectroscopic techniques in tandem with each other, and test kits based on solubility differences.[14, 25-28]

One technique that has experienced relatively little application with FAME detection, however, is the use of visible optical sensors. Optical sensors are often intrinsically easy to use, inexpensive, and can be mass produced for disposable applications. Moreover, combining dye-doped optical sensors to spectrophotometers makes remote sensing possible. Solvatochromatic dyes in particular have been used in a variety of applications such as chemical sensors and indicators.[29-36] In this study, a specific oxazine dye called Nile Blue Chloride (NBC) is applied to an optical sensor for FAME detection. Several authors have described these types of dyes as displaying positive solvatochromism leading to a large red shift in absorption and emission maxima when going from non-polar to polar solvents.[37,38] Solvatochromism describes the change in position and sometimes intensity of a UV-visible absorption band following a change in the polarity of the solvent.[30,35] The solvatochromatic behavior of NBC occurs from the large dipole moment change it undergoes during the transition between the ground and excited states. This corresponds well to the charge transfer between the diethylamino group which acts as an electron donor and aromatic acceptor.[35]

2.2. Experimental

2.2.1. Materials and Methods

All solvents were purchased from Fischer Scientific and used as received. Ethyl cellulose (49% ethoxy content) was purchased from MP biomedicals and Nile Blue chloride (NBC, 85%) was purchased from Sigma-Aldrich. Methyl hexanoate (98%) was purchased from Eastman, and methyl myristate (>98%), methyl oleate (>96%), and methyl behenate (>90%) were purchased from Fischer Scientific and used as received. These FAMEs were used for make standard solutions in kerosene. Biodiesel (B20) containing 20% v/v FAME was purchased from a Pilot gas station in Knoxville, Tennessee.

2.2.2. Sensor Fabrication and Analyte Exposure

Standard microscope slides (Corning) were cut to 1 cm^2 squares and used as the sensor substrate. The glass squares were washed in a piranha solution (concentrated H_2SO_4 and 30% H_2O_2 in 3:1 ratio) for 30 min, followed by washes with acetone, methanol, ethanol, rinsed with deionized water, and allowed to dry in the oven before use. N-type [100] silicon wafers were similarly cleaned for deposition of thin film sensors that were then used for characterization by SEM.

Ethyl cellulose (~0.750 g) was dissolved in a 1:1 mixture of toluene and ethanol and sonicated for approximately 4 h to ensure that the ethyl cellulose was completely dissolved in solution. The result was a viscous ethyl cellulose solution (7.5% wt EC). NBC (~1 mg) and methanol (350 µL) were added to 1.10 g of ethyl cellulose solution

with stirring. This mixture was allowed to stand and cure for several days in a capped vial prior to use. After curing, the mixture was pipetted onto a clean glass slide and drawn to the edges of the glass with a plastic pipette tip. The slide was then spun at ~2600 rpm for approximately 1 min in a custom built spin-coater. After spin-coating, a freshly made thin film sensors with a distinct blue color were placed in a Schlenk tube and pumped at 0.01 mmHg vacuum for 1 h. They were then stored prior to use.

The FAME mixture was made by combining methyl hexanoate, methyl myristate, methyl oleate, and methyl behenate in an evenly distributed 1:1:1:1 ratio. This mixture provides methyl esters with varying chain lengths (C6–C23) with methyl oleate offering a CH=CH bond in its chain. Different concentrations of the FAME mixture were made by diluting the mixture to the appropriate concentration with diesel. Sensors were submerged into their respective vials containing 20 mL of varying diesel/FAME concentrations while the solution was stirring. After satisfactory analysis time, the sensors were taken out of their vials and analysed using a UV-Vis spectrometer.

The sensor response to 20 mL of FAME, ranging from 0.5–30 ppm, is less than 30 min. To achieve this response time, two steps have been taken to allow faster diffusion of FAME into the sensor film and reduce the response time. First, the mixture of ethyl cellulose and NBC dye needs to be spin-coated at 2600 rpm (revolutions per minute) to make a thin sensor film. Second, the freshly-made sensor film is subjected to a dynamic vacuum (<0.01 mmHg) for 1 h to remove toluene and excess MeOH/EtOH in the film. After the vacuum treatment, the sensor remains blue, indicating that there is sufficient MeOH/EtOH around the NBC dye molecules in the sensor. These steps reduced the response time from originally over 1 h (without the vacuum treatment) to

<30 min.

2.2.3. Instrumentation

An Agilent 8453 UV-Vis spectrometer using two light sources, a deuterium and tungsten lamp, was used to acquire absorbance spectra of the sensing films. A quartz cuvette with a 1 mm pathlength was utilised to hold the sensor in place. Spectra were recorded in the range from 190 cm^{-1} to 1100 cm^{-1}. Peak deconvolution and baseline correction were achieved through Origin software. SEM images of the sensors before and after exposure to FAME were taken using a Leo 1525 Field Emission Scanning Electron Microscope.

Scanning electron microscopy (SEM) imaging was taken in order to characterise the surface of the FAME sensor before and after exposure to the FAME mixture. The images show “porous pitting” features consistent with the phase separation that occurs during the processing of the sensor with no discernible difference on the surface of the sensor before or after exposure (Figure 2.1). The porosity and polar features of the cellulose film allow FAME to preconcentrate and diffuse into the sensor, causing a color change.

2.3. Results and Discussion

2.3.1. Film and Sensor Characterization

Extensive research has been accomplished in recent years on the unique photo-physical properties that make oxazine dyes suitable for many chemical and biological

A

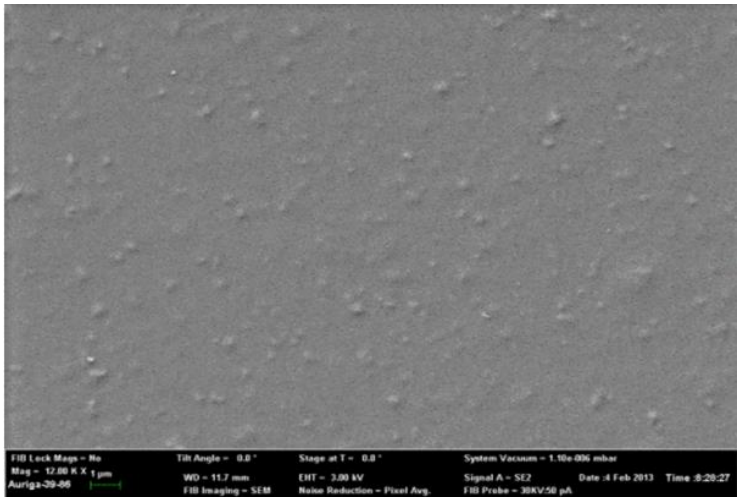

B

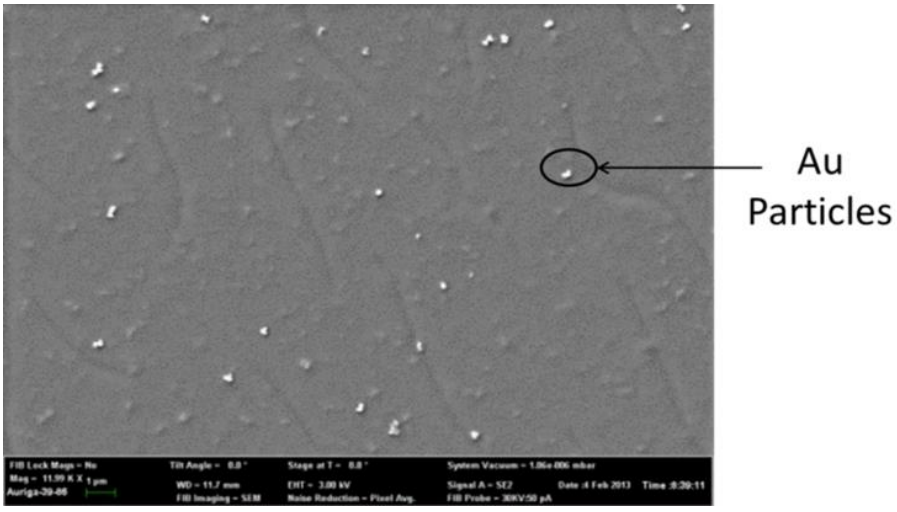

Figure 2.1. SEM surface images of the thin film sensors before (A) and after (B) exposure to FAME. The white particles in (B) are due to the sputtered gold particles needed on the sensor's surface to increase the conductivity for SEM imaging.

applications as well as the spectroscopic behaviour and interaction to different environments.[39-45] A simple procedure has been developed producing thin film sensors with high sensitivity towards FAME using NBC as the sensing agent. The sensor changes colors upon exposure to FAME and has been successfully used for quantitative FAME detection in the 0.5-200,000 ppm (20% v/v) range. The color change may be monitored by the naked eye or analysed by a visible spectrometer. Dye-doped optical sensors have been actively studied to detect different analytes using unique properties of specific dyes.[46-52] Several solvatochromatic dyes such as Reichardt's dye, Methylene Blue, Methyl Red, Coumarin, and NBC were tested in various solutions of kerosene, MeOH, and FAME. Only NBC showed the qualities necessary in preliminary tests to be used as the sensing agent. In the current work, initial solution tests demonstrated that NBC is insoluble in nonpolar solutions such as diesel, turns to a blue color in MeOH with an absorbance at ~625 nm, and changes to a pink color in a mixture of several different FAME solutions with an absorbance at ~525 nm (Figure 2.2). However, encapsulating the sensing dye into a polymer matrix for FAME detection proved to be challenging. Many different polymer matrices were examined such as sol gels and polyvinyl derivatives, and it was found that an ethyl cellulose polymer provided the most uniform and stable substrate. Sensor fabrication delivered an effective process to encapsulate NBC resulting in distinct blue colored thin films. These blue thin films have an absorbance at 610 nm. Exposing our sensor to a nonpolar solution (e.g., diesel) showed no color change, no dye leaching, and no influences on stability in the sensing film when put in an organic solvent which reinforces the choice of the polymer cellulose matrix.

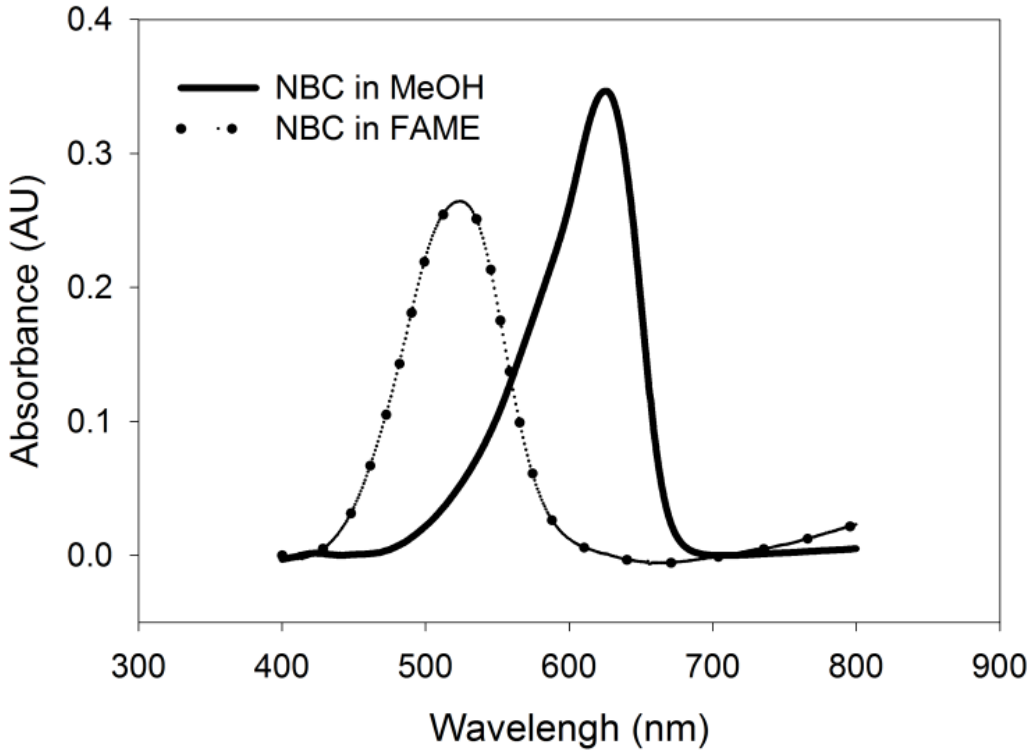

Figure 2.2. The absorbance of NBC when dissolved in MeOH (625 nm) and FAME (525 nm).

A distinct color change (blue to pink) is observed when the sensor is exposed to FAME, a less polar solution (Figure 2.3). This color change is believed to be largely attributed to FAME molecules replacing alcohols that surround the sensor during its fabrication, as a result of the positive solvatochromatic property of NBC. The spectrum of the sensor shows a new peak at 500 nm that corresponds to the sensor's pink color (Figure 2.4). The sensor was analyzed through spectrophotometry utilizing the newly defined peak at 500 nm that is associated with the physical change in sensor color. This peak was de-convoluted using Origin 8.1 Pro and was found to proportionally increase with increasing concentrations of the FAME mixture (Figure 2.5). The sensor provides a quick, direct, and disposable method for FAME determination that is unlike any other standard detection method[15,16-28] in the field such as GC-MS or FT-IR.

2.3.2. FAME Analysis

For low FAME concentrations of 0.5-30 ppm in diesel, the absorbance at 500 nm shows a linear relationship (Figure 2.6) both with standards and biodiesel samples made from a commercial biodiesel, B20. The standards were first measured to establish the calibration plot in Figure 2.6 with R^2 = 0.997. The limit of detection (3σ) for the sensor was found to be 0.22 ppm and the limit of quantification 0.73 ppm, indicating high sensitivity for FAME detection. The response of the real biodiesel samples, prepared from a serial dilution of B20, is also shown in Figure 2.6 insert. The biodiesel calibration is overlaid onto the calibration plot to demonstrate that the results fall within the standard error of the FAME calibration curve (Figure 2.6). For example, a 30 ppm biodiesel sample was evaluated using the FAME sensor. Using its absorbance value at

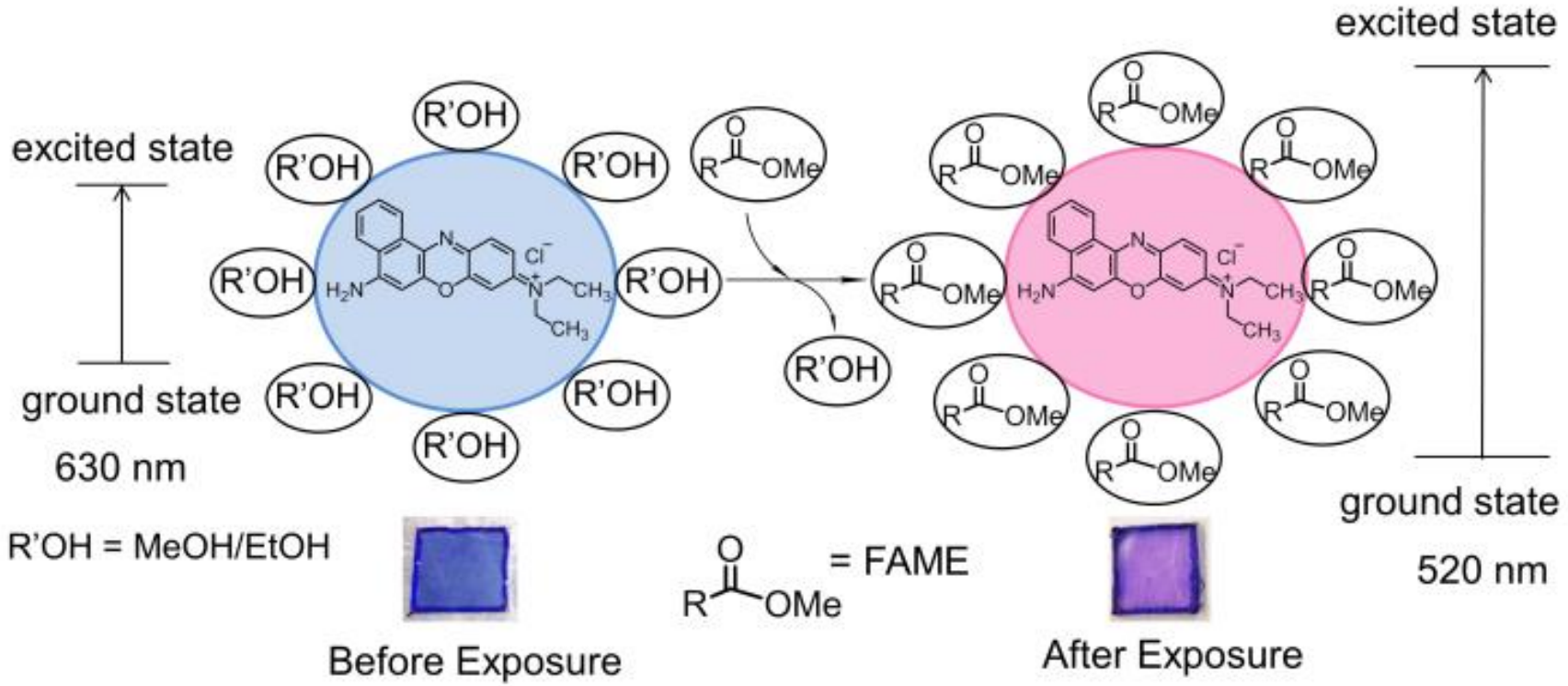

Figure 2.3. Shift in absorbance and a distinct color change from blue to pink occurring when the optical sensors are exposed to FAME.

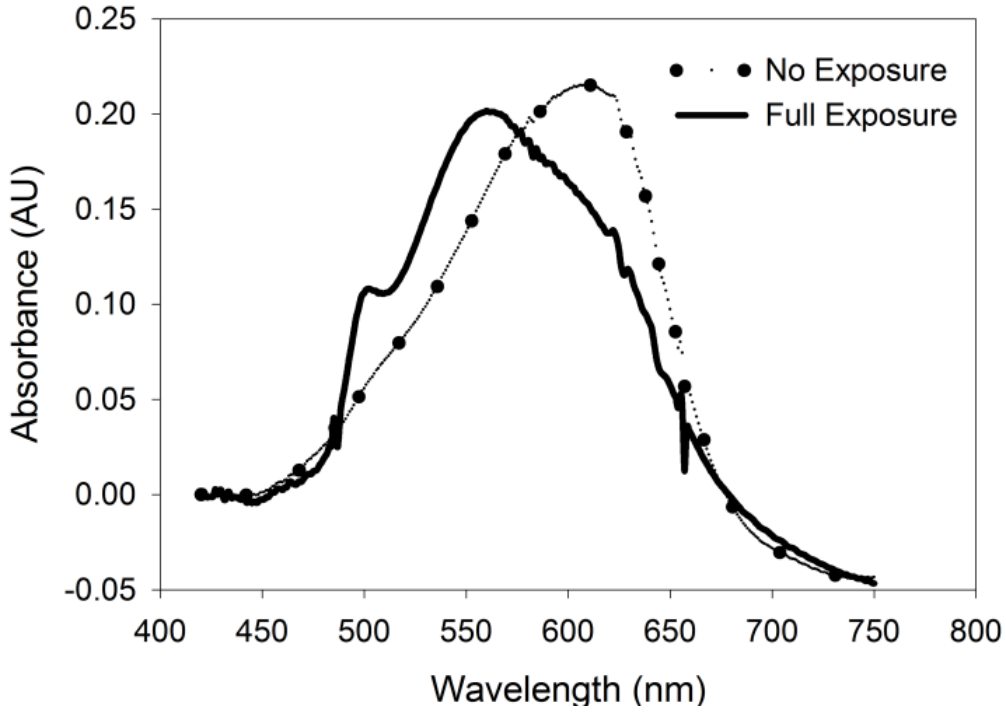

Figure 2.4. Absorbance spectra of the sensor showing the formation of a new peak at 500 nm.

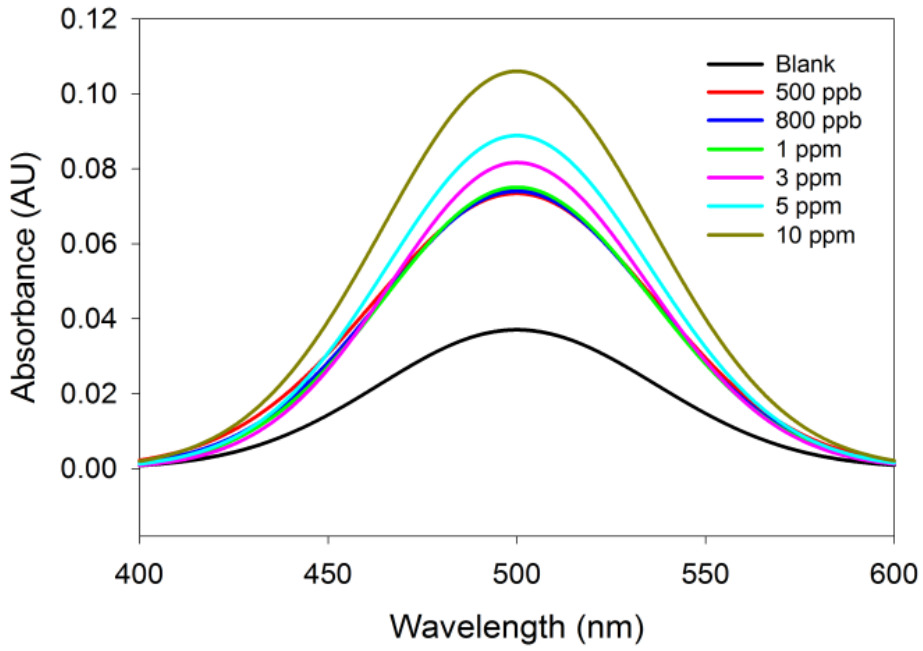

Figure 2.5. Absorbance spectra showing the peak at 500 nm increasing with increasing concentrations of FAME mixture (0–0.001% v/v).

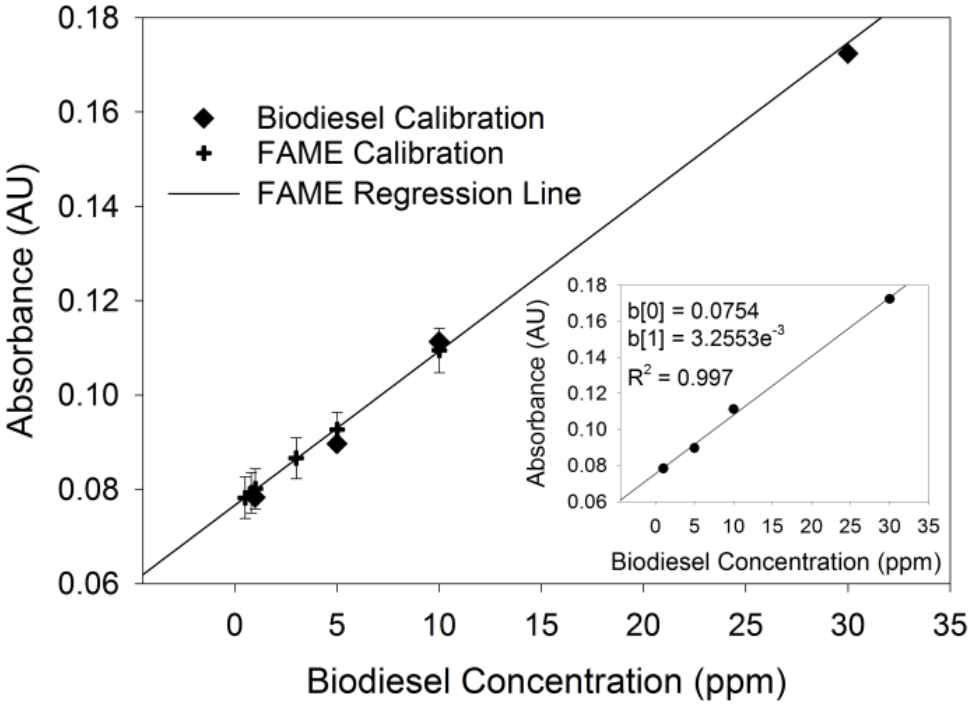

Figure 2.6. Calibration plot and confirmation using biodiesel samples in the 0.5-30 ppm range.

500 nm and the calibration data, the sensor gave the concentration of 29.3 ppm FAME with an accuracy of 97.7%. The results here verify the validity of the calibration plot established by the standards. The tests with the commercial biodiesel demonstrate the reliability and application potentials of the new FAME sensor. The color change from blue to pink is evident with the naked eye. The FAME sensor may thus also serve as a qualitative, disposable one.

At increasingly high FAME concentrations, more alcohol groups surrounding the dye inside the sensor are being replaced by FAME producing a greater color change. However, as more alcohol groups become replaced, the differences in color between 5–20% become less pronounced and give only subtle changes in absorbance providing essentially a saturation effect. This saturation curve may be modelled by a logarithmic function. Plots involving 0 and 100–200,000 ppm (20% v/v) FAME standards are shown in Figure 2.7. The absorbance A vs. ln ($x - x_o$) (x is concentration of FAME, x_o is found through the logarithmic fitting) gives a linear line with $R^2 = 0.995$ (Figure 2.7 insert). *At concentrations higher than 1,000 ppm, the sensor response time is less than 5 min.* With the naked eye, different shades of pink can be clearly detected corresponding to a conservative range of 1000 ppm–1% FAME. At concentrations lower than 1000 ppm and greater than 1% the color shades becomes too light and too dark to distinguish any color difference respectively. Therefore, these sensors may provide an effective and quick method for FAME determination with applications as a qualitative disposable sensor.

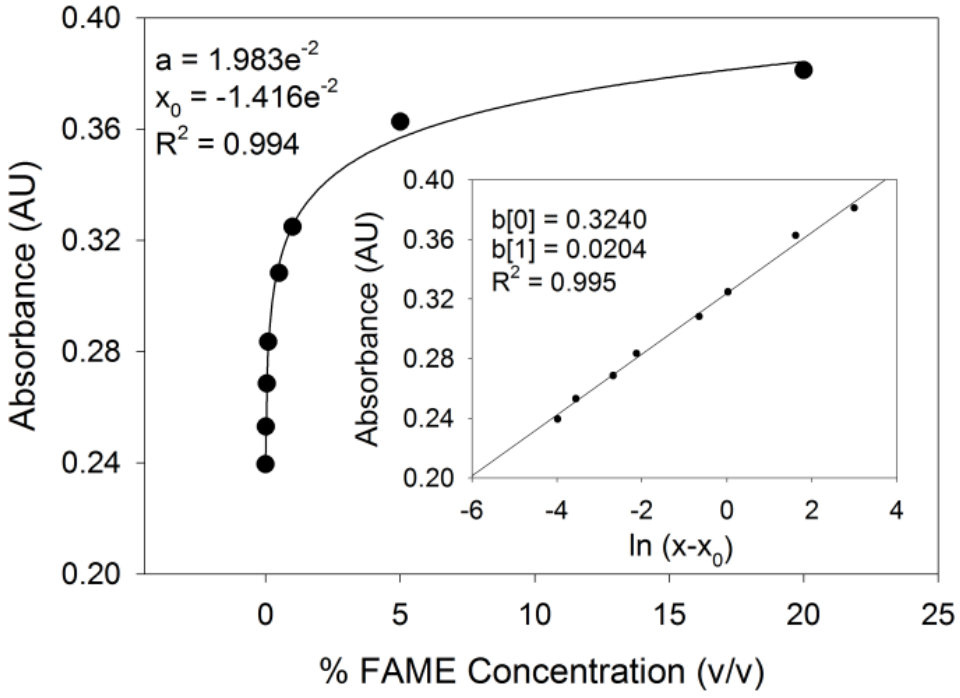

Figure 2.7. Detection of 100 ppm–20% v/v FAME mixtures modeled by a logarithmic curve function.

2.3.3. Stability Tests

Experiments were performed to test the stability of the FAME sensor over different periods of time. Extra sensors not used in previous experiments were kept in open air and then tested four months later against FAME sensors made a week ago and freshly made sensors made one day ago. These sensors were each exposed to real world samples of 1% biodiesel and examined by the UV-Vis spectroscopy. A side by side comparion in Table 2.1 shows that a freshly made sensor and a week old sensor have only a 0.3% error in absorbance at 502 nm while a sensor made 4 months ago left in open air had a 3% difference when compared to the freshly made sensor. This demonstrates that a sensor made several months ago is able to perform similarly to a freshly made FAME sensor that was fabricated only a day ago.

Table 2.1. Stability Tests

	Fresh Sensor	**Week Old Sensor**	**4 Month Old Sensor**
Absorbance at 502 nm (AU)	0.1622	0.1617	0.1577

2.3.4. B20 Sample Analysis

The FAME mixture used in previous experiments consisted of 4 diffeernt kinds of FAME ranging from C6 to C23 which was used as a mimic for biodiesel standards. However, the FAME mixture that was used as standards is not entirely representative of

the FAME composition found in biodiesel in the U.S and Europe, where methyl esters C16 and C18 dominate. Further tests have been performed using our FAME senosr on real world biodiesel samples (containing C16 or C18 fatty acids with unsaturation sites) over the range of 100 ppm–20% FAME instead of a FAME mixture to serve as methyl ester standards. The data was analyzed using UV-Vis spectrometry and modelled using a lograthmic curve function (Figure 2.8). The data is similar to previous experiments using FAME standards where the sensor undergoes a saturation effect. The absorbance (A) vs. ln ($x - x_o$) of the biodiesel data gives a linear line with R^2 = 0.993 (Figure 2.8). These studies using biodiesel give a better representation of the target analyte and the detection of FAME. This study along with previous studies shows that this FAME sensor can detect FAME at a full range from 1 ppm to 20%.

2.4. Conclusions

In conclusion, since Nile Blue Chloride is insoluble in diesel, it thus does not work to directly use the solvatochromatic properties of the dye in diesel and FAME. In the current approach, the dye, dissolved in alcohol, is made into a film. Diesel does not displace the alcohol surrounding the dye, thus keeping the blue color of the dye in alcohol. But FAME does replace the alcohol, changing the sensor color and leading to the detection of biodiesel. The approach here is thus not a traditional use of solvatochromism for analyte detection.

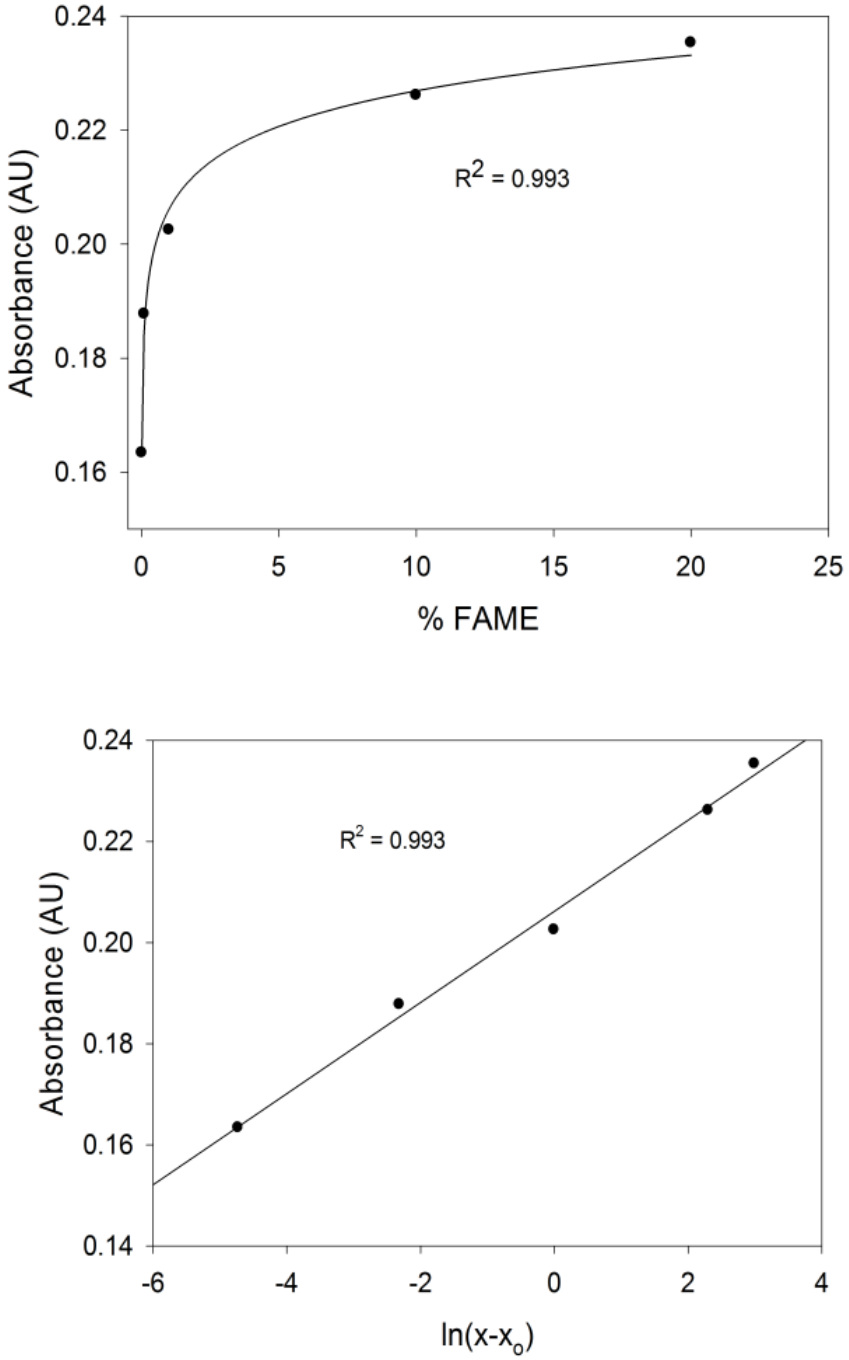

Figure 2.8. (Top) Detection of 100 ppm–20% v/v biodiesel modeled by a logarithmic curve function; (Bottom) Data plotted as a function of absorbance (A) vs. ln ($x - x_o$).

References

1. Sharma, Y.C.; Singh, B.; Upadhyay, S.N. *Fuel* **2008**, *87*, 2355–2373.
2. Canakci, M.; Erdil, A.; Arcaklioуglu, E. *Appl. Energy* **2006**, *83*, 594–605.
3. Karavalakis, G.; Tzirakis, E.; Stournas, S.; Zannikos, F.; Karonis, D. *Energ. Source. Part A.* **2009**, *32*, 376–383.
4. Lang, X.; Dalai, A.K.; Bakhshi, N.N.; Reaney, M.J.; Hertz, P.B. *Bioresour. Technol.* **2001**, *80*, 53–62.
5. ASTM International D975-09. *Standard Specification for Diesel Fuel Oils*.
6. European Standard EN 14214:2008+A1:2009 *Automotive Fuels. Fatty Acid Methyl Esters (FAME) for Diesel Engines. Requirements and Test Methods.*
7. Nygren, E.; Aleklett, K.; Höök, M. *Energ. Policy* **2009**, *37*, 4003–4010.
8. Froment, M. *FAST* **2010**, *46*, 8–13. (http://www.airbus.com/fileadmin/media_gallery/files/brochures_publications/FAST_magazine/fast46-5-jet-fuel.pdf, accessed on 20 February 2013).
9. FAME: Fuelling the Safety Debate, *Aerospace Technology*, 16 February 2012 (http://www.aerospace-technology.com/features/featurefame-fuelling-the-safety-debate, accessed on 20 February 2013)
10. Zeman, N. *Biodiesel Magazine*, 19 January 2010.
11. Parry, S. *The Telegraph*, 13 April 2010.
12. Farmery, M. *Yearbook and Directory 2012*, Energy Institute, UK, 20–22. (http://www.energyinst.org/_uploads/documents/2012-yearbook-and-directory-pdf.pdf, accessed on 20 February 2013) .
13. Pauls, R.E. *J. Chromatog. Sci.* **2011**, *49*, 384–396.

14. Kay, K.H.; Yasir, S.M.; Kudumpor, K. *Int. J. Chem. Eng. Appl*. **2012**, *3*, 307–310.

15. Rintoul, S. *Biodiesel Magazine*, 10 September 2012.

16. IP585/10, *Determination of Fatty Acid Methyl Esters (FAME) Derived from Biodiesel Fuel, in Aviation Turbine Fuel – GC-MS with Selective Ion Monitoring/Scan Detection*, The Energy Institute, London, UK.

17. Lissitsyna, K.; Huertas, S.; Morales, R.; Quintero, L.C.; Polo, L.M. *Chromatographia* **2012**, *75*, 1319–1325.

18. Pardo, V.L.; Fagundes, C.A.M.; Caldas, S.S.; Kurz, M.H.; Clementin, R.M.; D'Oca, M.G.M.; Primel, E.G. *J. Am. Oil Chem. Soc.* **2012**, *89*, 631–637.

19. Seeley, J.V.; Bates, C.T.; McCurry, J.D.; Seeley, S.K. *J. Chromatogr. A* **2012**, *1226*, 103–109.

20. Tariq, M.; Ali, S.; Ahmad, F.; Ahmad, M.; Zafar, M.; Kalid, N.; Khan, M. A. *Fuel Process. Technol*. **2011**, *92*, 336–341.

21. Kaminski, M.; Gilgenast, E.; Przyjazny, A.; Romanik, G. J. *Chromatogr. A*. **2006**, 1122, 153–160.

22. Carvalho, M.S.; Mendonça, M.A.; Pinho, D.M.M.; Resck, I.S.; Suarez, P.A.Z. *J. Braz. Chem. Soc.* **2012**, *23*, 763–769.

23. Mello, V.M.; Oliveira, F.C.C.; Fraga, W.G.; Nascimento, C.J.; Suarez, P.A.Z. *Magn. Reson. Chem.* **2008**, *46*, 1051–1054.

24. Monteiro, M.R.; Ambrozin, A.R.P.; Liao, L.M.; Ferreira, A.G. *Fuel* **2009**, *88*, 691–696.

25. Eide, I.; Neverdal, G.; Westad, F. *Energy Fuels* **2010**, *24*, 3661–3664.

26. Eide, I.; Zahlsen, K. *Energy Fuels* **2007**, *21*, 3702–3708.

27. Sitko, R.; Zawisza, B.; Kowalewska, Z.; Kocot, K.; Polowniak, M. *Talanta* **2011**, *85*, 2000–2006.

28. Chuck, C.J.; Bannister, C.D.; Hawley, J.G.; Davidson, M.G. *Fuel* **2010**, *89*, 457–461.

29. Nigam, S.; Rutan, S. *Appl. Spectrosc.* **2001**, *55,* 362A–370A.

30. Reichardt, C. *Chem. Rev.* **1994**, *94*, 2319–2358.

31. Marini, A.; Munoz-Losa, A.; Biancardi, A.; Mennucci, B. *J. Phys. Chem. B* **2010**, *114*, 17128–17135.

32. Galgano, P.D.; Loffredo, C.; Sato, B.M.; Reichardt, C.; El Seoud, O. A. *Chem. Educ. Res. Pract.* **2012**, *13*, 147–153.

33. Die, J. W. *Angew. Chem.* **1947**, *59*, 188–194.

34. Page, P.M.; McCarty, T.A.; Baker, G.A.; Baker, S.N.; Bright, F.V. *Langmuir* **2007**, *23*, 843–849.

35. Gilani, A.G.; Hosseini, S.E.; Moghadam, M.; Alizadeh, E. *Spectrochim. Acta A* **2012**, *89*, 231–237.

36. Ali, R.; Lang, T.; Saleh, S.M.; Meier, R.J.; Wolfbeis, O.S. *Anal. Chem.* **2011**, *83*, 2846–2851.

37. Jose, J.; Ueno, Y.; Burgess, K. *Chem. Eur. J.* **2008**, *15*, 418–423.

38. Peng, J.J.; Liu, S.P.; Wang, L.; He, Y.Q. *Spectrochim. Acta A* **2010**, *75*, 1571–1576.

39. Jose, J.; Burgess, K. *Tetrahedron* **2006**, *62*, 11021–11037.

40. Ghoneim, N. *Spectrochim. Acta A* **2000**, *56*, 1003–1010.

41. Gilani, A.G.; Moghadam, M.; Zakerhamidi, M.S. *Dyes Pigm*. **2012**, *92*, 1052–1057.

42. Kubinyi, M.; Grofcsik, A.; Pápai, I.; Jones, W.J. *Chem. Phys.* **2003**, *286*, 81–96.

43. Grofcsik, A.; Kubinyi, M.; Ruzsinszky, A.; Veszprémi, T.; Jones, W.J. *J. Mol. Struct.* **2000**, *555*, 15–19.

44. Hejazi, M.S.; Raoof, J-B.; Ojani, R.; Golabi, S.M.; Asl, E.H. *Bioelectrochemistry* **2010**, *78*, 141–146.

45. Ensafi, A.A.; Amini, M. *Sens. Actuat. B* **2010**, *147*, 61–66.

46. Mohr, G.J. *Sensor. Actuat. B* **2003**, *90*, 31–36.

47. Mohr, G.J. *Anal. Chim. Acta* **2004**, 508, 233–237.

48. Musto, C.J.; Lim, S.H.; Suslick, K.S. *Anal. Chem.* **2009**, *81*, 6526–6533.

49. Dansby-Sparks, R.N.; Jin, J.; Mechery, S.J.; Sampathkumaran, U.; Owen, T.W.; Yu, B.D.; Goswami, K.; Hong, K.; Grant, J.; Xue, Z-L. *Anal. Chem.* **2009**, *82*, 593–600.

50. Carrington, N.A.; Xue, Z.-L. *Acc. Chem. Res.* **2007**, *40*, 343-350.

51. Dansby-Sparks, R.N. ; Ouyang, R.-Z.; Xue, Z.-L. *Sci. China Chem.* **2009**, *52*, 1777–1788.

52. Canada, T.A.; Xue, Z.-L. *Anal. Chem.* **2002**, *74*, 6073–6079.

Part 3

Thin Film Optical Sensors for the Detection of Trace Chloroform

Abstract

Optical thin film sensors have been developed to detect chloroform in aqueous and nonaqueous solutions. These sensors utilize modified Fujiwara reactions, one of the only known methods for detecting halogenated hydrocarbons in the visible spectrum. The modified Fujiwara reagents, 2,2'-dipyridyl and tetra-n-butyl ammonium hydroxide (Bu^n_4NOH or TBAH), are encapsulated in an ethyl cellulose (EC) or sol-gel film. Upon exposure of the EC sensor film to $HCCl_3$ in petroleum ether, a colored product is produced within the film, which is analyzed spectroscopically, yielding a detection limit of 0.830 ppm (v/v) and quantification limit of 2.77 ppm. In aqueous solution of $HCCl_3$, reaction in the sol-gel sensor film turns the sensor from colorless to dark yellow/brown with a detection limit of 500 ppm. To our knowledge, these are the first optical quality thin film sensors using Fujiwara reactions for halogenated hydrocarbon detection.

3.1. Introduction

Chlorinated hydrocarbons (CHCs) pose a serious threat to the environment. CHCs such as chloroform ($HCCl_3$)[1] are widely used in many industries as a solvent, refrigerant, and pesticide.[2,3] The extensive use and production of $HCCl_3$ is on the scale of thousands of tons per year worldwide which results in increased disposal of $HCCl_3$ into the environment in the form of aqueous wastes. One of the greatest concerns is that $HCCl_3$, with a solubility of 8.7(0.5) g/L or [5.8(0.3) x 10^3 μL/L] in water at 23-24 °C,[4] easily causes the pollution of groundwater and sediments. Generally, CHCs in low concentrations in air or in water can cause damage to the liver, kidneys, and central nervous system. Most CHCs, including $HCCl_3$, are also suspected carcinogens.[5-7] Moreover, it has been shown that organic solvents, such as $HCCl_3$ used in the manufacturing processes for drug products, are often not completely eliminated in the manufacturing process.[8-11] Thus, low levels of residual organic solvents are present in most pharmaceutical products. The acceptable level of $HCCl_3$ at 60 ppm in pharmaceuticals is given in guidelines issued by the International Conference on Harmonization (ICH).[8-11] Therefore, monitoring the concentration of $HCCl_3$ in groundwater and quality control of residual $HCCl_3$ in pharmaceutical samples is vital for the environment and the pharmaceutical industry.[11,12]

Several common methods have been established for $HCCl_3$ detection including GC-MS usually in tandem with preconcentration such as purge and trap, solid-phase microextraction (SPME), and headspace/SPME analysis.[13-19] While these methods provide sensitive and adequate detection limits, they often require relatively expensive, non-portable equipment and trained technicians. In addition, they are time consuming

and difficult to apply for on-site monitoring. There have been drives to develop a simple, direct, and low cost method to analyze $HCCl_3$ as an environmental pollutant as well as determining residual concentration in pharmaceuticals. Infrared spectroscopy has also been studied for CHC detection in water.[20-22]

Detection of CHCs in the visible range is generally based on Fujiwara reactions *in solution*.[23-28] The Fujiwara reaction for the spectroscopic detection of $HCCl_3$ was first reported in 1916 and originally relied on a two phase system consisting of an aqueous layer of NaOH along with a liquid pyridine layer to which $HCCl_3$ was added.[29] This mixture was then heated to give an intense red color that was monitored spectroscopically for $HCCl_3$ detection and quantification.

Many studies have modified the original Fujiwara procedure to a single phase system where the reaction relies on the use of excess pyridine for the detection and quantification of halogenated compounds.[25-28] However, pyridine itself is a toxic, offensive-smelling compound.[30-32] We have recently developed new alternative approaches using solid dipyridines (SDPs) such as 2,2'-dipyridyl, 4,4'-dipyridyl or 1,2-bis(4-pyridylethane) and a new base, tetra-n-butyl ammonium hydroxide (TBAH), for the detection of $HCCl_3$.[33] The mechanism for the modified Fujiwara reactions is described for trihalogenated hydrocarbons (HCX_3) and shown in Figure 3.1. First, a strong base removes the acidic proton in HCX_3 to yield a trihalogenated anion ($:CX_3^-$). This unstable anion loses a halide anion to give a reactive carbene species ($:CX_2$) that is able to react with dipyridine yielding a colored product.[34,35] *In nonaqueous solutions*, the reactions of CHCs with SDPs and TBAH give colored species with detection limits of 0.17 ppm for $HCCl_3$ using visible spectroscopy.[33] Although our earlier approach using

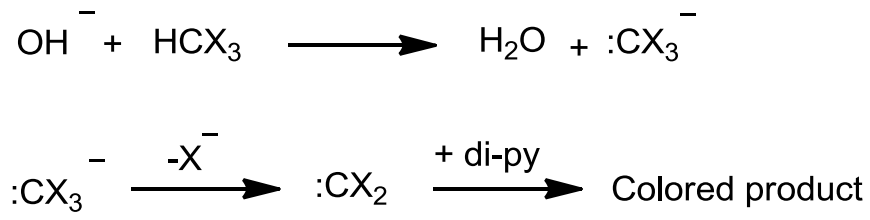

Figure 3.1. Modified Fujiwara reaction mechanism (di-py = dipyridine).

the modified Fujiwara reactions removed the requirement to use liquid pyridine, one major limitation is that the process is conducted in solution, specifically CHCs in THF solutions, using a cuvette (10 mm pathlength) and a spectrophotometer. It is more desirable to use optical thin film sensors that in part preconcentrate CHCs into the films to react with SDPs and the base, forming color products for CHC detection.

In this study, procedures have been developed to fabricate optical sensors encapsulating modified Fujiwara reagents (2,2'-dipyridyl and TBAH) to detect $HCCl_3$ in aqueous and nonaqueous solutions. Ethyl cellulose (EC) polymers and sol-gels were evaluated as the matrix for the optical sensors. Upon exposure to $HCCl_3$ the sensor produces a colored product which is visible to naked eyes or is analyzed using visible spectroscopy. Coupling spectroscopy to the sensors would allow for online monitoring and remote sensing applications. Optical thin film sensors have a great deal of versatility since they may be doped with a variety of different sensing agents, and are intrinsically easy to use and inexpensive to produce. The sol-gel-based sensor was designed for the analysis of $HCCl_3$ in water with a detection limit of 500 ppm. The color change of the sol-gel sensor could be monitored by naked eyes. The EC-based sensor was designed for the analysis of $HCCl_3$ in organic solvent and it demonstrates a linear response in the 5-500 ppm range with a detection limit of 0.830 ppm (v/v) and quantification limit of 2.77 ppm. To our knowledge, the current work represents the first optical thin film sensors based on Fujiwara reactions.

3.2. Methods

3.2.1. Chemical Reagents and Materials

Tetra-n-butylammonium hydroxide (TBAH, 40% v/v, Lancaster), tetraethoxysilane (TEOS, 99.9%, Alfa Aesar), methyltrimethoxysilane (MTMS, 97%, Acros), 3,3,3-trifluoropropyltrimethoxysilane (TFPTMOS, 98%, Gelest), Sufasil (Thermo Scientific™ Hydrocarbon-Soluble Siliconizing Fluid), 2,2'-dipyridyl (99%, Acros), acetylsalicylic acid (99%, Fischer Scientific), and ethyl cellulose (EC, 49% ethoxy content, MP biomedicals) were used as received. Solvents were purchased from Fischer Scientific and used as received. Standard microscope slides (Corning) were cut to 1 cm^2 rectangles and used as the sensor substrate. Solutions prepared using deionized (DI) water were prepared from a Barnstead International e-pure four-holder deionization system (18 MΩ cm).

3.2.2. Fabrication of Ethyl Cellulose and Sol-gel Films

A two-pronged approach was employed in developing sensor films to detect trace CHCs. The first approach was the use of polymer films to encapsulate the solid dipyridines and TBAH. Several polymers, including polystyrene (PS), poly(2-vinylpyridine), poly(4-vinylpyridine), and ethyl cellulose (EC), were tested. EC was found to be the best polymer to use as the matrix. EC is porous enough to allow organics to diffuse through the polymer and rigid enough to hold up under use. EC (~0.750 g) was dissolved into a mixture of toluene and EtOH (1:1) and sonicated for 4 h forming a viscous EC solution (7.5% wt EC). Approximately 1.5 g of EC solution was transferred

into a vial along with 0.85 g of 2,2'-dipyridyl and 200 µL of TBAH and stirred thoroughly for 1 h. This solution was directly pipetted onto glass substrates, drawn to the edges of the glass with a plastic pipette tip, and allowed to cure at 4 ^{o}C in a refrigerator overnight. In order to increase the amount of TBAH base in the system, the cured EC films were removed from the refrigerator after 12 h and an additional layer of TBAH in EC was pipetted onto the top of the EC films and spread across the surface with a plastic pipette tip. Then, the films were allowed to cure again at 4 ^{o}C overnight to allow the TBAH base to penetrate into the EC film.

The second approach was the use of sol-gel based materials. *It should be pointed that both 2,2'-dipyridyl and TBAH are bases, and sol-gel reactions, catalyzed by base, are highly sensitive to the presence of base. It is thus extremely challenging to place the two bases in a thin sol-gel film.* Sol-gel precursors TEOS (2 mL) and MTMS (1.5 mL) were mixed and added to 2 mL of ethanol. This solution was stirred thoroughly for 15 min and then 0.85 g of 2,2'-dipyridyl was added. The solution was stirred again for 30 min to ensure that dipyridyl was completely dissolved. Afterwards, 300 µL of H_2O was added to the sol-gel solution to allow the mixture to hydrolyze and 5 mL of TBAH was added dropwise to saturate the sol-gel solution with the base. The entire solution was allowed to stir again for another 30 min and then the solution was pipetted onto glass substrates and drawn to the edges of the glass with a plastic pipette tip. The films were then cured at 4 ^{o}C for 12–48 h to help prevent any cracking and allow the sol-gel sensors to harden, yielding crack-free transparent films.

In the case where moisture sensitive over-coatings were evaluated, 3,3,3-trifluoropropyltrimethoxysilane (TFPTMOS) and Surfasil were utilized. The sol-gel

precursor TFPTMOS was mixed in a 1:1 ratio with TEOS. H_2O (100 µL) and 1 M HCl (100 µL) were added to the solution and the mixture was stirred for 48 h to allow the over-coating sol-gel solution to hydrolyze. This over-coat solution was then pipetted directly onto the sol-gel sensors and allowed to cure at 4 ^oC overnight. SurfaSil was used as received and directly pipetted onto the sol-gel sensors and then allowed to cure at 4 ^oC overnight.

3.2.3. Analyte Exposure and Instrumentation

Different concentrations of $HCCl_3$ were made by diluting $HCCl_3$ to the appropriate concentration with either petroleum ether, pentane, or DI water. Sensors were submerged into their respective vials containing 20 mL of varying chlorforom concentrations. After satisfactory analysis time, the sensors were taken out of their vials and analyzed using visible spectrometry.

An Agilent 8453 UV-Vis spectrometer using two light sources, a deuterium and tungsten lamp, was used to acquire absorbance spectra of the sensing films. A quartz cuvette with a 1 cm pathlength was utilized to hold the sensor in place. A blank glass substrate was then placed in the cuvette along with solution that did not contain CHC and this was used as the blank for the visible spectra. To reduce the noise from the visible spectrometer, data were collected by filling the cuvette with each sensor's respective analyte solution along with the sensor standing up in the cuvette. Spectra were taken at several different areas of the sensor in order to obtain a good representation of the sensor film. Spectra were recorded in the range from 190 cm^{-1} to 1100 cm^{-1}. Data smoothing, peak deconvolution, and baseline correction were

achieved through Origin Pro 8.1 software. SEM images of the sol-gel and EC sensors were taken using a Zeiss Auriga Scanning Electron Microscope.

A Hewlett Packard HP 6890 Series GC system equipped with a HP 5973 Mass Spectrometer was used for GC-MS measurements. Gas chromotagraphy was carried out in a 30.0 m x 250 µm i.d. x 0.25 µm thick capillary column. Helium was used as the carrier gas with a constant flow rate of 0.8 mL min^{-1}. The initial temperature was set at 30 ^{o}C and held for 3 min, ramped at 10 ^{o}C up to 100 ^{o}C, and a second rate at 15 ^{o}C up to 250 ^{o}C.

3.3. Results and Discussion

3.3.1. EC Sensor Characterization and Response

For the Fujiwara reaction to generate a colored product within the sensing film, the concentration of dipyridyl and TBAH need to be maximized. Spin-coating or dip-coating techniques are widely used in fabricating thin films onto glass substrates. In the currenty studies, these techniques produce uniform thin films but are not effective in retaining the dipyridyl and TBAH reagents needed to produce a distinct colored product in the film at low concentrations. Therefore, the EC solution was directly pipetted onto glass substrates to improve the amount of reagents in each film fabricated. The resulting sensor film is thicker but more responsive. SEM measurements show a “porous pitting” feature in the EC films that is consistent with the phase separation during the processing of the sensor (Figure 3.2). This also enlarges the surface area of the sensor, thus improving its sensivitity. The thickness of the EC film as measured by

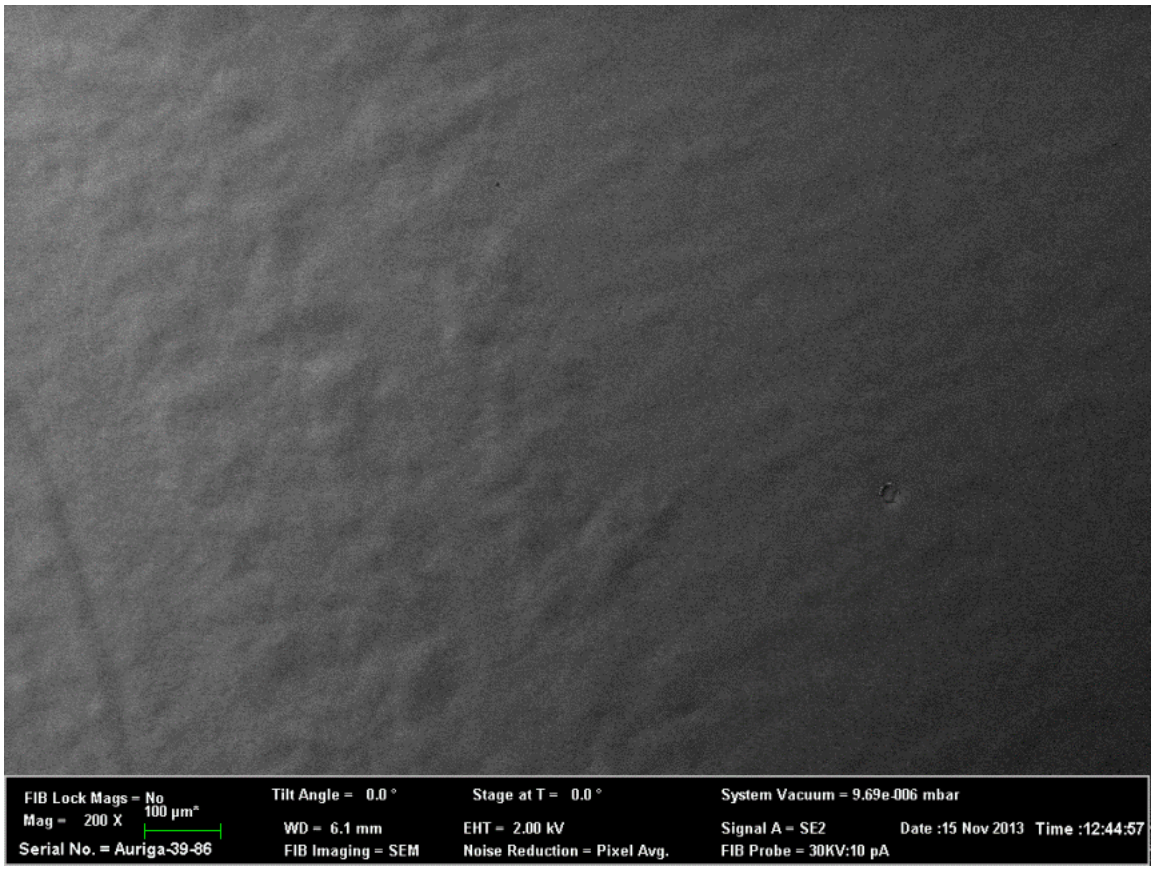

Figure 3.2. SEM image of the EC sensor surface.

SEM imaging was found in the range of 5–10 µm. The addition of an extra layer of TBAH onto the EC sensor and letting TBAH penetrate into the film increased the sensitivity of the EC sensor as well. However, it was found that storing these EC sensors under open atmosphere significantly diminished the sensor's ability to form a colored product when exposed to $HCCl_3$. This is most likely due to the slow neutralization of TBAH by acidic CO_2 in open air. The best results came from storing the sensors at 4 ^oC or under nitrogen.

Exposing the EC sensors to different concentrations of $HCCl_3$ in aqueous solutions did not produce a colored product within the sensing film. When excess aqueous solution is present, it may compete with the bipyridine for the carbene intermediate, decomposing $:CX_2$ before it reacts with the dipyridine to give the colored product in the Fujiwara reaction.[33] Overcoatings applied to this sensor were unsuccessful in providing a colored product. However, a colored product was observed (Figure 3.3) within the EC sesnsor in nonaqueous solution (petroleum ether, pentane) with a response time of approximately 1 h at concentrations ranging from 5 to 500 ppm $HCCl_3$. A distinct peak around 430–450 nm was observed in the visible spectra for the EC sensors which correlates with the colored product from the Fujiwara reaction. This peak intensity decreased with decreasing concentrations of $HCCl_3$, as shown in Figure 3.4. Using this peak, a calibration curve was created with $R^2 = 0.9978$ (Figure 3.5). The limit of detection (3σ) for the sensor was found to be 0.830 ppm and the limit of quantification (10σ) 2.77 ppm. Several additional $HCCl_3$ concentrations were tested by spiking nonaqueous solutions and measuring these with the EC sensors. The data were overlaid onto the calibration curve in Figure 3.5. The data from the spiked

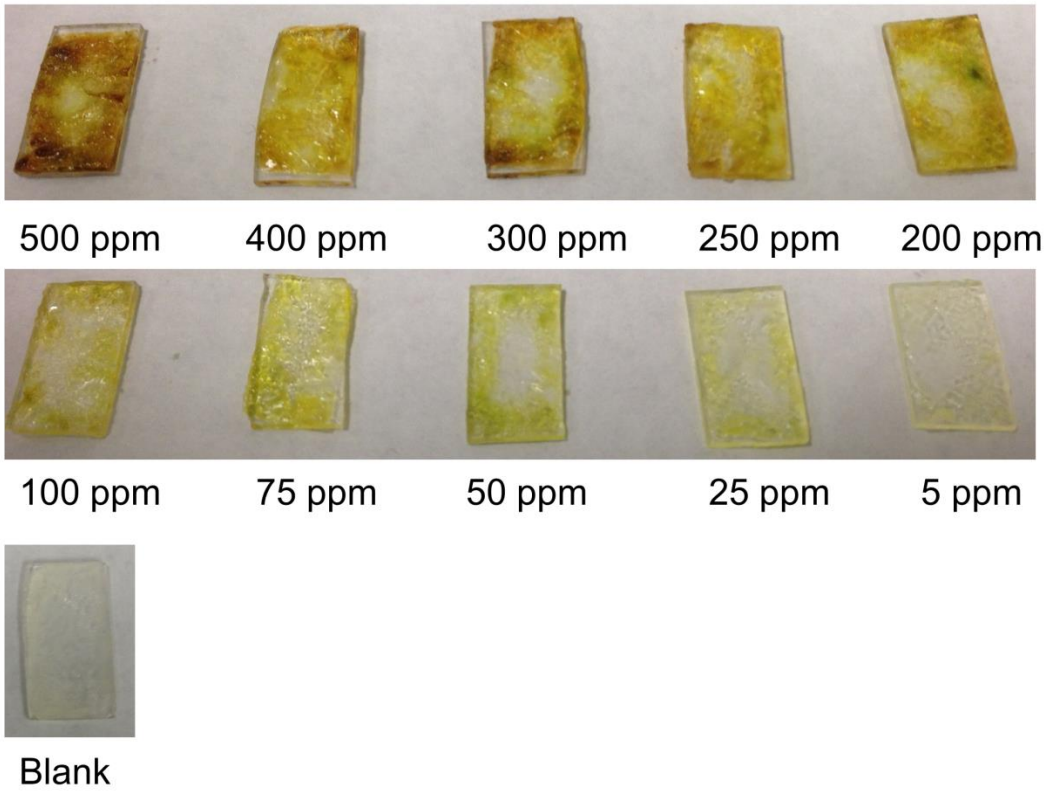

Figure 3.3. $HCCl_3$ concentrations ranging from 5 to 500 ppm and the resulting colored product from the Fujiwara reaction.

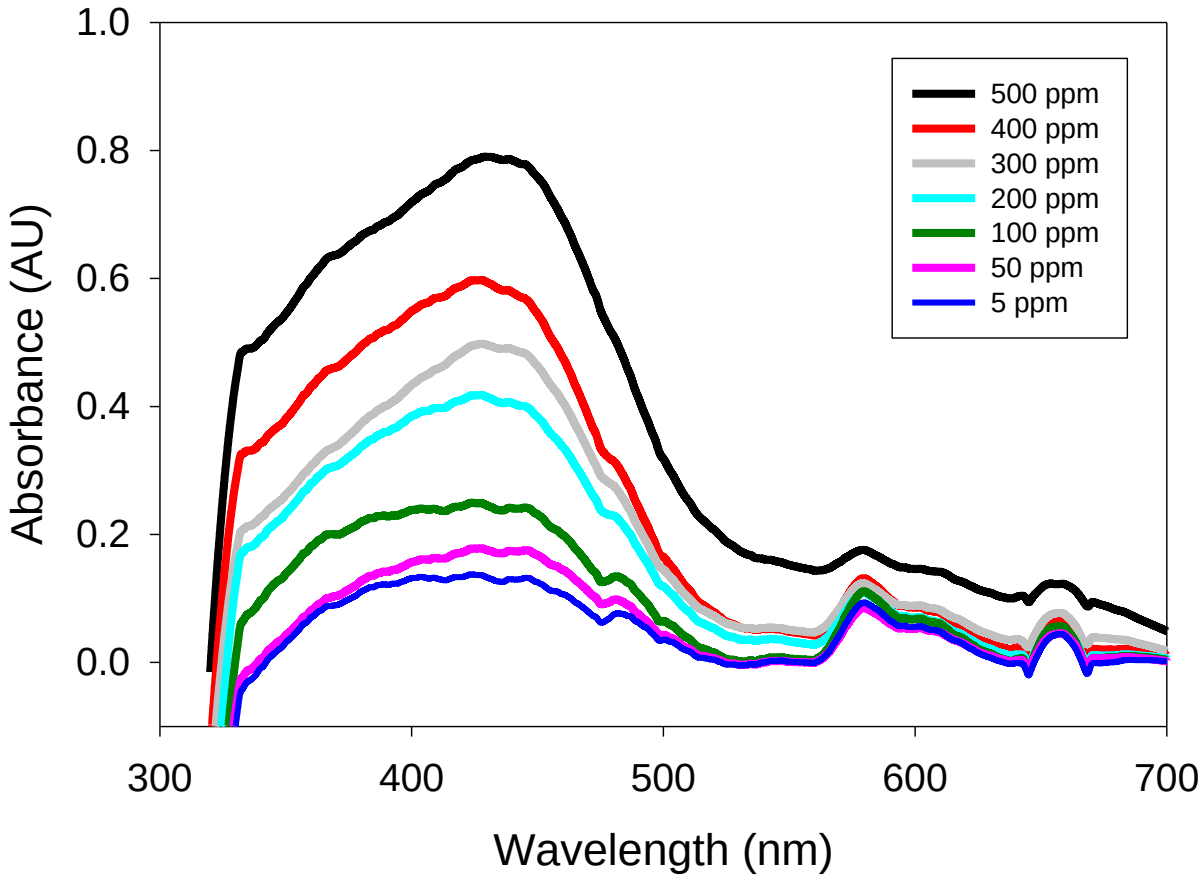

Figure 3.4. Visible spectra showing a decrease in absorbance at approximately 430–450 nm with decreasing $HCCl_3$ concentrations.

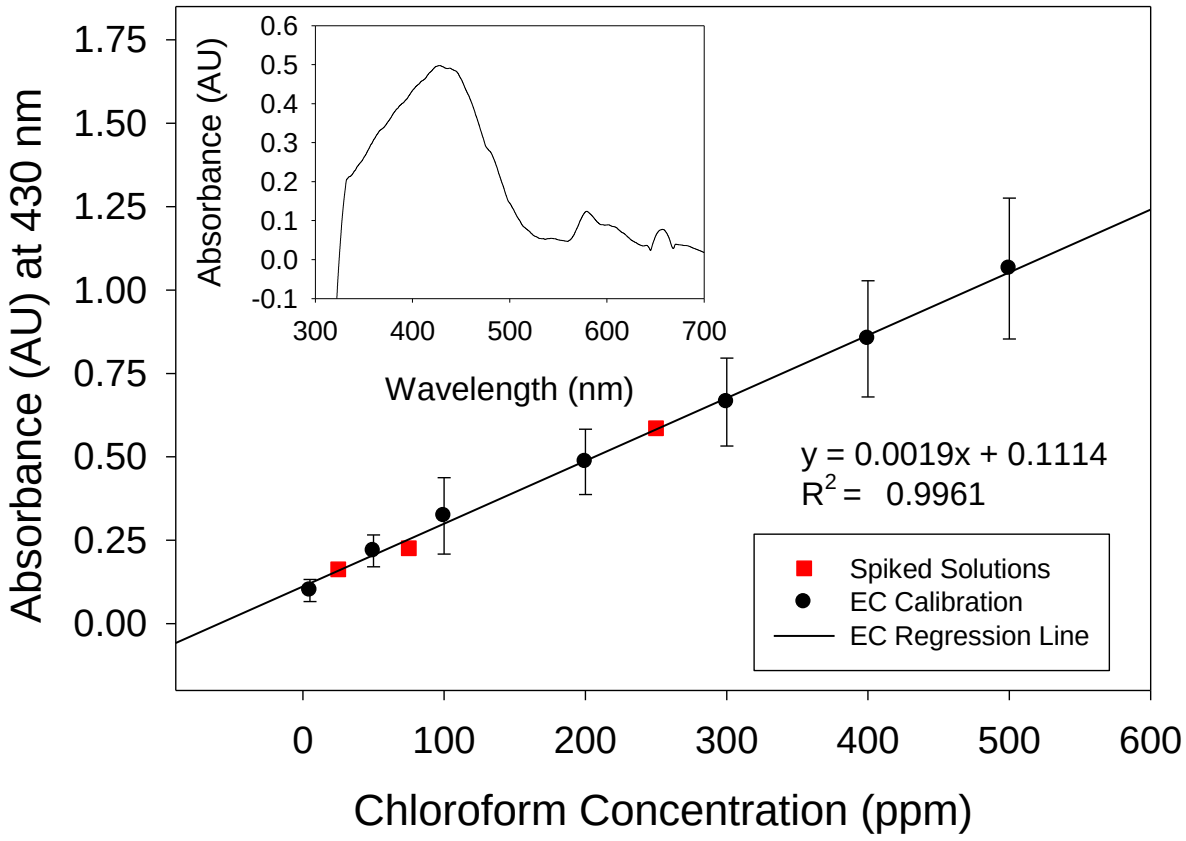

Figure 3.5. Calibration plot of the EC sensor using $HCCl_3$ standards with spiked standards overlaid onto the plot. Inset shows a standard visible spectrum of the sensor from 320–700 nm.

samples fall within the standard error of the EC calibration curve. For example, a 250 ppm $HCCl_3$ sample was evaluated by the EC sensor. Using its absorbance value at 430–450 nm and the calibration data, the sensor gave the concentration of 249.6(3) ppm with 0.12% error. The results here were compared below to GC-MS analysis on the same analyte samples to verify the validity and reliability of the calibration plot established by the standards and EC sensors. These sensors may provide an effective method for the direct determination of $HCCl_3$ with applications as a qualitative and quantitative disposable sensor.

3.3.2. Comparison of the $HCCl_3$ Measurements by the EC Sensor with Those by GC-MS

A comparison of GC-MS and optical sensing was conducted for $HCCl_3$ detection. While detection methods for $HCCl_3$ using GC-MS rely on a preconcentration step such as a purge and trap on a sorbent in order to achieve adequate sensitivity and detection limits,[13-19] this study focused on measurements using GC-MS without preconcentration to compare the results with the direct response of our optical sensors coupled to a visible spectrometer. The same $HCCl_3$ solution samples (5-400 ppm) to test the EC sensor was used here in the GC-MS measurements. $HCCl_3$ concentrations below 5 ppm did not display a discernable peak that could be verified with MS and were thus not taken into account for analysis. With the parameters set for the GC-MS, the resulting chromatogram displays a peak for $HCCl_3$ at 2.4–2.7 min retention time for each concentration (Figure 3.6). This peak was analyzed using MS and was verified as $HCCl_3$. It was observed that the integration of each peak area was proportional to the

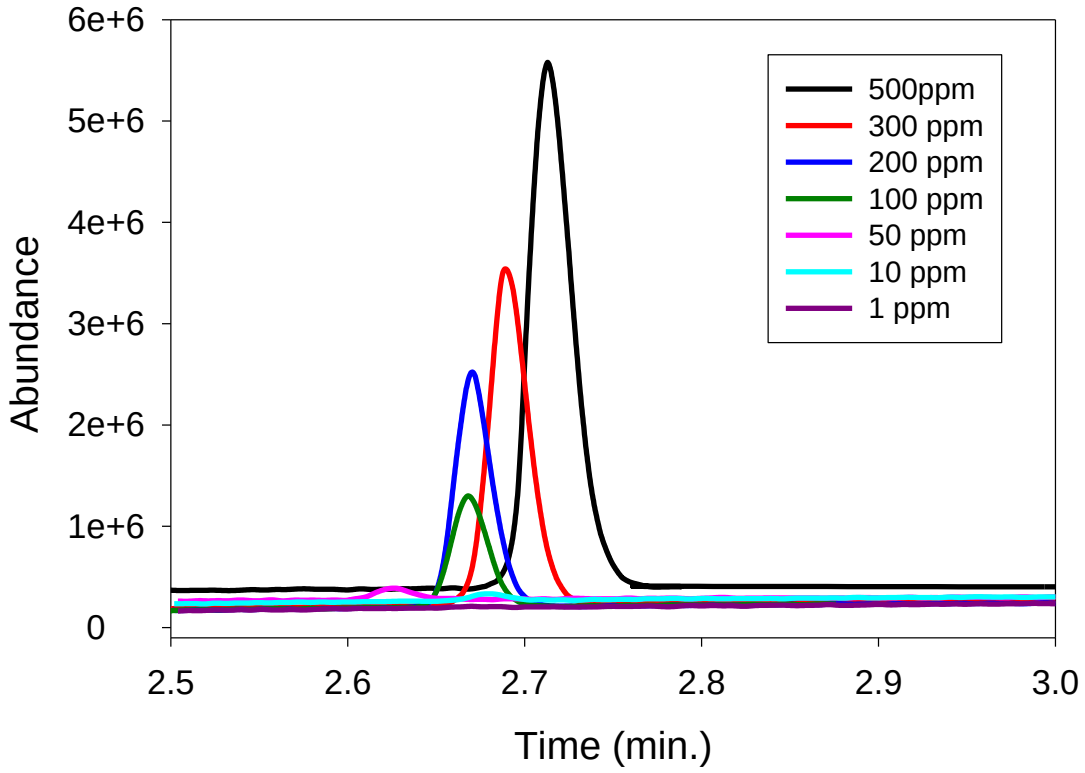

Figure 3.6. Chromatogram displaying the various concentrations of $HCCl_3$ peaks at 2.4–2.7 min retention time.

concentration of $HCCl_3$ analyte. A calibration plot was created showing good linearity for the analysis using GC-MS with $R^2 = 0.995$ (Figure 3.7). Additional $HCCl_3$ concentrations were evaluated by spiking the pentane solution. These measurements were overlaid onto the calibration plot as well. This data fell within the standard error for the GC-MS calibration plot. Samples of 250, 75, and 25 ppm showed a 4.69%, 6.89%, and 3.66% error respectively. Table 3.1 gives the comparison of GC-MS and optical sensors for the spiked $HCCl_3$ samples. This comparison shows that our optical sensor is able to correctly determine higher $HCCl_3$ concentration (250 ppm) more accurately than the GC-MS but does not accurately outperform the GC-MS in determining $HCCl_3$ concentrations at lower concentrations (75 and 25 ppm). Without a preconcentration step, the calculated limit of detection for the GC-MS method was found to be 80 ppb and limit of quantification 267 ppb. However, these results confirm that our EC optical sensors give the correct $HCCl_3$ concentrations and thus may be used as a direct qualitative and quantitative sensor for $HCCl_3$ analysis.

Table 3.1. Comparison of GC-MS and EC Sensors Detecting Spiked Solutions of 250, 75, and 25 ppm $HCCl_3$.

	250 ppm	**75 ppm**	**25 ppm**	R^2
GC-MS (% Error)	4.69%	6.89%	3.66%	0.9977
EC Sensors (% Error)	0.12%	10.83%	5.16%	0.9961

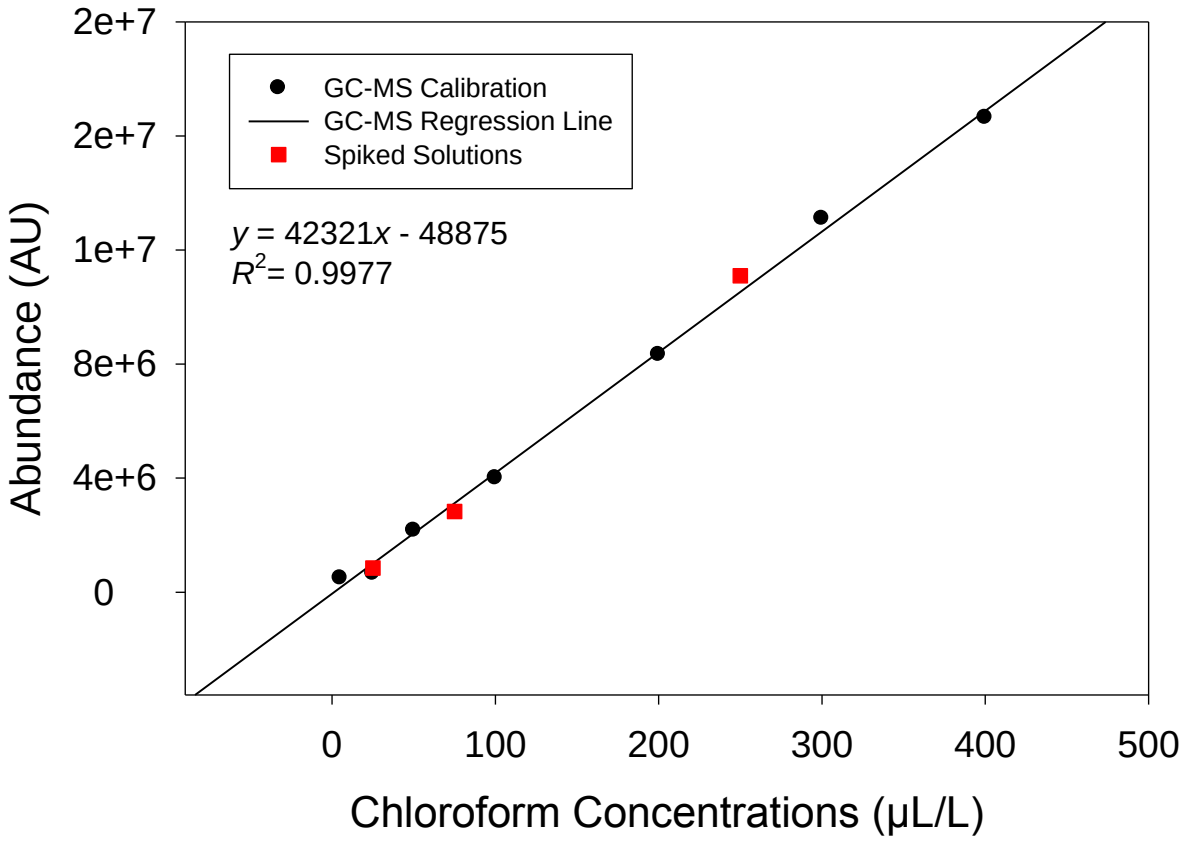

Figure 3.7. GC-MS calibration plot of $HCCl_3$ standard samples ranging from 5–400 ppm (v/v) with spiked samples overlaid onto the plot.

3.3.3. Application in a Pharmaceutical Sample

The analytical reliability and application potential for the proposed method was evaluated by measuring residual $HCCl_3$ in nonaqueos sample solutions containing acetylsalicylic acid, an active pharmaceutical ingredient (API) of aspirin. Prior to the analysis, 100 mg of acetylsalicylic acid, a low dosage amount of API in aspirin, was dissolved in minimal THF and transferred to a nonaqueous sample containing residual $HCCl_3$ ranging from 20 to 500 ppm. The EC sensors were then exposed to each sample solution and spectroscopic measurements were performed to evaluate the colored product produced within the sensing film layer. A well defined peak around 440 nm was observed and shown to increase proportionally with the $HCCl_3$ concentrations (Figure 3.8). This indicates the successful use of the proposed method for the detection of residual $HCCl_3$ in a pharmaceutical sample. The API did not cause any obvious interference in the performance of the EC sensor, and the sensor showed good sensitivity to detect below the concentration limit of $HCCl_3$ (60 ppm) allowed in a pharmaceutical.

3.3.4. Sol-gel Sensor Characterization and Response

For our sol-gel sensor, it was found that saturating the sol-gel solution with 5 mL of TBAH served two purposes. This amount of TBAH helped to base-catalyze the sol-gel solution and left an adequate amount of TBAH in solution to interact with the dipyridyl and $HCCl_3$ analyte. An additional benefit from base-catalyzed sol-gel films is that they tend to have greater porosity due to the formation of highly condensed particulate sols and thus have larger diffusion rates and more surface area to interact

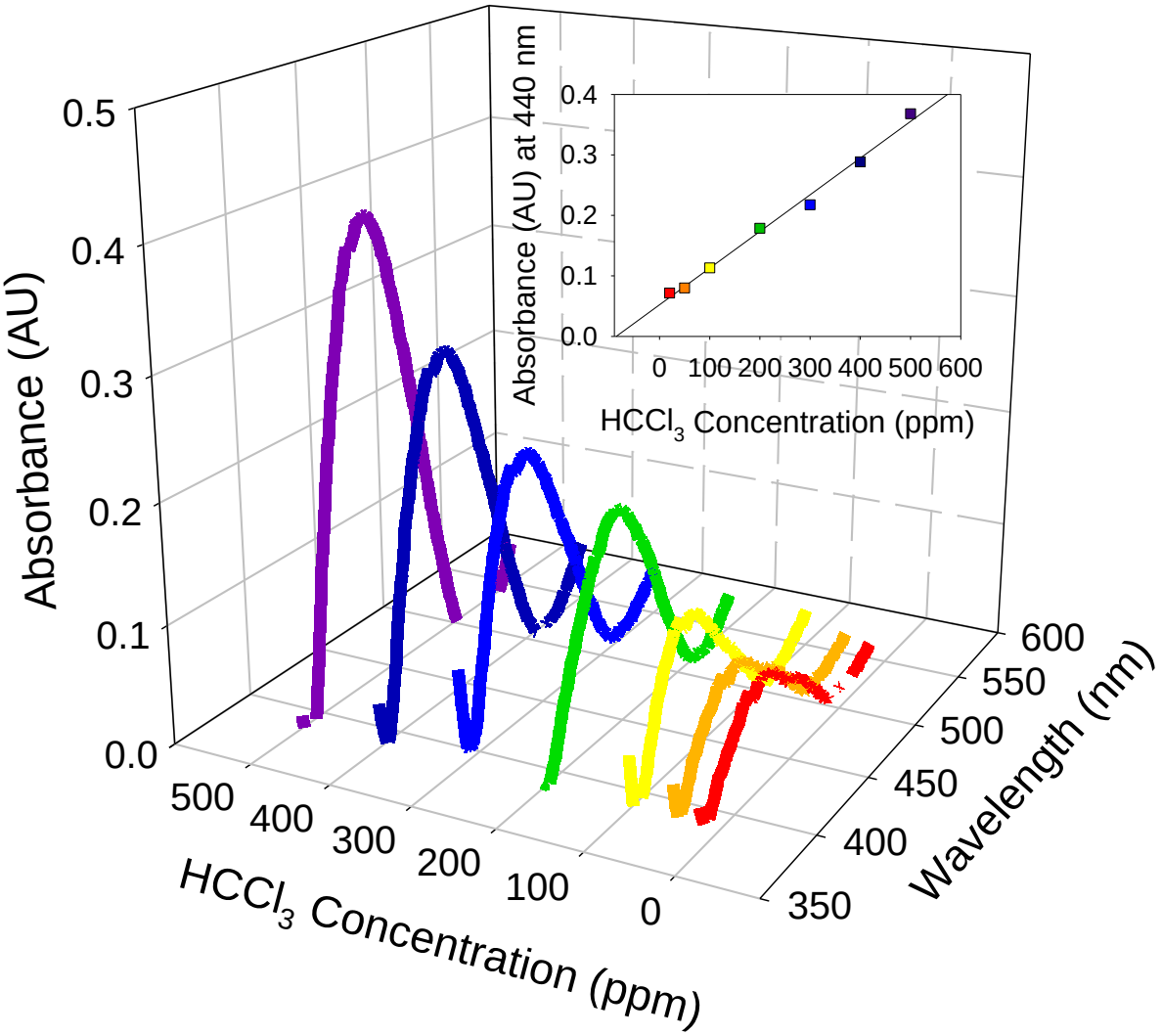

Figure 3.8. Visible spectra of nonaqueous samples with residual $HCCl_3$ ranging from 20 to 500 ppm in the presence of an API.

within the sensing layer to produce a response.[36-37] The sol-gel solution was directly pipetted onto glass substrates and cured under the same conditions as the EC sensors above. Surfasil and TFPTMOS were evaluated as moisture sensitive over-coatings to protect the sol-gel sensors in aqueuos solutions. The use of Surfasil ontop of the sensor caused the sensor to lose a significant degree of optical quality as did TFPTMOS to a lesser extent. SEM images of the sol-gel sensors show a fairly uniform coating on the surface with some structural defects, possibly due to contractions of the film during the curing process (Figure 3.9A) and at higher magnification, SEM images show the encapsulation of the solid dipyridyl (Figure 3.9B). The thickness of the sol-gel sensors as measured by SEM imaging ranged from 9 to 18 µm. Compared to the EC sensors, the sol-gel sensors had a slightly thicker film most likely due to the additional moisture sensitive over-coating applied to the sol-gels.

The sol-gel sensors were evaluated under excess aqueous solutions and found to show a dinstinct colored product in solutions of diluted $HCCl_3$. As previously reported,[38] the Fujiwara reaction must be conducted in a low moisture environment but when an excess amount of water is present, the reaction is inhibited and there is no formation of a colored product in the solution. However, in this study the addition of Surfasil and TFPTMOS allow a moisture proof over-coating that appears to have prevented water from entering the sol-gel sensor while allowing organics, $HCCl_3$, to diffuse within the sensor producing a colored product from the Fujiwara reaction. In the sol-gel sensors, a distinct colored product was detected in concentrations ranging from 625 to 7000 ppm, yielding a detection limit of 500 ppm. However, it was found that the optical quality is reduced from the over-coatings, causing a large amount of

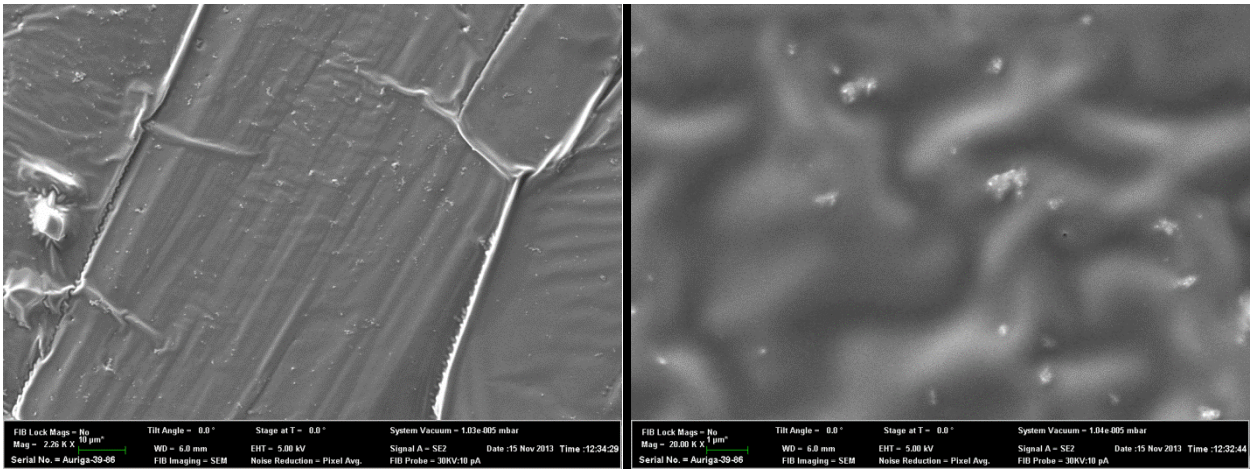

Figure 3.9. (A) SEM surface images of the sol-gel sensors; (B) Higher magnification image showing the encapsulation of the dipyridyl.

scattering. Several samples that were tested provided broad shoulder spectrums instead of clear peaks (Figure 3.10). The sol-gel sensor is, however, adequate for $HCCl_3$ detection at ≥500 ppm that is significantly lower than the solubility (8,700 ppm) of $HCCl_3$ in water. To our knowledge, the approach described here provides the first optical sensors for qualitative and direct detection of a halogenated hydrocarbon compound using the Fujiwara reaction in aqueous solutions.

The in-depth testing showed that the amount of base in the sol-gel reactions was crucial in obtaining a colored product using the Fujiwara reactions. It was determined that the sol-gel solutions should be saturated with (Bu^n_4NOH, TBAH) in order to provide the best opportunity for the resulting sol-gel sensors to react with $HCCl_3$. In addition, the sol-gel solutions should contain as much solid pyridine derivative as possible. These approach lead to optically transparent thin film sensors (Figure 3.11).

3.4. Conclusion

The optical sensors developed in this work utilizing the modified Fujiwara reaction in the EC thin films have proved to be useful for $HCCl_3$ detection in organic solution with a detection limit of 0.83 ppm and quantification limit of 2.77 ppm. Calibrations from the EC sensor resulted in good linearity in nonaqueous solutions, demonstrating the use of the sensor as a qualitative and quantitative sensor. The sol-gel method presented in this study gives the first optical sensor based on the Fujiwara reaction to qualitatively detect CHCs in an aqueous solution. The sensors are easy to fabricate and inexpensive. The EC sensor may be coupled to visible spectroscopy and/or with a fiber optic bundle for direct measurement studies in the field for

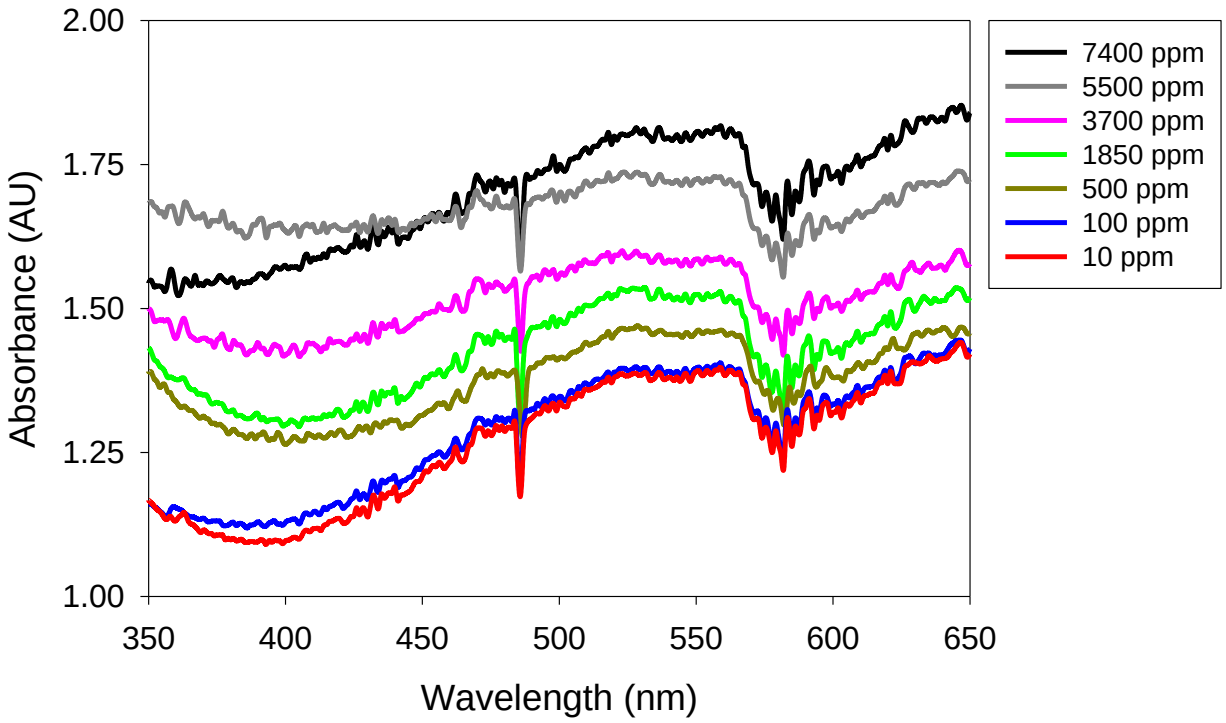

Figure 3.10. Visible spectra showing the large broad shoulder from 500 to 550 nm in the sol-gel sensors.

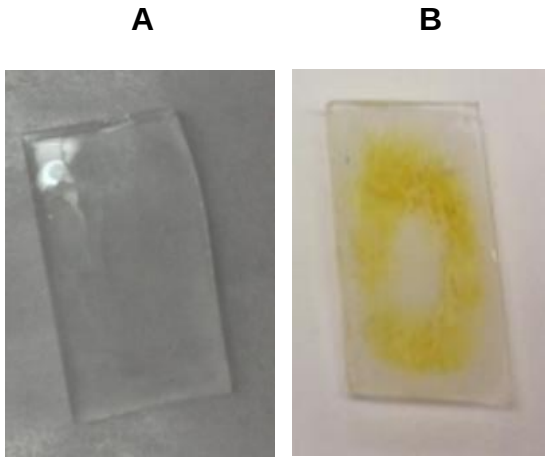

Figure 3.11. (A) Sol-gel sensor where the solution was directly pipetted upon the glass substrate and allowed to cure in the refrigerator to prevent cracking; (B) Sol-gel sensor after exposure to 625 ppm aqueous $HCCl_3$ solution.

pharmaceuticals or water quality.

References

1. Holbrook, M.J. *Kirk-Othmer Encyclopedia of Chemical Technology*, 5th ed., Wiley, New York, 2004, pp. 279–290.
2. Rossberg, M.; Lendle, W.; Pfleiderer, G.; Tögel, A.; Dreher, E.-L.; Langer, E.; Rassaerts, H.; Kleinschmidt, P.; Strack, H.; Cook, R.; Beck, U.; Lipper, K.-A.; Torkelson, T.R.; Löser, E.; Beutel, K.K.; Mann, T. *Ullmann's Encyclopedia of Industrial Chemistry*, Wiley, 2006 pp. 1–186.
3. Petrelli, G.; Siepi, G.; Miligi, l.; Vineis, P. *Scand. J. Work Environ. Health*. **1993**, *19*, 63–65.
4. K. Broholm, S. Feenstra, *Environ. Toxicol. Chem*. 1995, *14*, 9-15.
5. *U.S. Code of Federal Regulations, Occupational Safety and Health Standards on Toxic and Hazardous Substances,* 29 CFR 1910.1000, Tables Z-1, Z-2, and Z-3.
6. US EPA Seminar Publication. Chapter 3. EPA/625/R-93/002.
7. Ferguson, J.F.; Pietary, J.M.H. *Environ. Pollut.* **2000**, *107*, 209–215.
8. Vali, S.J.; Garg, L.K.; Sait. S.S. *J. Chem. Pharm. Res*. **2012**, *4*, 4312–4218.
9. Grodowska, K.; Parczewski, A. *Acta Pol. Pharm*. **2010**, *67*, 3–12.
10. Jacobs, P.; Dewé, W.; Flament, A.; Gibella, M.; Ceccato, A. *J. Pharmaceut Biomed.* **2006**, *40*, 294–304.
11. Klick, S.; Sköld, A.*J. Pharmaceut Biomed.* **2004**, *36*, 401–409.
12. McCulloch, A. *Chemosphere*. **2003**, *50*, 1291–1308.
13. Martínez, E.; Lacorte, S.; Llobet, I.; Viana, P.; Barceló, D. *J. Chromatogr. A.* **2002**, *959*, 181–190.

14. Huybrechts, T.; Dewulf, J.; Moerman, O.; Van Langenhove, H. *J. Chromatogr. A.* **2000**, *893*, 367–382.

15. Alonso, A.; Fernández-Torroba, M.A.; Tena, M.T.; Pons, B. *Chromatographia*. **2003**, *57*, 369–378.

16. Lara-Gonzalo, A.; Sánchez-Uría, J.E.; Segovia-García, E.; Sanz-Medel, A. *Talanta*. **2008**, *74*, 1455–1462.

17. Flórez Menéndez, J.C.; Fernández Sánchez, M.L.; Sánchez Urıa, J.E.; Fernández Martınez, E.; Sanz-Medel, A. *Anal. Chim. Acta.* **2000**, *415*, 9–20.

18. Wang, Z.; Li, K.; Fingas, M.; Sigouin, L.; Menard, L. *J. Chromatogr. A.* **2002**, *971*, 173–184.

19. Plummer, L.N.; Busenberg, E.; Eberts, S.M.; Bexfield, L.M.; Brown, C.J.; Fahlquist, L.S.; Katz, B.G.; Landon, M.K. *J. Hydrol. Eng.* **2008**, *13*, 1049–1068.

20. Silva, A.M.S.; de A. Viana, E.; Pimentel, M.F.; Almeida, Y.; Raimundo Jr, I.M. *J. Brazil Chem. Soc.* **2011**, *22*, 1470–1477.

21. Jakusch, M.; Mizaikoff, B.; Kellner, R.; Katzir, A. *Sensor Actuat. B-Chem.* **1997**, *38*, 83–87.

22. Mizaikoff, B. *Anal. Chem.* **2003**, *75*, 258–267.

23. Bhattacharjee, M.; Cherian, L.; Gupta, V.K. *Microchem. J.* **1991**, *43*, 109–111.

24. Pillai, A. K.; Rastogi, R.; Gupta, V.K. *Indian J. Chem. Techn.* **1999**, *6*, 294-296.

25. Milanovich, F.P.; Brown, S.B.; Colston, B.W.; Daley, P.F.; Langry, K.C. *Talanta*. **1994**, *41*, 2189–2194.

26. Zavar, M.H.A.; Rounaghi, G.H.; Chamsaz, M.; Ashraf, N. *Asian J. Chem*. **2009**, *21*, 2903–2910.

27. Luo, W.; Chen, Z.; Zhu, L.; Chen, F.; Wang, L.; Tang, H. *Anal. Chim. Acta*. **2007**, *588*, 117–122.

28. Carrington, N.A.; Rodman, D.L.; Goswami, K.; Xue, Z.-L. *J. Appl. Polym. Sci*. **2007**, *104*, 1043–1048.

29. Fujiwara, K. *Sitz. Nat. Ges. Rostock.* **1916**, *6*, 33–43.

30. The health rating for pyridine in the Materials Safety Data Sheet: 3-Severe (Life) (http://www.jtbaker.com/msds/englishhtml/P7456.htm).

31. *Toxicological Profile for Pyridine*, Agency for Toxic Substances and Disease Registry, U.S. Public Health Service, 1992. http://www.atsdr.cdc.gov/toxprofiles/tp52.pdf.

32. *The Safe Drinking Water and Toxic Enforcement Act of 1986* (http://www.oehha.ca.gov/prop65/out_of_date/51702notice.html), The Office of Environmental Health Hazard Assessment of the California Environmental Protection Agency.

33. Rodman, D.L.; Carrington, N.A.; Qiu, H.; Goswami, K.; Xue, Z.-L. *Anal. Chim. Acta*. **2005**, *548*, 143–147.

34. Uno, T.; Okumura, K.; Kuroda, Y. *J. Org. Chem*. **1981**, *46*, 3175–3178.

35. Kofron, W.G.; Kirby, F.B.; Hauser, C.R. *J. Org. Chem*. **1963**, *28*, 873–875.

36. Dansby-Sparks, R.N.; Jin, J.; Mechery, S.J.; Sampathkumaran, U.; Owen, T.W.; Yu, B.D.; Goswami, K.; Hong, K.; Grant, J.; Xue, Z.-L. *Anal. Chem*. **2010**, *82*, 593–600.

37. Allain, L.R.; Sorasaenee, K.; Xue, Z.-L. *Anal. Chem*. **1997**, *69*, 3076–3080.

38. Hine, J. *J. Am. Chem. Soc*. **1950**, *72*, 2438–2445.

Part 4

Fluorescent-dye Doped Thin-film Sensors for the Highly Sensitive Detection of Alcohol Vapors

Abstract

Fluorescence sensors based on a trifluoroacetophenone compound doped in ethyl cellulose (EC) thin films have been developed for the detection of methanol, ethanol, and 2-propanol (isopropanol, Pr^iOH) vapors. Thin-film sensors are prepared with 4-dibutylamino-4′-(trifluoroacetyl)stilbene (Chromoionophore IX or CIX) as the fluorescent dye and its solution in EC was spin-coated onto glass slides. The luminescence intensity of the dye (555 nm) is quenched when exposed to alcohol vapor. Tested in the range of ca. 0–1.5 x 10^4 ppm (wt) for MeOH and EtOH, and ca. 0–2.3 x 10^4 ppm for Pr^iOH, the sensors gave detection limits of 9, 13, 21 ppm and quantification limits of 32, 43, and 70 ppm, respectively. To enhance the sensitivity of the sensors, TiO_2 particles have been added to the films to induce Mie scattering, which increases the incident light interaction with the sensing films. The sensors in this work have been designed to work in a multianalyte platform for the simultaneous detection of multiple gas analytes.

4.1. Introduction

Alcohol vapor detection is an area of intense interest. At the John C. Stennis Space Center (SSC) in Mississippi, the leading NASA testing facility for liquid fuel rocket testing and certification, there are a variety of ground test sensing needs including chemical sensors for isopropyl alcohol (Pr^iOH) vapor.[1] A rocket engine called the J-2X, created back in 2007 by NASA, was unique in that it could start up in atmosphere and vacuum conditions.[1] In order to test the J-2X engine's abilities, a new A-3 test stand was started back in 2007 with the purpose of simulating vacuum conditions. Chemical steam generators were used to generate a vacuum environment with steam being generated through the combustion of Pr^iOH, liquid oxygen (LOX), and water to produce approximately 2100 kg/s of steam.[1,2] NASA desired techniques for near-real time detection that was miniaturized and suitable for remote chemical detection of Pr^iOH in these test plumes generated from chemical steam generators. Valuable information regarding the efficiency as well as information on the environmental impact of these chemical steam generators could be obtained by placing working sensors in different locations around the plume for spatial and temporal responses. Initial work on optical sensors for the detection of Pr^iOH is discussed in this chapter. The ultimate goal is to develop sensors for various test plume constituents that could be incorporated into a miniaturized multi-analyte testing device for the simultaneous detection of different plume constituents.

While the importance of Pr^iOH vapor detection has been stated, interest can also be extended to other alcohol vapors such as methanol (MeOH) and ethanol (EtOH). Since fossil fuels are not a renewable source of energy, the need for promising

alternatives such as alcohols has steadily increased in demand. Fuels heavily blended with ethanol have shown promise in the automotive industry.[3] In addition, methanol has been actively studied in fuel cell technologies.[4] However, the increasing use of methanol for fuel cells may lead to the greater exposure of methanol vapors to the general public due to, e.g., unburned fuel in the form of exhaust or from evaporation during refueling.[3] Methanol vapor can cause nausea, headaches, and even blindness.[5-7] In 2002, an experimental physicist developed Parkinson's disease from the delayed toxic effect of long term exposure to methanol vapors without showing any signs of acute toxicity.[8] While ethanol is a renewable energy source, it is known to be corrosive to stainless steel and other metals/alloys,[8,9] and more studies on ethanol gas tank corrosion are required. Since ethanol and gasoline have different physical and thermodynamic properties, engines in vehicles, especially flex fuel vehicles, need to be optimized for performance accordingly.[10] Ethanol has a lower vapor pressure than gasoline which could lead to potential cold start engine problems particularly in flex fuel vehicles.[11] These issues establish a need for a sensor to detect a variety of alcohol vapor analytes.

Methods developed to sense alcohol vapor are largely based on the solvatochromatic effect (or their physical changes inside the sensor matrices). Stevens and Akins have developed a fluorescence sensor using the dye Coumarin 481 specifically for methanol vapor at 150 ppm.[12] The sensor in that study displays fluorescence quenching upon exposure to methanol as a result of physical changes inside the sensor matrix. However, the fluorescence intensity is not fully recoverable possibly because of an irreversible morphological change in the film.[12] Bangalore and

coworkers have shown that detection of methanol vapor from 400 to 7000 ppm in air can be accomplished by open path FT-IR spectroscopy, but this method requires quite bulky and expensive instruments that are not field deployable.[13] Pang and coworkers have used the sol-gel method to fabricate a planar waveguide ring resonator sensitive to ethanol with spectral dips that are red shifted when exposed to ethanol.[14] However, this technique has a small dynamic range (0–160 ppm) and the sensitivity of the resonant wavelength may be detected more precisely by spectroscopy than from loss measurements.[14] Hunter and coworkers have developed a technique for the measurement of ethanol concentrations in aqueous mixtures with a detection limit of 40 ppm, in which ethanol vapor is transported by a permeable membrane to a microelectromechanical (MEMS) chemi-capacitor array.[15] The dielectric constant of a polymeric material in the micro-capacitors increased upon absorption of ethanol vapor, leading to the measurement. There has been ongoing and continued research in the field of alcohol detection such as miniature GC[16] and bioelectronic gas sensors (biosniffers)[17] to improve and advance alcohol analyzers based on other methods. All of the aforementioned techniques are based on physical (rather than chemical) detection methods.

Currently optical sensors have been convenient to use for a variety of analytes because of its cost effectiveness, easy of production, and can be made into disposable chemical sensors if required. Mohr and coworkers have produced an optical sensor for alcohols using a synthesized fluorescent compound Chromoionophore IX (CIX) prepared in a poly(vinyl chloride) (PVC) membrane for the detection of alcohols *in the*

liquid phase.[18-20] We have adapted and developed sensors based on the fluorescence of CIX for the detection of methanol, ethanol, and 2-propanol *in the gas phase*.

With the goal of detecting various alcohols in the gas phase, optical sensors were developed using an ethyl cellulose (EC) thin-film matrix to encapsulate the dye in our studies. Their preparation has been optimized to produce highly sensitive sensors for alcohol vapors. TiO_2 particles were used in the sensor films to induce Mie scattering, which increased the incident light interaction with the sensing films, and enhanced the sensitivity of the sensor.[21] The sensors show fast and reversible responses. The optical sensors have also been designed to function in a multianalyte platform for the simultaneous detection of multiple gas analytes. The studies here follow our earlier work in the development of optical sensors for chemicals in both liquid and gas phases.[22-28]

4.2. Experimental

4.2.1. Chemical Reagents and Materials

Ethyl cellulose (49% ethoxy content, MP Biomedicals), tridodecylmethylammonium chloride (TDMACl, 98%, Sigma-Aldrich), methyltriethoxysilane (MTEOS, Aldrich), tetramethoxysilane (TMOS, Aldrich), R706 TiO_2 (DuPont), and dioctyl sebacate (DOS, Sigma-Aldrich) were used as received. Methanol (99.9%), ethanol (99.9%), 2-propanol (99.9%), and other chemicals were purchased from Fisher Scientific. Chromoionophore IX (CIX) was either purchased from Fluka or prepared by the reported procedure.[20]

Standard microscope slides (Corning) were used to cut 1 cm^2 glass sensor substrates. They were washed in a piranha solution (concentrated H_2SO_4 and 30% H_2O_2 in 3:1 ratio) for 30 min, followed by rinses first with deionized water and then with acetone, methanol, and ethanol. These slides were then dried in an oven before use. N-type [100] silicon wafers were similarly cleaned for deposition of thin film sensors that were then used for characterization by scanning electron microscopy (SEM).

A 0.9900% CO_2 gas tank (Airgas), odorless kerosene (Acros), acetone (Fischer), hexanes (Fischer), 29% aqueous ammonia solution, and food products, specifically bread, were used in the interference tests. To expose CO_2 gas to Sensor **A**, the CO_2 gas tank was directly connected to one of the flowmeters. After establishing a N_2 baseline, CO_2 gas (0.9900%) was introduced into the gas stream. In the interference tests involving kerosene, acetone, hexanes, and aqueous ammonia, approximately 50 mL of each analyte were placed into a temperature controlled jacketed gas impinger for their respective tests. After a baseline was established for Sensor **A**, nitrogen gas was introduced to the impinger to bubble the specific interferent vapor into the sensor flowcell, where the response was recorded.

4.2.2. Experimental Procedures (Sensors A, B and C)

A custom-built spin-coater was used to make the thin films. Ethyl cellulose (~0.235 g) was dissolved in a 4:1 mixture of toluene (8 mL) and ethanol (2 mL) to give a solution (2.5% wt EC) which, after several tests, was found to be of the optimal for the deposition of the sensor thin films. This solution was sonicated for 20 min and stirred to ensure that ethyl cellulose was completely dissolved. Then CIX (1–2 mg) and TDMACl

(0.28 mg) were dissolved into 1.00 g of the solution with stirring. The ethyl cellulose solution containing the dye was pippetted on a cleaned glass slide (~1 cm^2), which was on the spin coater, and drawn to the edges of the glass slide with a plastic pipette tip. The slide was then spun at ~2600 rpm (revolutions per minute) for approximately 30 s. Schlenk tubes were used to store the freshly made thin-film sensors (Sensor **A**) under vacuum prior to use.

Sensors were also prepared by incorporating TiO_2 particles (360 nm diameter) to induce the Mie scattering. In the preparation of these sensors, R706 TiO_2 particles (~3.7 mg) were added to EtOH (5 mL) and sonicated for 20 min to disperse the particles. The EtOH solution containing the TiO_2 particles (100 µL) was added with additional EtOH (1.9 mL) and then mixed with toluene (8 mL) to give an ethyl cellulose solution (2.5% wt EC). Sonication was used to ensure that ethyl cellulose was completely dissolved. Thin film sensors on glass slides were prepared from this EC solution (Sensor **B**) in a process similar to that described above, and then stored under vacuum in a Schlenk tube before use.

Sensor **C** was prepared on silicon wafers as Sensor **A**.

4.2.3. Instrumentation and Analytical Procedures

A Perkin-Elmer LS55 luminescence spectrometer with a pulsed Xe source was used for fluorescence measurements. The spectrometer was set at the following parameters: λ_{ex} = 445 nm, λ_{em} = 555 nm, 10 nm slits, 810 V PMT detector voltage, and a 515 nm emission cutoff filter. For time-based signal measurements, a signal reading was taken every 0.1 s. To improve the signal-to-noise ratio (S/N), signal averaging was

used by the arithmetic mean of a point and the points before and after. Sensors were placed in a brass flow cell constructed to fit with a front surface sample cell holder purchased from Perkin-Elmer.

The vapor pressure of each alcohol at various temperatures was calculated by using the Antoine equation (Eq. 4.1), where *A*, *B* and *C* are constants over a defined temperature (*T* in K) range.[29]

$$\log p = A - \frac{B}{T + C} \qquad (4.1)$$

A custom-made, jacketed gas impinger containing an alcohol liquid was used. The lid for the bubbler contained a medium frit gas diffuser immersed in the alcohol, and the lid was sealed by an O-ring and clamp. On top of the lid, there was a gas inlet for nitrogen gas and an outlet for the alcohol-saturated gas. The temperature of the jacketed impinger was controlled by a Thermo Haake temperature controller at -15.0, -7.0, and 0.0 ºC to give 1.000% MeOH (wt%, 1.549 x 10^4 ppm), 1.000% EtOH (1.587 x 10^4 ppm), and 1.000% Pr^{i}OH (2.310 x 10^4 ppm), respectively. Two separate mass flow controllers (MKS Instruments) (Figure 4.1) were connected to the inlet of the flow cell in the fluorescence spectrometer, and they were used to control the ratio of nitrogen gas and the gas from the impinger to obtain an accurate alcohol concentration. The outlet of the flowmeter was linked to a sealed vial which was attached to a separate bubbler to prevent the backflow of gases.

SEM images of Sensor **C** were taken using a Leo 1525 Field Emission Scanning Electron Microscope.

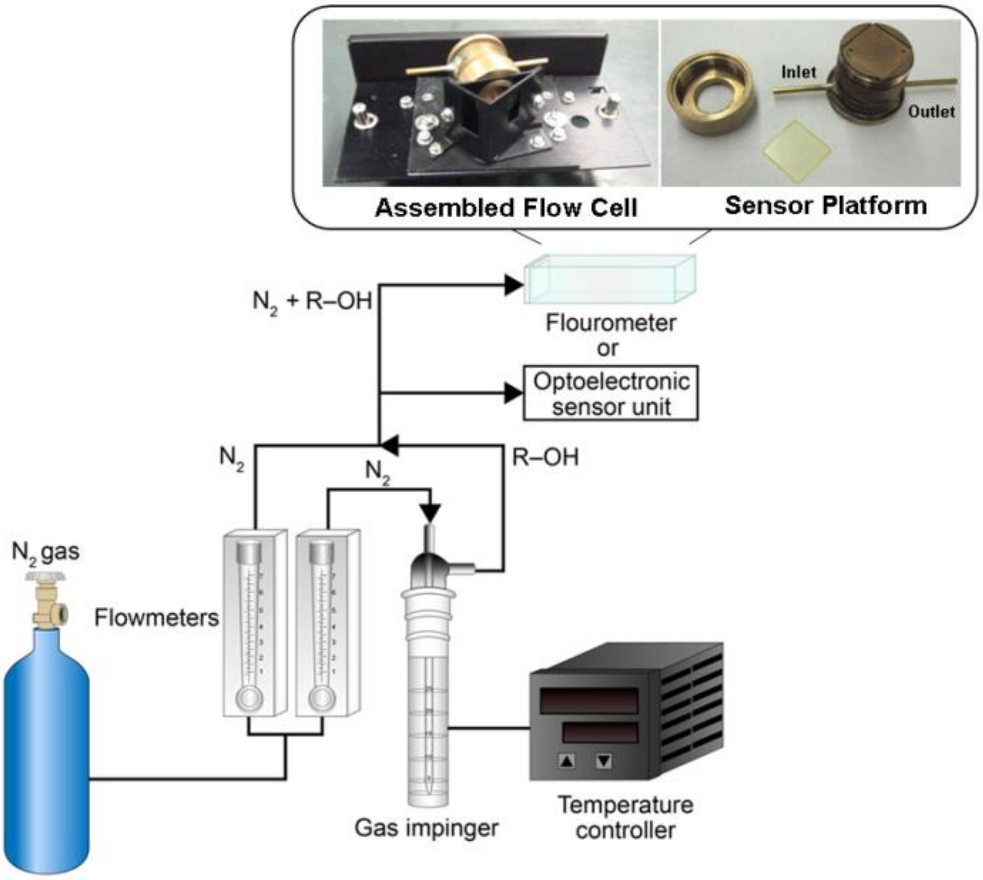

Figure 4.1. Schematic diagram of the instrumental set-up.

4.3. Results and Discussion

4.3.1. Dye Sensing Mechanism

The CIX dye, a trifluoroacetyl, reacts with alcohol to give a hemiacetal (Figure 4.2) and in the process quenches the fluorescence of the dye. However, formation of the hemiacetal takes approximately 20 h to complete. Mohr and coworkers found that a quaternary ammonium salt, TDMACl, catalyzes the reaction resulting in an immediate conversion of the trifluoroacetyl group to the hemiacetal upon exposure to alcohol.[20] To our knowledge, the dye, CIX, has not been used for gas phase detection of alcohols *or* encapsulated in an ethyl cellulose matrix.

4.3.2. Matrix Effects on Sensor Response

Initially, PVC sensors (Sensor **D**) were made following the formulation by Mohr and coworkers.[20] Upon exposure to air for several days, the PVC films lost a majority of their orange color, but were still responsive when tested under 1.000% Pr^{i}OH pulses. The sensors, with an excitation peak at 450 nm, produced an emission peak at 540 nm (Figure 4.3). During pulses of nitrogen and 1.000% Pr^{i}OH vapor, Sensor **D** showed quick response times by displaying a decrease in emission intensity and fast recovery times suitable for online measurements (Figure 4.4). In order to increase the sensitivity, Sensor **E** was prepared with twice the dye content. In the 0.036–1.000% Pr^{i}OH vapor range (Figure 4.5), Sensor **E** showed better sensitivity. However, the signal was noisy and it required signal averaging and baseline correction to adjust for the baseline drift.

Sol-gel sensors (Sensor **F**) were then explored as another alternative matrix for

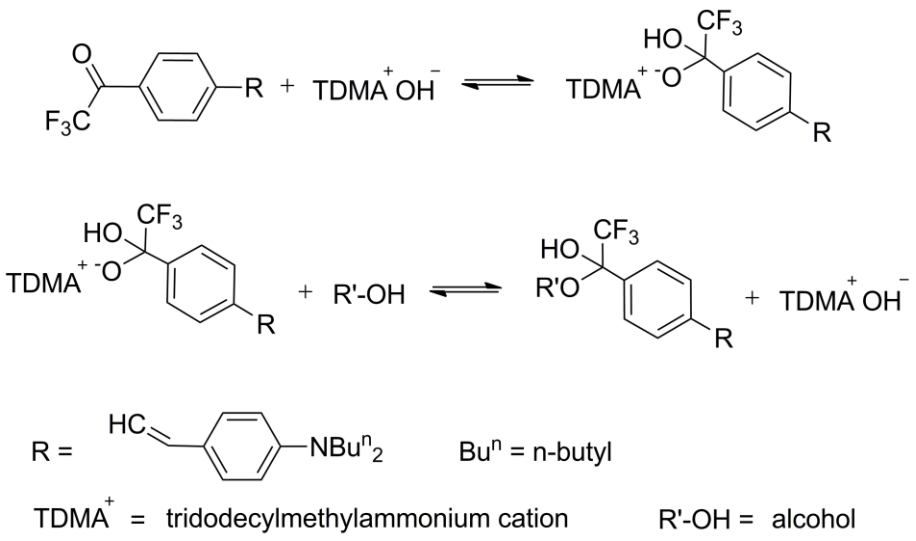

Figure 4.2. Proposed mechanism for the reaction between the dye and an alcohol catalyzed by TDMACl.[18]

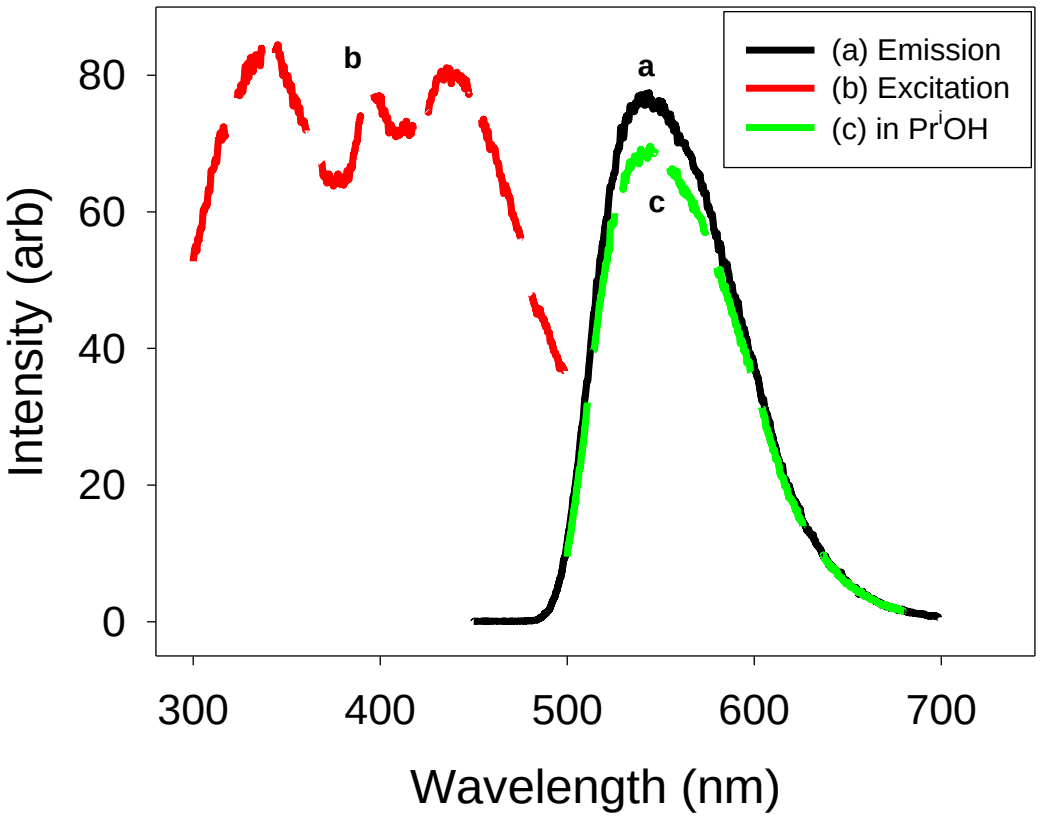

Figure 4.3. Excitation/Emission spectra of PVC Sensor **D** and signal quenching upon exposure to 1.092 mol% Pr^{i}OH vapor.

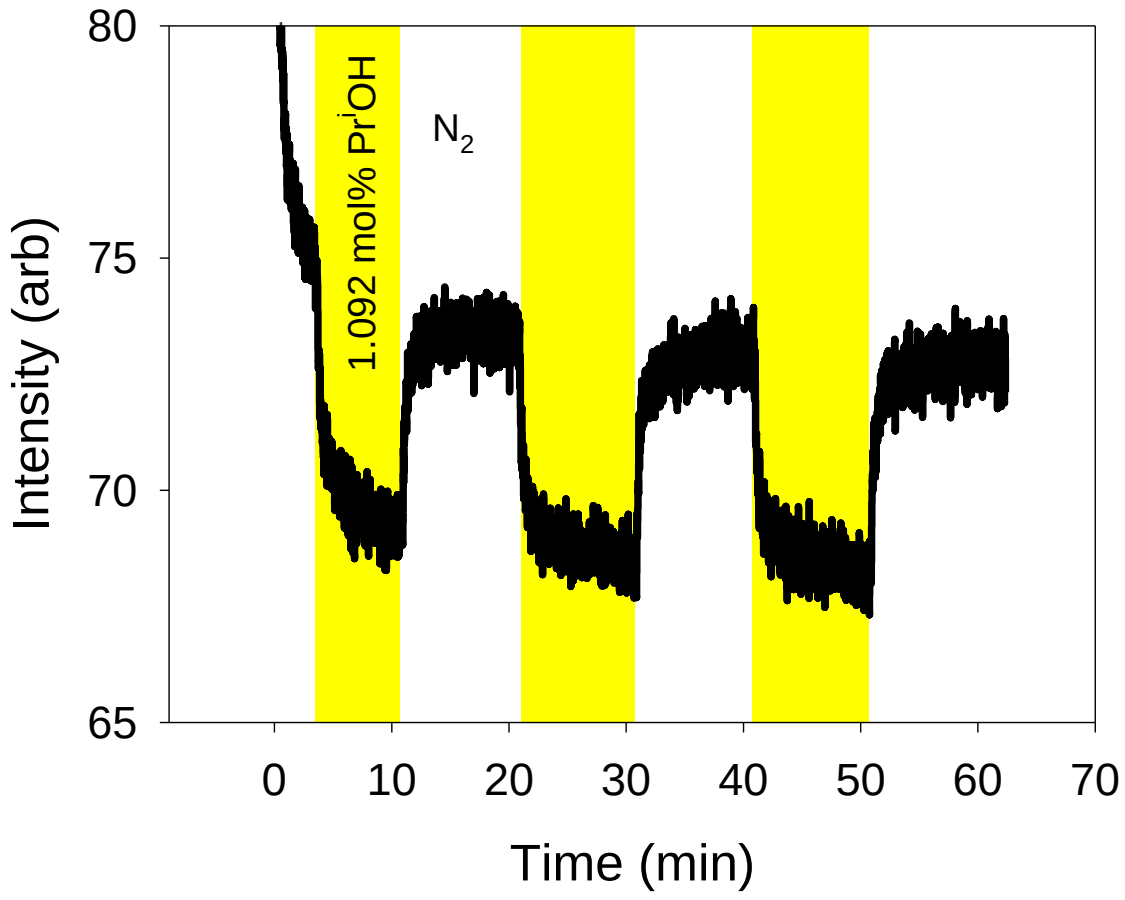

Figure 4.4. Time-based emission of Sensor **D** at 540 nm demonstrating a signal quenching response when exposed to 1.092 mol% $Pr^{i}OH$ in nitrogen gas without signal averaging or background correction.

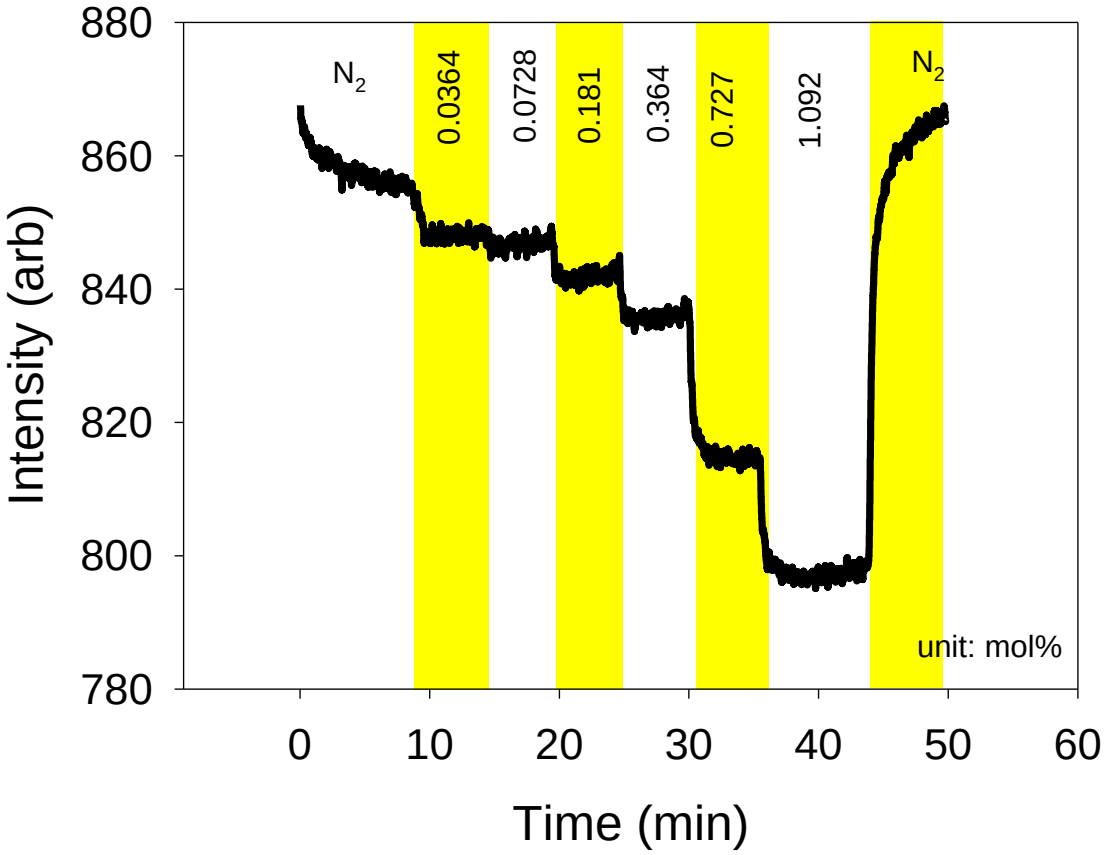

Figure 4.5. Response of Sensor **D** to 0.0364–1.092 mol% Pr^{i}OH with signal averaging and baseline correction.

CIX. Figure 4.6 shows the response of the sol-gel sensor to 1.000% Pr^iOH pulses. Initially, the response to Pr^iOH was quick, but after switching back to nitrogen gas, the response was higher than the initial baseline, indicating that the sol-gel matrix perhaps has an affinity for alcohols and once exposed to alcohols reversibility may be problematic.

After several comparison tests, ethyl cellulose (EC) was found to be the best matrix to encapsulate the dye CIX. A focus on EC as the matrix for CIX also helped to provide consistency with other sensors previously studied by Innosense LLC in a multi-channel sensing platform. Sensor **A** produced an emission peak at 555 nm when the dye was excited at 445 nm (Figure 4.7).

Figure 4.8A shows a section of a uniform pitted surface of Sensor **C** on a silicon substrate at 900x magnification from SEM imaging. Figure 4.8B displays a cross section of Sensor **C** at 3000x magnification that has a thickness of 1–2 µm, highlighted by the two parallel lines in the image. The surface of the sensor shows features ("pitting") consistent with phase separation that occurs during the processing of the sensor.

4.3.3. Mie Scattering with TiO_2 Particles

In order to increase the sensitivity of the indicator dye, TiO_2 particles were incorporated into ethyl cellulose thin films. TiO_2 particles scatter wavelengths in the visible range about equally.[21] The scattering of light by the TiO_2 particles within the sensing matrix allows for a more effective interaction of light with the indicator molecules in the sensing layer, thus effectively increasing the path length without using

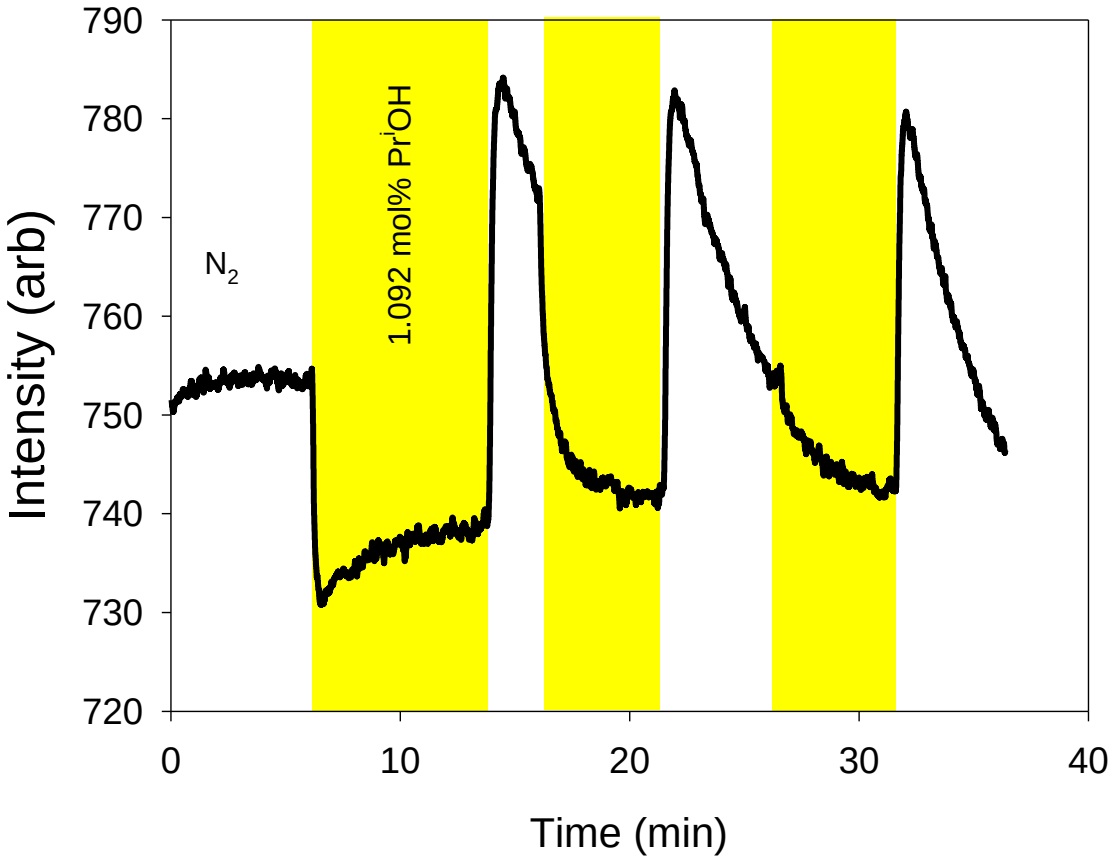

Figure 4.6. Response of the sol-gel Sensor **F** on exposure to 1.092 mol% pulses of $Pr^{i}OH$ vapor; Emission was detected at 580 nm.

A

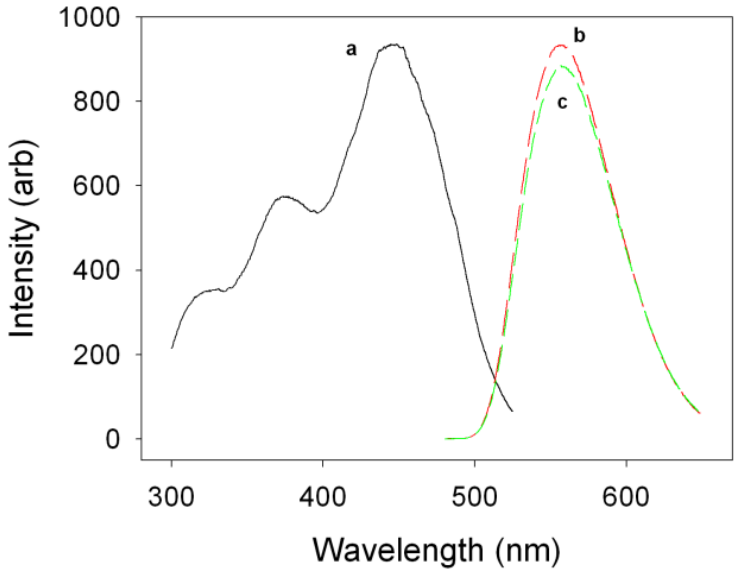

B

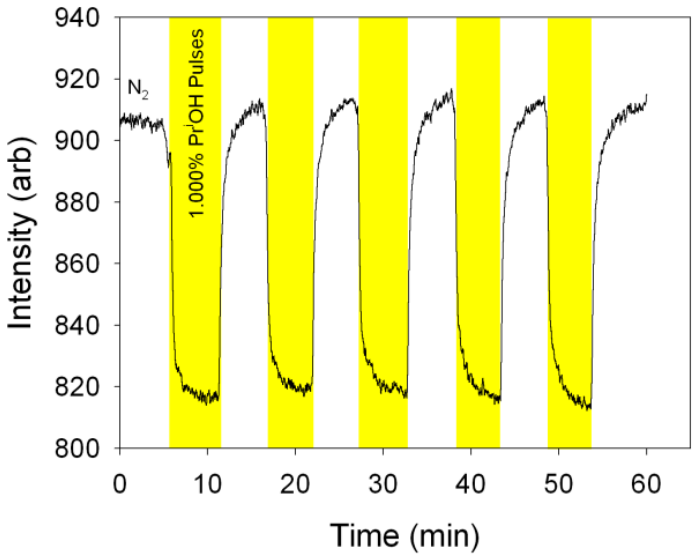

Figure 4.7. (A) Spectra of Sensor **A**: (a) excitation; (b) emission; (c) emission after exposure to 1.000% Pr^{i}OH; (B) Time-based emission at 555 nm demonstrating a signal quenching response when exposed to 1.000% Pr^{i}OH in nitrogen gas without signal averaging or background correction. arb = arbitrary unit.

A

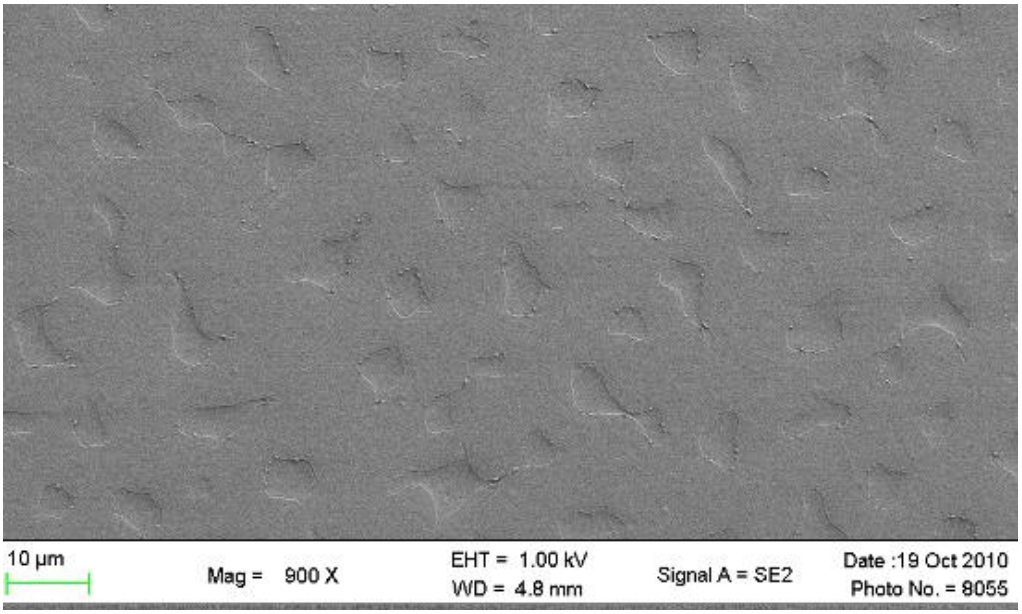

B

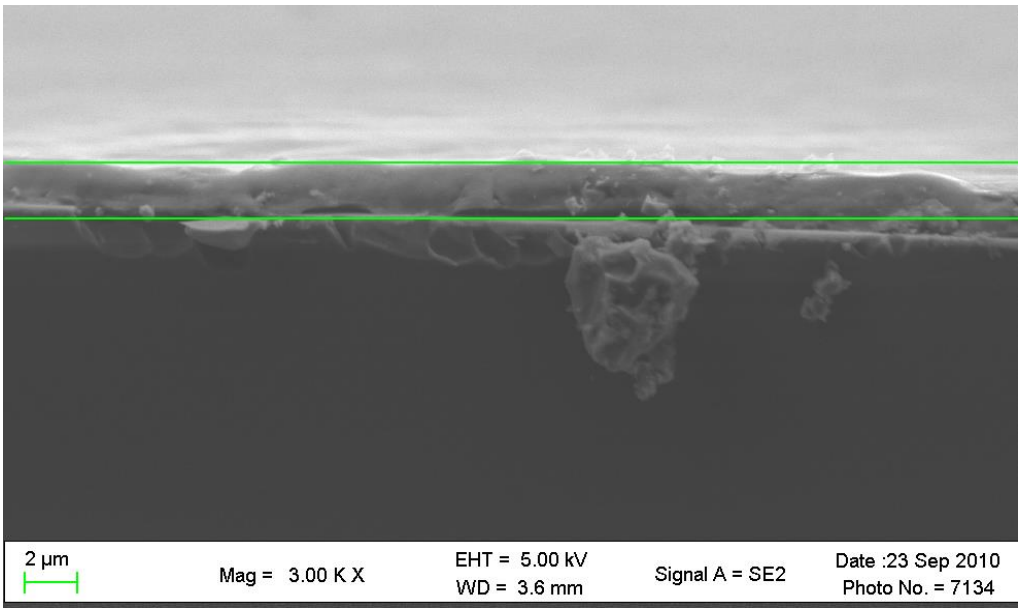

Figure 4.8. SEM images of Sensor **C**: (A) Surface; (B) Cross section.

thicker sensing layers.[21] The optimum particle size would be approximately 0.5 times sensing matrix allows for a more effective interaction of light with the indicator molecules in the sensing layer, thus effectively increasing the path length without using thicker sensing layers.[21] The optimum particle size would be approximately 0.5 times the wavelength of interest which, in this case, would be around 250–350 nm for the emission wavelength of 550 nm from the dye. This method was adapted from CO_2 sensors that we developed recently.[27] Figure 4.9 shows the response of TiO_2-doped Sensor **B**. The addition of TiO_2 R706 particles resulted in an increase in the emission intensity. This is most likely because the median size of R706 particles, at 360 nm,[30] is close to the 250–350 nm range indicated above. Moreover, according to the DuPont's R706 product sheet, small TiO_2 particles scatter blue light more effectively than those with larger particle sizes.[30] In addition, R706 is ideal for the prototype optoelectronic device using a blue LED as its light source discussed below.

4.3.4. Storage Conditions and Long Term Studies

Unlike the PVC sensors (Sensors **D** and **E**), the EC sensors (Sensor **A**) were able to keep their fluorescent orange color and demonstrated durability under ambient environment. An EC matrix helped to stabilize the baseline response which was observed by the small difference between the original and baseline corrected response (Figure 4.10) when the sensor was exposed to Pr^iOH vapor. Since the EC thin-film sensors do not lose their initial sensitivity in ambient environment, a long term study was performed to test the durability of the sensors. In order to simulate real-world field tests, Sensor **A**s were wrapped in a lint-free cloth and then covered in aluminum foil to

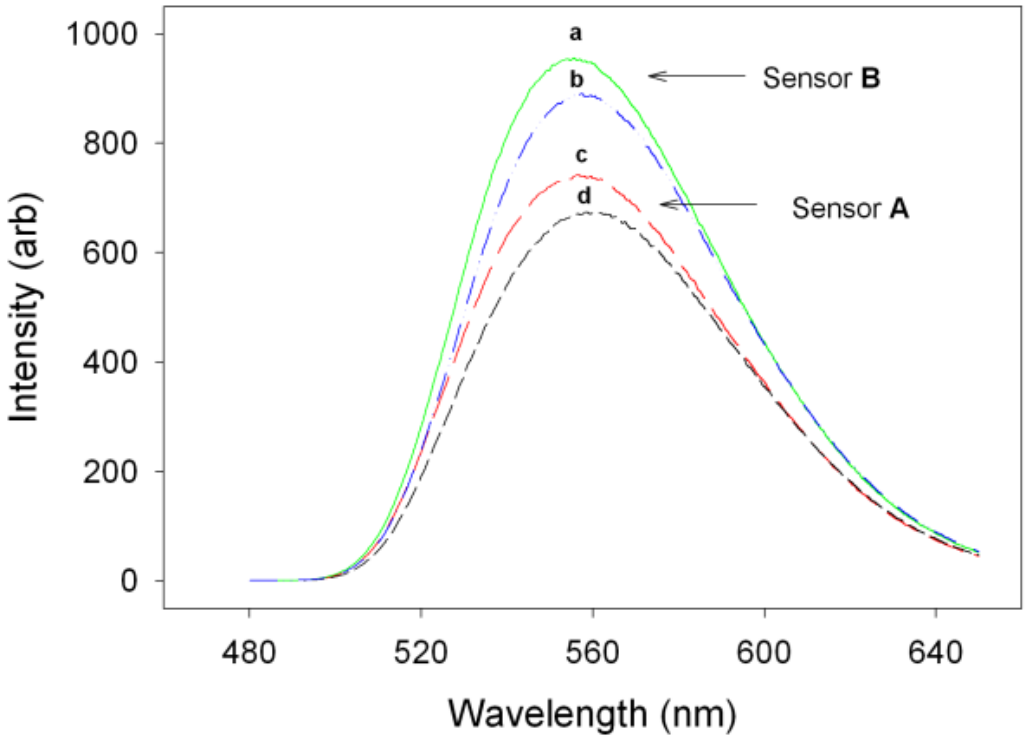

Figure 4.9. Comparison between Sensor **A** and TiO_2-doped Sensor **B**: (a) Sensor **B**; (b) Sensor **B** when exposed to 1.000% Pr^iOH; (c) Sensor **A**; (d) Sensor **A** when exposed to 1.000% Pr^iOH.

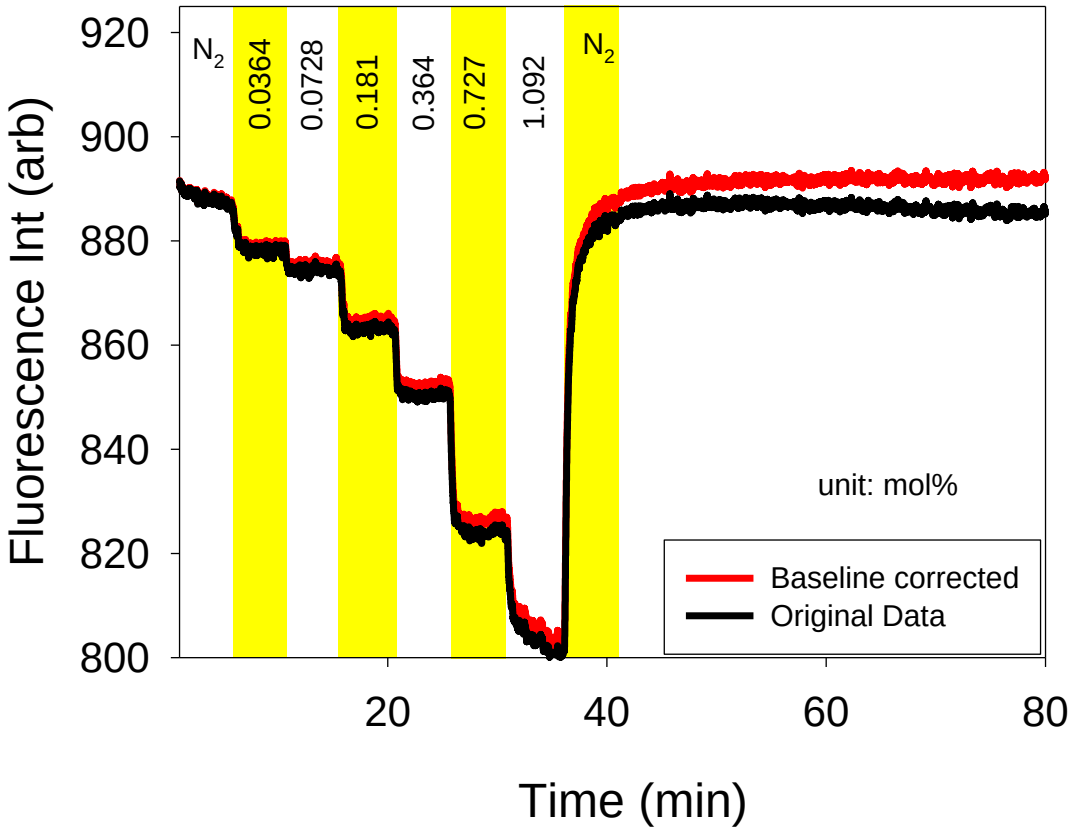

Figure 4.10. Response of Sensor **A** to Pr^{i}OH vapors.

protect the sensors from light. Afterwards, the sensors were placed in sealable bags. Fluorescence measurements were performed every 2 weeks on the same sensor (Sensor **A1**), which was compared to a freshly opened sensor from the same batch. Over a period of eight months, Sensor **A1** began to fluctuate in baseline (Figure 4.11) but the sensor still showed sensitivity when exposed to alcohol vapor ($Pr^{i}OH$). In comparison, freshly opened sensors for each measurement showed a baseline and sensitivity similar to that of Sensor **A1** from month 1. This long term study demonstrates that Sensor **A** is able to optimally detect alcohol for 3 months before it needs to be replaced, and the sensor can remain sensitive for up to a year.

4.3.5. Multi-channel Prototype Platform

To demonstrate that these alcohol sensors can be used in the field, InnoSense LLC has designed and built a miniaturized multi-channel optoelectronic device that can test up to seven different sensors simultaneously from a blue or amber LED light source. Each channel has a slot for an optical filter to enable absorbance or fluorescence based measurements and longpass filters (500 nm) were used to examine the EC-CIX alcohol sensors. Within the optoelectronic sensor unit, there is a built-in temperature and humidity probe to monitor temperature and relative humidity during the testing period. Therefore, any contribution from humidity can be subtracted from the signal, thus giving the signal arising from the alcohol analyte itself. The optoelectronic sensor unit can be connected to a PC where data acquisition is monitored by LiveGraph software. The sensor unit was evaluated by testing three alcohol sensors (Sensor **A**) and an EC blank and exposing these sensors to varying concentrations of $Pr^{i}OH$

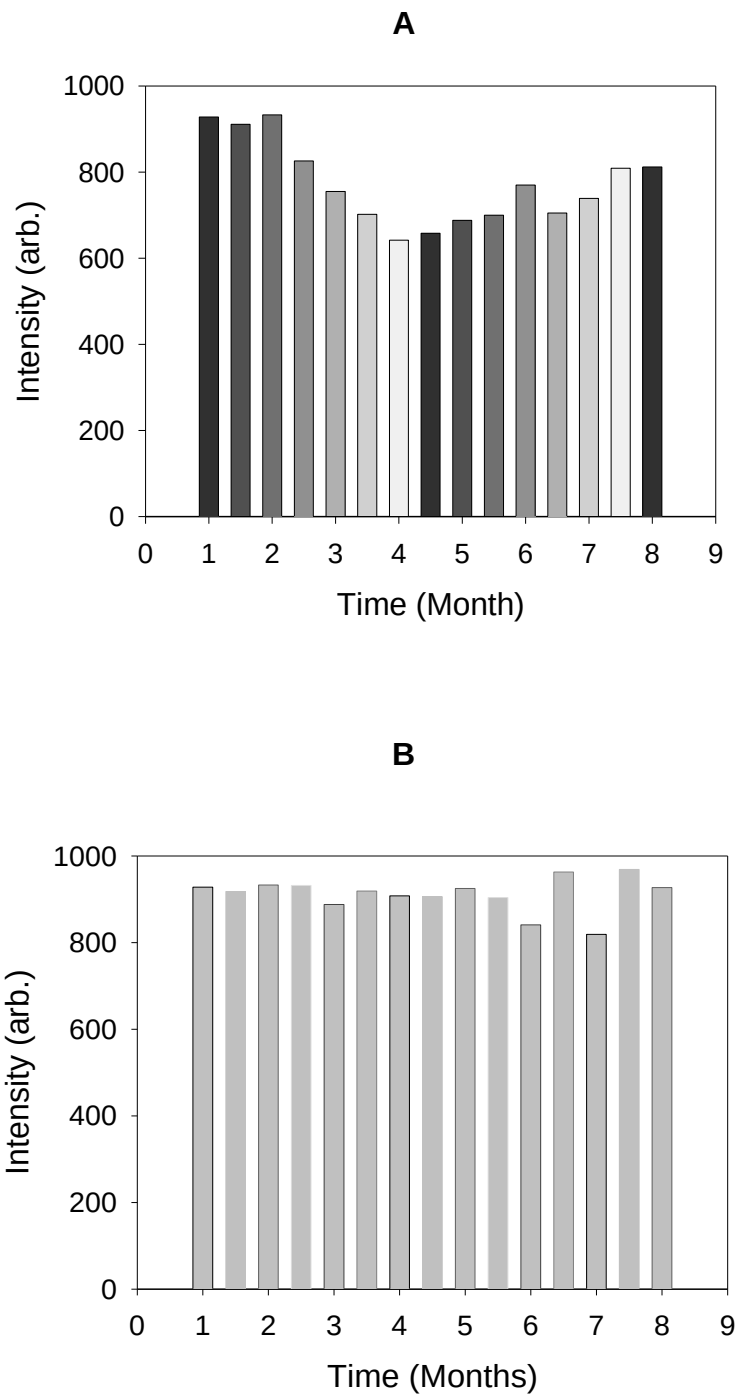

Figure 4.11. Baseline study of Sensor **A**: (A) one sensor over an 8-month period; (B) freshly opened sensors over an 8-month period.

ranging from 0 to 1.000%. Data were taken every 5 s. Figure 4.12 displays the results from the sensor unit. Each alcohol sensor shows a similar response to the other and demonstrates an expected decrease in signal upon exposure to $Pr^{i}OH$.

4.3.6. Analytical Performance

As indicated earlier, reactions of the dye CIX with alcohols forming hemiacetals are selective. Primary alcohols with increasing chain lengths show an increasing ratio of the trifluoroacetyl form rather than the product hemiacetals.[20] Figure 4.13 shows the sensitivity of the EC sensor towards MeOH, EtOH, and $Pr^{i}OH$, respectively. Linear calibrations are obtained over large concentration ranges. The detection limits are 9, 13, 21 ppm, and the quantification limits are 32, 43, and 70 ppm, respectively, for MeOH, EtOH, and $Pr^{i}OH$ vapors. The data shows that the sensors are in general more sensitive to less bulky alcohols. Since CIX reacts with different alcohols, it is important to place the sensor in a specific location where the type of alcohol is known. For example, the alcohol sensor could be positioned to detect methanol leaks from fuel cells that are used in microelectronics or be adapted into breathalyzers for ethanol intoxication.

Compared to other previously mentioned studies of alcohol sensors, the EC-CIX sensors developed in this study have a much higher dynamic range and lower limit of detection for the alcohols investigated. Commercial alcohol gas sensors such as the ones used in breathalyzers usually have a sensor accuracy of $\pm$0.01 blood alcohol content (BAC), according to commercial product specifications, which indicates the readings can vary by as much as 100 ppm.[31-33]

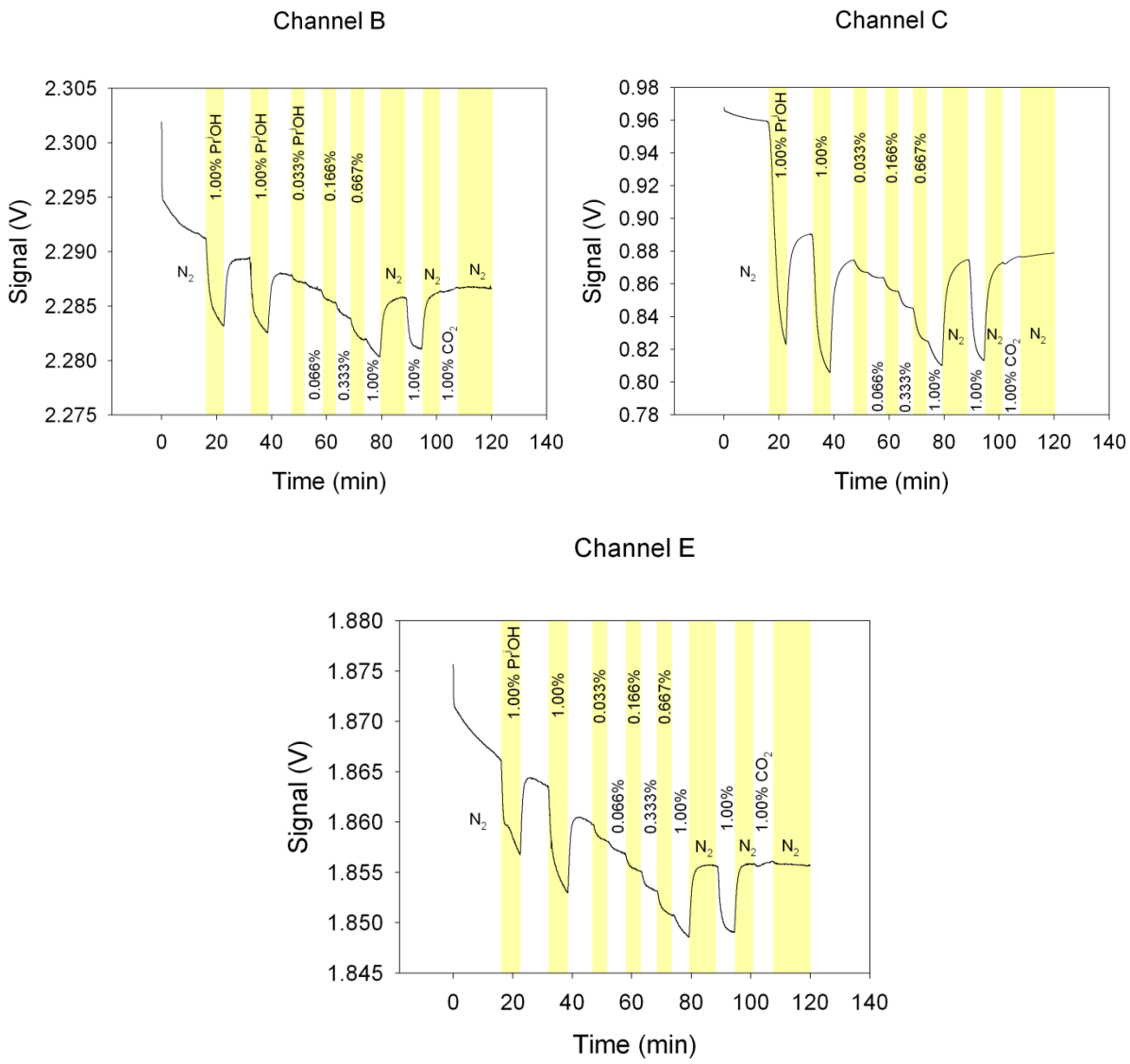

Figure 4.12. Response of three alcohol sensors (Sensor **A**) in the prototype optoelectronic device in channels B, C, and E when exposed to $Pr^{i}OH$ vapor and CO_2.

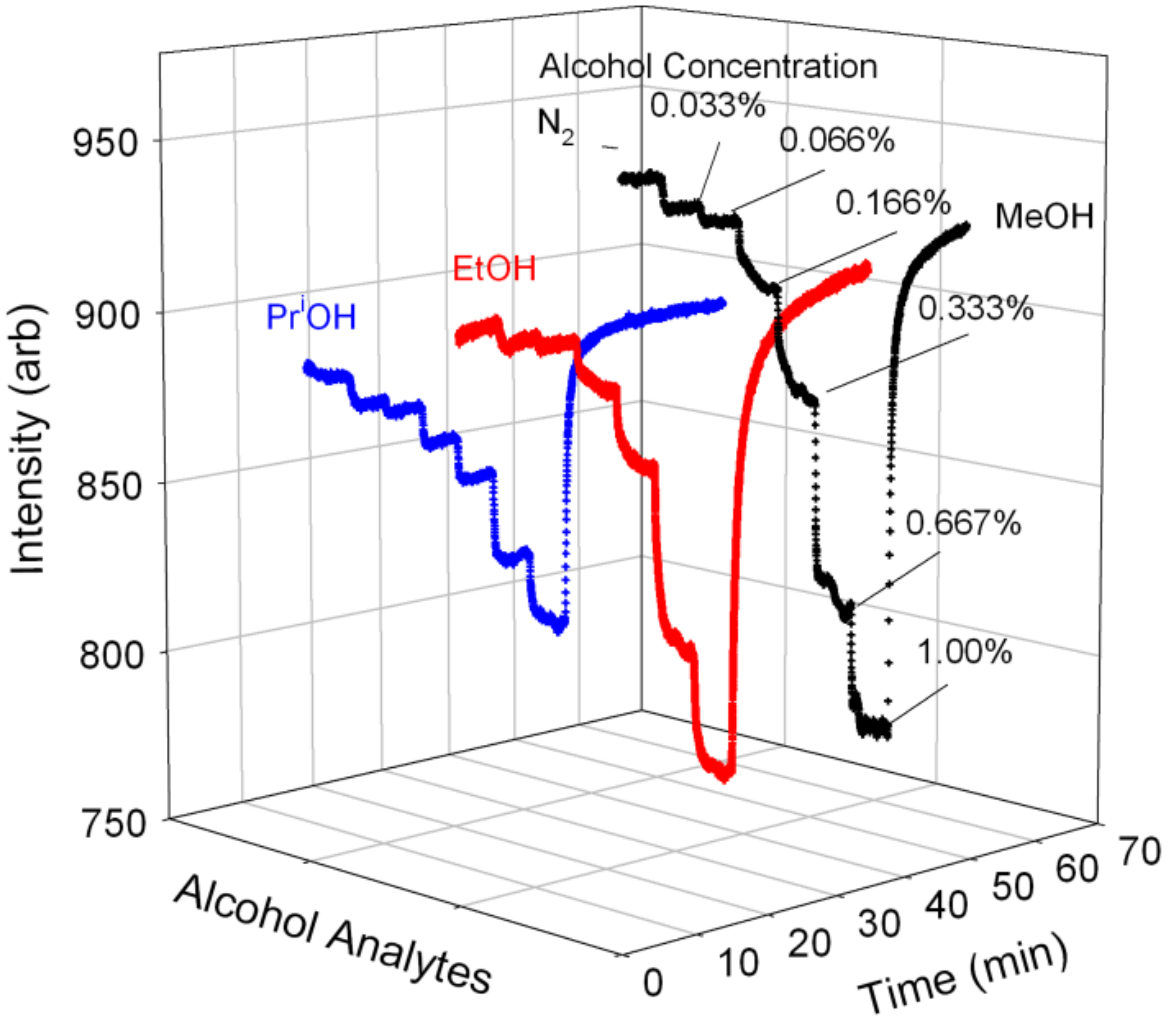

Figure 4.13. Response of Sensor **A** to MeOH vapors - Calibration: $y = 0.1517x + 0.0021$ ($R^2 = 0.998$) based data in the range of 0–1.000% (0–1.549 x 10^4 ppm) MeOH, EtOH vapors - Calibration: $y = 0.3476x - 0.0045$ ($R^2 = 0.996$) based data in the range of 0–1.000% (0–1.587 x 10^4 ppm) EtOH, and Pr^iOH vapors - Calibration: $y = 0.0926x + 0.0123$ ($R^2 = 0.998$) based data in the range of 0–1.000% (0–2.310 x 10^4 ppm) Pr^iOH.

4.3.7. Temperature and Interference Study

An Agilient 8653 UV-Vis spectrometer, connected to a thermostattable cell holder in order to control temperature, was used to analyze the response of the EC-CIX alcohol sensor under various temperatures without exposure to analytes such as Pr^iOH. Figure 4.14 shows that as temperature increases the absorbance of the sensor increases. At approximately 60 ^oC, the increase in absorbance due to temperature begins to taper off. Also, as the absorbance of the sensor increases, the EC-CIX sensor red-shifts 10 nm from 450 to 440 nm under increasing temperature (Figure 4.14).

Another challenge for detection in optical sensors is interferences. To evaluate the response of the alcohol sensor to interferent vapors, carbon dioxide (CO_2), kerosene, ammonia (NH_3), moisture (H_2O), hexanes, and acetone were directly exposed to Sensor **A** in triplicate and recorded. Kerosene is a rocket fuel, and CO_2 is a major component of rocket plumes. NH_3 is a primary product of hydrazine (H_2NNH_2) decomposition, and hydrazine has been used as a liquid rocket propellant.[34,35] Moisture is a byproduct generated through the combustion of 2-propanol with liquid oxygen in order to simulate a vacuum for rocket testing.[1] Acetone, and hexanes are some of the interferences that have been attributed to false positives in general commercial alcohol sensors.[36]

As expected, Figure 4.15 shows that CO_2 gas has a minute effect on Sensor **A**, and the observation is consistent with the fact that CO_2 does not react with the CIX dye. Exposing Sensor **A** to kerosene vapors caused the fluorescence of the sensor to slightly quench in intensity, suggesting that the introduction of the hydrophobic kerosene to the

A

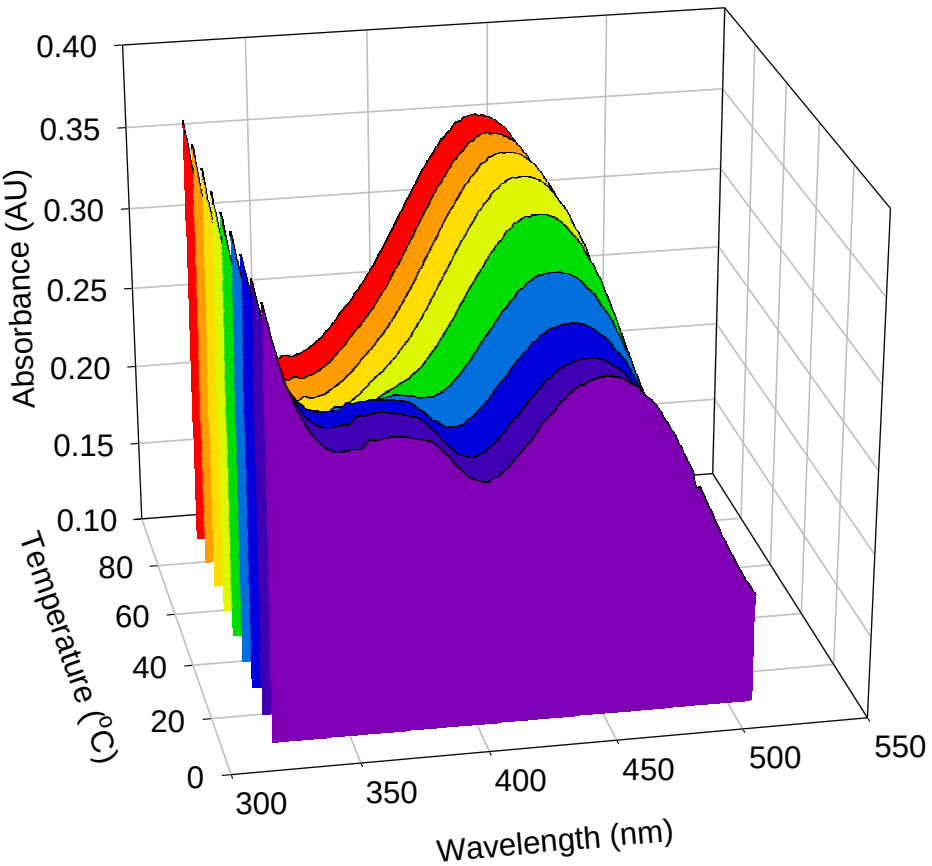

B

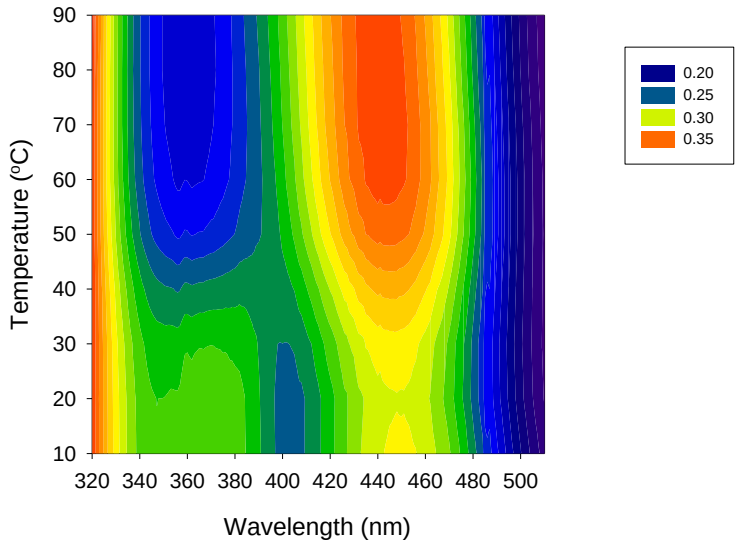

Figure 4.14. UV-Vis measurement of the response of the EC-CIX sensor to (A) temperature and (B) the resulting change in wavelength.

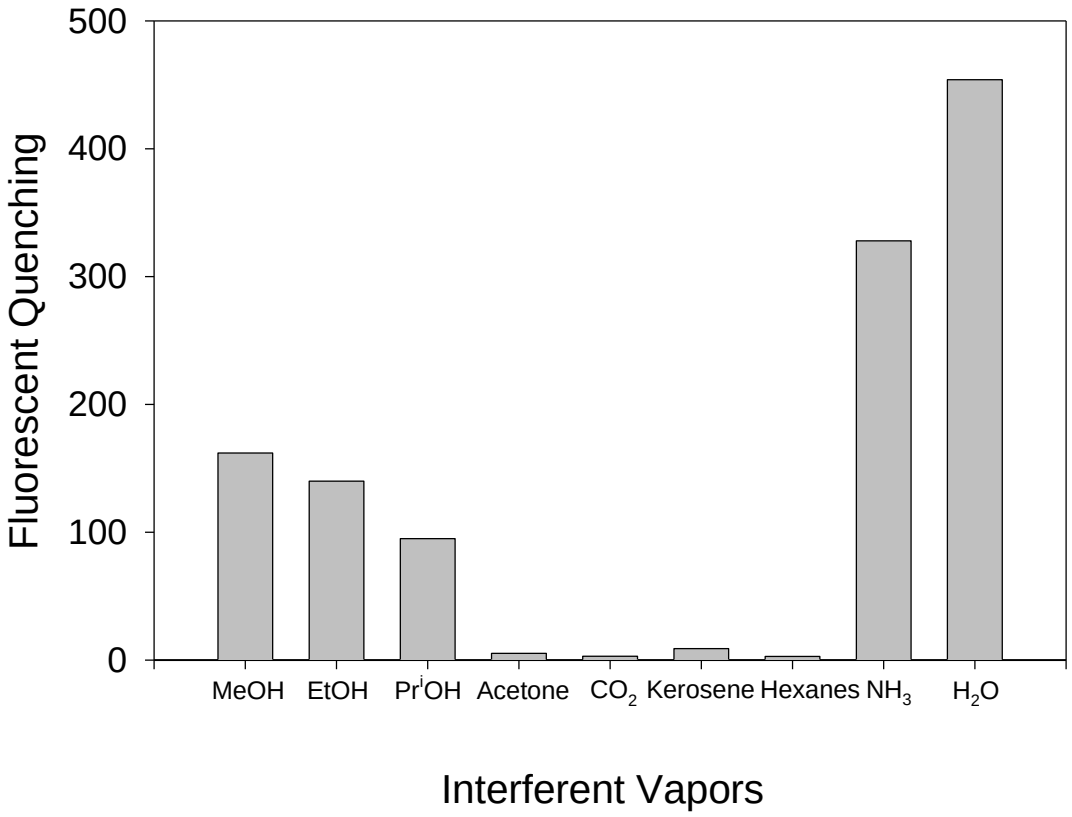

Figure 4.15. Response of the alcohol sensor to interferent vapor CO_2, kerosene, ethylene glycol, and NH_3.

sensor film may have changed the environment, shifting *to a small degree* the equilibrium of the reaction between the CIX dye and alcohol (Figure 4.2). It is expected that vapors of other organic hydrocarbons may lead to a similar, small effect. However, exposing Sensor **A** to ammonia vapor and moisture caused a large decrease in fluorescence of the sensor. Other amines, especially primary amines, may react with the CIX dye and quench its fluorescence.[37] Moreover, moisture can react with the CIX dye, a ketone, forming geminal diols and thus affect the reaction of the dye with alcohol.[37] Since Sensor **A** is being used in an optoelectronic sensor unit with a built in humidity probe, the relative humidity can be measured during the testing period. Thus, the relative humidity can be measured and be subtracted from the signal. Studies are also underway to develop a dual optical sensing approach to address the impact of moisture, and the results will be reported in the future.

General alcohol sensors such as commercial breathalyzers may also be susceptible to outside interferences such as chemicals in the environment, leading to readings higher than normal and false positives.[36] The US National Highway Traffic Safety Administration (NHTSA) establishes guidelines and screenings for commercial breathalyzers in order to be approved as an alcohol sensing device.[38] These guidelines do not require a certain limit of detection to be met but require devices to conform to a set of tests to evaluate the precision and accuracy of the alcohol sensing device.[38]

One of the major flaws of IR breathalyzers is the lack of specificity, since it is often the methyl group in ethanol that is being detected.[36] Thus the sensor will treat any compound with a methyl group as ethanol which includes many chemical compounds whose molecular structures are compatible with IR filters. Two IR wavelengths and an

algorithm for the detection of interferents have been used in new breathanalyzers to calculate the ratio of absorbance values at the two measured wavelengths.[36] Also, the instrumentation for IR breathanalyzers can be complex with some requiring five filters to address volatile interferences.[39] Although such an approach reduces interference, acetone, e.g., was found to still have an effect on the new, IR-based breathanalyzers.[40] Semiconductor breathalyzers have been shown to absorb many substances which can give positive alcohol readings even when no ethanol is present.[36] Studies have confirmed the existence of a wide variety of compounds on the human breath.[41] Acetone and hexanes are among chemicals that are commonly found on the breath of normal, healthy individuals but are of insignificant levels to affect breathalyzers. However, dieters and diabetics not in control of their blood sugar can have acetone levels hundreds or even thousands of times higher than normal which may create falsely high results in a semiconductor breathalyzer.[36] Breathalyzers based on fuel cell technology give concerns due to sensitivity loss and sensor degradation after long term exposure in dry conditions.[42] The primary reason for sensitivity loss and sensor degradation is from the loss of electrochemically active surface area of the platinum electrode, which is seemingly irreversible.[42] Another concern for fuel cell sensors, albeit to a lesser extent, is the loss of proton conductivity as a result of membrane dehydration but can be alleviated by rehydrating the membrane in humid conditions.[42] There has been a report of a false-positive breath-alcohol test using a fuel-cell based analyzer after a ketogenic diet.[43]

In comparison to commercial breathalyzers, Sensor **A** appears to be less prone to common interferences of current commercial alcohol sensors. Sensor **A** was directly

exposed to interferents that are known for commercial breathalyzers such as acetone, and hexanes but gave a minute response to these interferences (Figure 4.15). The small responses are perhaps a result of solvent effects, as acetone and hexanes do not react with the CIX dye.[44] The interference study here demonstrates that interferences without active N-H or O-H groups are unlikely to interfere with the response of Sensor **A**. The current study looks into a new method centered on a fluorescence based system for the detection of alcohol and provides an improvement over existing alcohol sensors by limiting the possible interferences that may affect a reading such as chemicals or dry conditions.

4.4. Conclusion

In this study, the CIX dye was incorporated into EC films in order to detect alcohol vapors. The ethyl cellulose sensor for alcohol vapors was sensitive to MeOH, EtOH, and $Pr^{i}OH$. To induce Mie scattering, TiO_2 particles were added to the alcohol sensors to increase the interaction of light with the indicator material which enhanced the sensitivity of the sensors. The use of TiO_2 particles increased the signal of the emission intensity by approximately 30%. The alcohol gas sensor reported in this study has a much higher dynamic range and lower limit of detection for the alcohols studied than the other gas alcohol sensors reported earlier using microelectronics and resistivity. Sensor **A** was tested with a miniaturized multi-channel testing platform, showing that they could be used under real world field testing conditions. The research here shows that EC-CIX sensors may be considered an option as a highly sensitive alcohol sensor for detection in rocket plumes as well as being adapted and providing an

improvement to general alcohol sensing devices.

References

1. NASA Stennis Space Center, *Environmental Assessment for the Construction and Operation of the Constellation Program A-3 Test Stand*, May 2007. http://www.ssc.nasa.gov/environmental/docforms/eas/eas.html Accessed on February 8, 2012.
2. Tejwani, G.D.; McVay, G.P.; Langford, L.A.; St. Cyr, W.W. *Planning for Plume Diagnostics for Ground Testing J-2X Engines at the SSC*; NASA: Stennis Space Center, 2006.
3. Costantini, M.G.; *Environ. Health Perspect*. **1993**, *101*, 151–160.
4. Flipsen, B. *J. Fuel Cell Sci. Technol*. **2010**, *7*, 061014–8.
5. http://www.epa.gov/ttn/atw/187polls.html. Accessed on February 8, 2012.
6. Young, J.A.; *J. Chem. Educ*. **2006**, *83*, 1131.
7. http://www.osha.gov/dts/chemicalsampling/data/CH_251600.html. Accessed on 8 February 2012.
8. Finkelstein, Y.; Vardi, J. *NeuroToxicology* **2002**, *23*, 521–525.
9. Federal Register 75: 213 (November 4, 2010) p. 68094–68150. Available from: Environmental Protection Agency; Accessed on December 1, 2010.
10. Torsner, E. Corros. *Eng. Sci. Technol*. **2010**, *45*, 42–48.
11. Oliverio, N.; Jiang, L.; Yilmaz, H.; Stefanopoulou. A. *J. Fuels Lubr*. **2009**, *2*, 229–241.
12. Stevens, N.; Akins, D.L. *Sens. Actuators B*. **2007**, *123*, 59–64.
13. Bangalore, A.S.; Small, G.W.; Combs, R.J.; Knapp, R.B.; Kroutil, R.T. *Anal. Chim. Acta.* **1994**, *297*, 387–403.

14. Pang, F.; Han, X.; Chu, F.; Geng, J.; Cai, H.; Qu, R.; Fang, Z. *Sens. Actuators B*. **2007**, *120*, 610–614.

15. McCorkle, D.L.; Warmack, R.J.; Patel, S.V.; Mlsna, T.; Hunter, S.R.; Ferrell, T.L. *Sens. Actuators B.* **2005**, *107*, 892–903.

16. Morey, T.E.; Booth, M.M.; Prather, R.A.; Nixon, S.J.; Boissoneault, J.; Melker, R.J.; Goldberger, B.A.; Wohltjen, H.; Dennis, D.M. *J Anal Toxicol*. **2011**, *35*, 134–142.

17. Gessei, T.; Sato, H.; Kazawa, E.; Kudo, H.; Saito, H.; Mitsubayashi, K. *Microchim. Acta* **2009**, *165*, 179–186.

18. Mohr, G.J.; Citterio, D.; Spichiger-Keller, U.E. *Sens. Actuators, B.* **1998**, *49*, 226–234.

19. Mohr, G.J.; Spichiger-Keller, U.E. *Anal. Chim. Acta*. **1997**, *351*, 189–196.

20. Mohr, G.J.; Lehmann, F.; Grummt, U.; Spichiger-Keller, U.E. *Anal. Chim. Acta.* **1997**, *344*, 215–225.

21. Wriedt, T. *Part. Part. Syst. Char*. **1998**, *15*, 67–74.

22. Allain, L.R.; Xue, Z.-L. *Anal. Chem*. **2000**, *72*, 1078–1083.

23. Allain, L.R.; Canada, T.A.; Xue, Z.-L. *Anal. Chem.* **2001**, *73*, 4592–4598.

24. Canada, T.A.; Xue, Z.-L. *Anal. Chem*. **2002**, *74*, 6073–6079.

25. Canada, T.A.; Beach, D.B.; Xue, Z.-L. *Anal. Chem*. **2005**, *77*, 2842–2851.

26. Rodman, D.L.; Pan, H.; Clavier, C.W.; Feng, X.; Xue, Z.-L. *Anal. Chem*. **2005**, *77*, 3231–3237.

27. Carrington, N.A.; Thomas, G.H.; Rodman, D.L.; Beach, D.B.; Xue, Z.-L. *Anal. Chim. Acta*. **2007**, *581*, 232–240.

28. Dansby-Sparks, R.N.; Jin, J.; Mechery, S.J.; Sampathkumaran, U.; Owen, T.W.; Yu, B.D.; Goswami, K.; Hong, K.; Grant, J.; Xue, Z.-L. *Anal. Chem*. **2010**, *82*, 593–600.

29. Dean, J.A. *Lange's Handbook of Chemistry*, 15th ed., McGraw-Hill: New York, 1999, p. 5.30.

30. DuPont's R706 product sheet. Accessed on 8 February 2012. http://www2.dupont.com/Titanium_Technologies/en_US/products/706/CO_B_H_56619_7_706_Grade_Description.pdf

31. AlcoMate AL-7000 product sheet. Accessed on 25 July 2012. http://alcomate.net/prodmanuals/manual_Premium.pdf

32. AlcoHawk Precision product sheet. Accessed on 25 July 2012 http://www.q3i.com/pdfs/AlcoHAWK-Precision-Datasheet.pdf

33. Bactrack S30 product sheet. Accessed on 25 July 2012. http://www.bactrack.com/breathalyzer/images/s30-ownersmanual.pdf

34. Schmidt, E.W.; Wucherer, E.J. *Proceedings of the 2nd International Conference on Green Propellants for Space Propulsion (ESA SP-557)*. 7-8 June 2004, Chia Laguna (Cagliari), Sardinia, Italy. Editor: A. Wilson. http://adsabs.harvard.edu/full/2004ESASP.557E...3S, Accessed on 8 March 2012.

35. Plemmons, D.H.; Mehta, M.; Clark, B.C.; Kounaves, S.P.; Peach Jr., L.L.; Renno, N.O.; Tamppari, L.; Young, S.M.M. *J. Geophys. Res*. **2008**, *113*, E00A11.

36. Taylor, L.; Oberman, S. *Drunk Driving Defense*. 6th ed., Aspen: New York, 2006.

37. Mohr, G.J.; Citterio, D.; Demuth, C.; Fehlmann, M.; Jenny, L.; Lohse, C.;

Moradian, A.; Nezel, T.; Rothmaier, M.; Spichiger. U.E. *J. Mater. Chem.* **1999**, *9*, 2259–2264.

38. Federal Register 73: 62 (March 13, 2008) p. 16956–16960. Available from: National Highway Traffic Safety Administration; Accessed on 26 July 2012.

39. Jones, A.W.; Anderson, L. *J. Breath. Res*. **2008**, *2*, 1-7.

40. Watterson, J.H. *J. Anal. Toxicol*. **2009**, *33*, 109–117.

41. Conkle, J.P.; Camp, B.J.; Welch. B.F. *Arch. Environ. Health*. **1975**, *30*, 290–295.

42. Prest, L. M.S. Thesis, University of Ontario Institute of Technology, 2011.

43. Jones, A.W.; Roessner, S. *Int. J. Obesity* **2007**, *31*, 559-561.

44. Loudon G.M. *Organic Chemistry*, 3rd ed., Benjamin/Cummins Publishing Company, 1995, p. 654.

Part 5

Fingerprinting Method for Kerosene Vapor Detection

Abstract

The ability to detect hydrocarbons is a topic of interest for NASA. Hydrocarbons in test plumes may interfere with the line of sight and complicate the analysis of current optical emission/absorption measurements. A variety of different indicator dyes have been utilized to develop optical sensors as a fingerprinting method to detect hydrocarbon/kerosene vapors. Reichardt's dye, Coumarin 153, and Resorufin were encapsulated into several polymer films or sol-gels and their response to kerosene was evaluated. The solvatochromatic properties of these dyes have been exploited to measure the fluorescent or absorbance response when exposed to kerosene. These sensors were then tested using a multichannel prototype test box developed by our collaborators at InnoSense LLC in order to evaluate the capability of the prototype for detecting kerosene vapor.

5.1. Introduction

Hydrocarbons are used to fuel many of NASA's rockets and are expected to remain a major component in the future of the space program.[1] Built in the 1960s, the John C. Stennis Space Center (SSC) in Mississippi has become the leading testing facility for NASA on rocket engine fuel testing and certification.[2] In recent years at SSC, there has been an assortment of ground test sensing needs including chemical sensors for hydrocarbon detection. Unburnt hydrocarbon fuels need to be detected to reduce their impacts on the environment and the safety of ground personnel. Therefore, NASA has a need at space launch ground testing facilities for near real time detection methods for hydrocarbons that are suitable for remote chemical detection in test plumes produced from chemical steam generators. The initial work covered in this part discusses methods utilizing optical sol-gel and polymer sensors for the detection of hydrocarbons with the ultimate goal to produce sensors that can be incorporated into a miniaturized multi-analyte testing device and placed in the plumes produced from chemical steam generators. Valuable data on rocket engine efficiency as well as information on the environmental impact could be gathered from the sensors and test unit placed at different locations around the test plume for spatial and temporal responses.

5.2. Experimental

5.2.1. Chemical Reagents and Materials

Bis[3-trimethoxysilyl)propyl]amine) (ATMOS, Gelest), methyltriethoxysilane (MTEOS, 98% Acros), methyl trimethoxysilane (MTMOS, 97% Acros), methyl

triethoxysilane (MTEOS, 98% Acros), 3-glycidoxypropyltrimethoxysilane (GPTMS, 97% Acros), 3-aminopropyltriethoxysilane (APTES, 99% Acros), polyvinyl chloride (PVC, Sigma Aldrich), bis(2-ethylhexyl) sebacate (DOS, Sigma Aldrich), ethylcellulose (EC, 49% ethoxy content, MP Biomedicals, Inc.), methanol (MeOH, ACS certified, Fisher), ethanol (EtOH, ACS certified, Fisher), toluene (ACS certified, Fisher), Reichardt's dye (Aldrich), Coumarin 153 (Sigma Aldrich, 99%), Resorufin (TCI America, 85%), Chromoionophore IX (Fluka), tridodecylmethylammonium chloride (TDMACl, 98%, Sigma Aldrich), and kerosene (ACS certified, Fisher) were used as received. Tetrahydrofuran (ACS certified, Fisher) was modified by drying over potassium/benzophenone, then distilled, and stored under N_2 before being used. DI water (18 MΩ cm) was obtained from a Barnstead International e-pure 4-holder deionization system and used to prepare aqueous solutions. Gas phase analytes were combined with nitrogen flow from a standard high purity N_2 gas tank (Airgas) or bled off from a liquid N_2 tank.

Glass slides (Fisher) were cut using a diamond tipped scriber in order to make glass sensor substrates. For sol-gel preparation, glass substrates were washed in a piranha solution (concentrated H_2SO_4 and 30% H_2O_2 in 3:1 ratio) for 30 min, followed by rinses first with deionized water and then with acetone, methanol, and ethanol to ensure maximum Si-OH formation on the surface of the glass. These slides were then dried in an oven overnight and left to open air for 1 to 2 days before use. N-type [100] silicon wafers were similarly cleaned for deposition of thin film sensors that were then used for characterization by scanning electron microscopy (SEM).

5.2.2. Instrumentation

For fluorescence measurements, a Perkin-Elmer LS55 luminescence spectrometer with a pulsed Xe source was utilized. A custom build spin coater was used to create films onto glass substrates. Films were placed in a brass flow cell that was created to be compatible with a front facing sample cell holder accessory to attach to the Perkin Elmer spectrometer. In order to make room for the brass flow cell and gas tubing, the sliding mechanism of the sample cell holder accessory was removed. A custom-made, jacketed gas impinger (Figure 5.1) stored the kerosene analyte being examined. The lid for the bubbler contained a medium frit gas diffuser immersed in kerosene liquid and the lid was sealed by an O-ring and clamp. The lid also contained a gas inlet for nitrogen gas and an outlet for kerosene saturated gas. The gas impinger was connected to a Thermo Haake temperature controller so that the liquid's temperature could be carefully regulated. Two separate mass flow controllers (MKS Instruments) were connected to the inlet of the flow cell in the fluorescence spectrometer, and they were used to control the ratio of nitrogen gas and the gas from the impinger to obtain an accurate concentration. The outlet of the flowcell was linked to a sealed vial which was attached to a separate bubbler to prevent the backflow of gases. For absorbance measurements, an Agilent 8453 photodiode array UV-Vis spectrophotometer was used along with a peltier thermostated cell holder for temperature control. Sensors were placed inside a 2 mm pathlength quartz cuvette with a plastic gas inlet and outlet tubes placed on the top of the cuvette which was tightly sealed with parafilm to create a gas-tight flow cell.

A prototype optoelectronic detection unit created for placement in test plumes

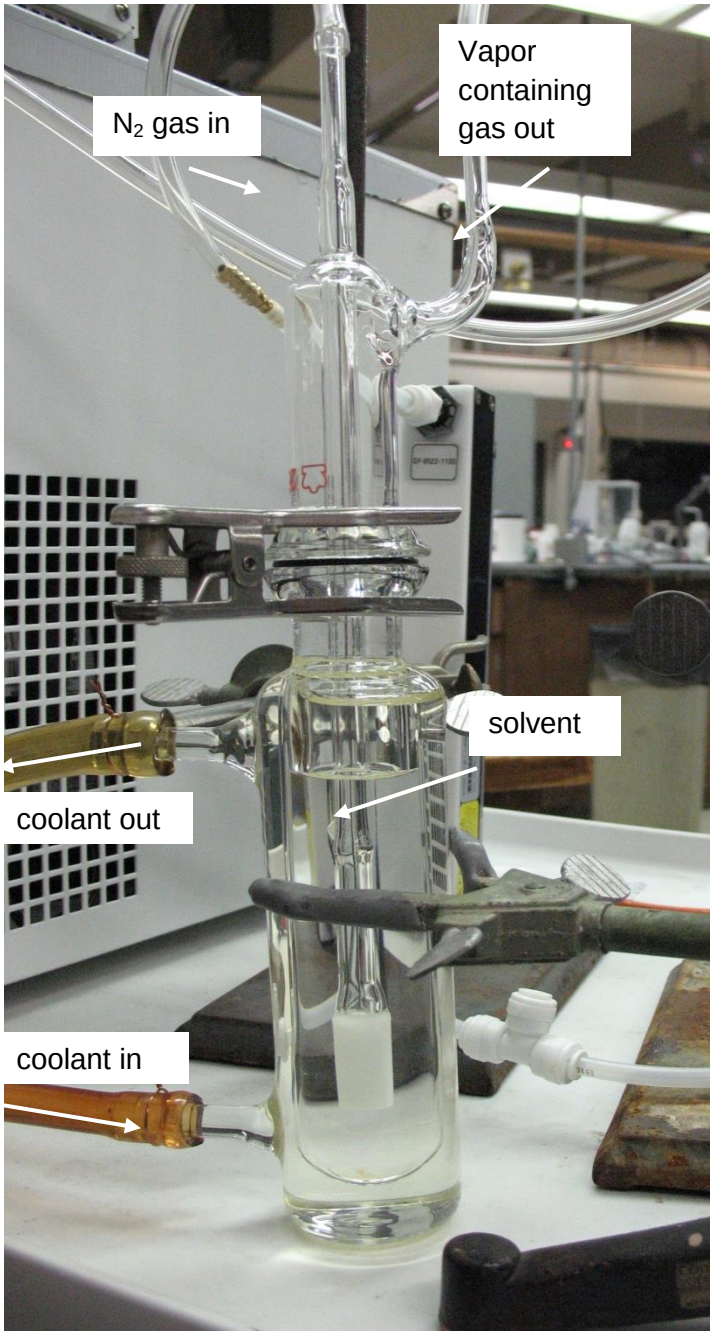

Figure 5.1. Gas saturator/bubbler for generating analytical quantities of kerosene in N_2 gas streams.

was made by collaborators at InnoSense LLC used to obtain data from completed optical sensors (Figure 5.2). The prototype was outfitted with a dual cube sensor unit with a blue and amber LED that each contained seven channels for sensor placement. The prototype unit also contained valves on each cube so that gas tubing could be fitted onto the unit and act as a flowcell for analytes gases. Attached to the prototype were a motherboard in an enclosure and a USB minihub/miniboard to connect to a computer interface.

5.2.3. Experimental Procedures

Several dyes were studied for the detection of kerosene gas. Reichardt's dye was encapsulated into a PVC film matrix by dissolving 1 mg of dye in 1.5 mL of THF, 20 mg of PVC, and 40 mg of DOS plasticizer. The solution was stirred for 1 h followed by spin coating on glass substrates at ~2600 rpm and then stored under vacuum for 24 h before testing. Reichardt's dye was also encapsulated into a sol-gel according to a previously published procedure.[3] However, the procedure was modified because the solution would gel too quickly before films could be made. The solution was made by dissolving 7.5 mg of Reichardt's dye in 200 µL ATMOS, 100 µL MTMOS, 10 µL H_2O, and 250 µL MeOH. This mixture was stirred for 1 h before spin-coating the solution onto glass slides.

The fluorescent dye Coumarin 153 was tested for kerosene sensing as well. This dye was encapsulated into a sol-gel matrix by mixing 2 mg of Coumarin 153 with 200 µL of MTEOS, 100 µL of MTMOS, 10 µL of H_2O, and 250 µL of MeOH. The solution was stirred for 1 h and spin-coated onto glass substrates. The resulting films

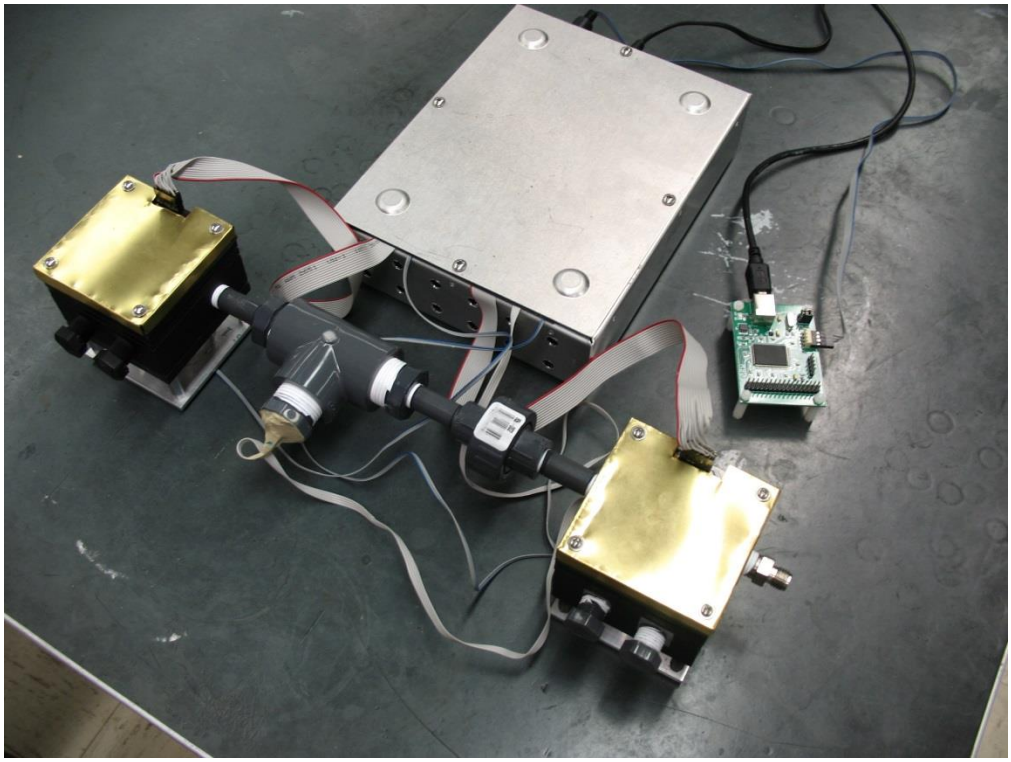

Figure 5.2. InnoSense LLC optoelectronic prototype unit.

were stored under static vacuum for at least 24 h before testing. To produce sensing films containing Resorufin, 2 mg of Resorufin was combined with 1.5 mL of EtOH, 250 µL of APTES (3-aminopropyltriethoxysilane), 250 µL of GPTMS (3-glycidoxypropyltrimethoxysilane), and 25 µL of TBAOH (tetrabutylammonium hydroxide). The solution was stirred until thoroughly mixed and then coated onto glass slides and stored under static vacuum.

5.2.4. Analytical Procedures

Several indicator dyes were selected and tested for their potential response to kerosene. A Perkin Elmer LS55 luminescence spectrometer using a standard 1 cm quartz cuvette or front facing sample cell holder accessory unit fitted with a custom flow cell was utilized for fluorescence based tests of dyes and sensing films in solution or solid phase. When time based signal measurement studies were conducted, a signal reading was usually integrated over 1 s and signal averaging was used to improve the signal noise by averaging each data point with two data points preceding and following it. For absorbance measurements, a UV-Vis (photodiode array detector) spectrometer was utilized to monitor changes in absorbance spectra of indicator dyes in relation to the changing concentration of analytes. A prototype multichannel test device developed by InnoSense LLC was evaluated for detection of kerosene vapor. This current unit is being tested to eventually be used in test plumes to detect certain hydrocarbon constituents.

In order to generate kerosene gas vapor, N_2 gas was connected to a double walled glass vessel containing a gas saturator/bubbler with liquid kerosene inside. The

lid of the saturator/bubbler contained a fine glass frit gas diffuser that extended into the analyte solution allowing N_2 to flow into the solution in order to saturate the gas stream with kerosene analyte. The glass vessel was sealed with an O-ring and clamp. Integrated on top of the lid was a gas inlet and outlet for N_2 and analyte saturated N_2 respectively. The analyte saturated N_2 vapor could then be further diluted when combined to another line and mixing it with various amount of pure N_2 gas.

5.3. Results and Discussion

5.3.1. Dye Selection/Testing for Kerosene Vapor

In order to detect kerosene, a fingerprinting-type method was closely studied using up to 3 different dyes that produce a unique response to kerosene or constituents of kerosene such as hydrocarbons. Generally, many of these dyes were solvatochromatic. When they are exposed to solvents of different polarities, the absorbance spectrum of the dye shifts. Optical sensors were developed using dyes including Reichardt's dye, Coumarin 153, and Resorufin. The dyes were encapsulated in several different polymer matrices such as sol-gel, PVC, or EC and their response to kerosene vapor was evaluated.

5.3.2. Reichardt's Dye Indicator

Reichardt's dye (Figure 5.3) was chosen for its potential sensitivity towards kerosene vapor. It is a solvatochromatic dye that has an electronic transition of 350 nm when the solvent is changed from tetrahydrofuran to methanol.[4] Initially, a sol-

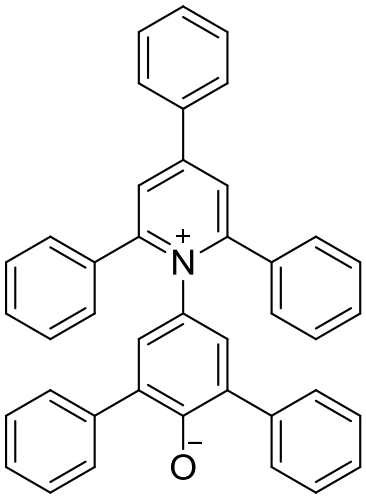

Figure 5.3. Structure of Reichardt's indicator dye.

gel formulation was used to encapsulate Reichardt's dye. Since the dye is hydrophobic in nature, a non-polar media is required. Using alkoxide precursors such as tetramethyl orthosilicate (TMOS) causes the dye to precipitate. When the sol-gel reaction is acid catalyzed, the phenolate group of the dye may be protonated which can adversely affect the sensitivity of the dye. Therefore, the dye was successfully encapsulated using slightly basic non-polar conditions using a previously published report.[3] The recipe uses 25 µL of ATMOS (bis[3-trimethoxysilyl)propyl]amine), 45 µL of MeOH, 30 µL of H_2O, 30 µL of MTMOS (methyltrimethoxysilane), and 30 µL of 10 mM of Reichardt's dye in MeOH. This recipe is advantageous because ATMOS has long chain spacer units that contain both hydrophobic and hydrophilic groups, providing a good mixture of polar and non-polar environment for the dye. Addtionally, the amino-containing precursors provide the slightly basic sol-gel conditions needed to prevent protonation of the dye.[4] However, after attempting to reproduce this formulation several times, it was found that the solution would gel instantly within 2 minutes of mixing. Therefore, the recipe was modified by adding additional MeOH and using less H_2O to help slow the hydrolysis so that the solution would not gel as fast. The new recipe stayed in solution and was able to be mixed thoroughly for 1 h before spin-coating the solution onto glass substrates. The film produced a dark blue color after spin-coating the purple solution onto the glass substrate and the comparison of the solution and film is given in Figure 5.4.

The response to kerosene vapor was tested using the gas saturator system described above in Section 5.2.2. Pulses of kerosene were introduced to the sol-gel sensor and the effects on the absorbance were monitored. The sol-gel sensor shows an absorption peak at 610 nm and upon exposure to kerosene the absorption peak red

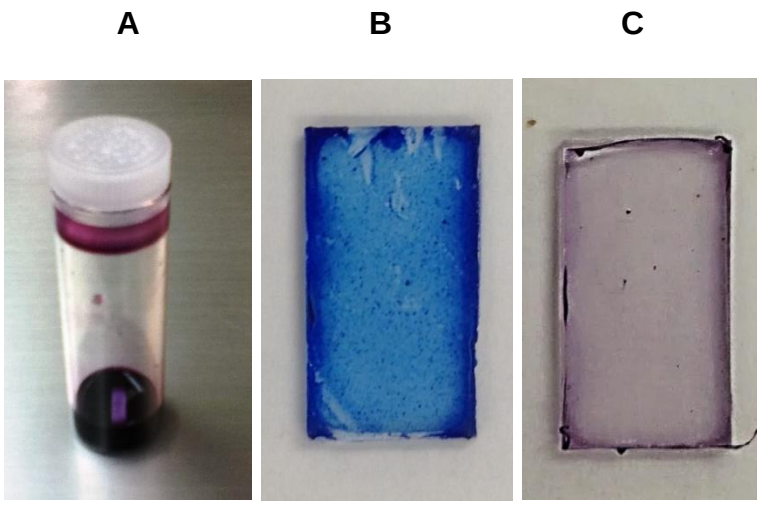

Figure 5.4. (A) Solution of the modified sol-gel recipe; (B) Blue sensor after spin coating; (C) The same sensor becoming purple after exposure to kerosene vapor for 5 min.

shifts to 650 nm (Figure 5.5A). A time-based study focusing on the 610 nm and 650 nm wavelengths shows that the sensor displays an increase in absorbance after exposure to kerosene vapor and a decrease in absorbance after the kerosene vapor is turned off (Figure 5.5B). The response at 650 nm showed greater sensitivity towards kerosene vapor which could be seen by the greater increase in absorbance when exposed to kerosene vapor. There was also an overall downward drift throughout the experiment but the sensor did display some reversibility to kerosene when targeting these specific wavelengths. Alternative films were also studied to encapsulate Reichardt's dye. A polyvinyl chloride matrix was evaluated. To produce the sensing films, 1 mg of Reichardt's dye was dissolved in 1.5 mL of THF, 20 mg of PVC, and 40 mg of DOS plasticizer. The films were spin-coated at 2600 rpm on glass slides and stored under vacuum for 24 h before testing. In PVC, the films were yellow in color and tested using a fluorometer to observe if there was better sensitivity or reversibility towards kerosene vapor using fluorescence. The emission response of the PVC sensor shows a peak at approximately 500 nm and a slight quenching response can be observed when exposed to a pulse of kerosene vapor and reversibility after sweeping the sensor with N_2 gas (Figure 5.6A). Time-based fluorescent measurements of the sensor showed an initial quick response to kerosene vapor, but displayed an upward drift during the kerosene pulse (Fig 5.6B). Sweeping the sensor with N_2 gas exhibited a small amount of reversibility but subsequent pulses gave a reduced response to kerosene vapor. There was also a slight downward drift throughout the entire experiment.

A

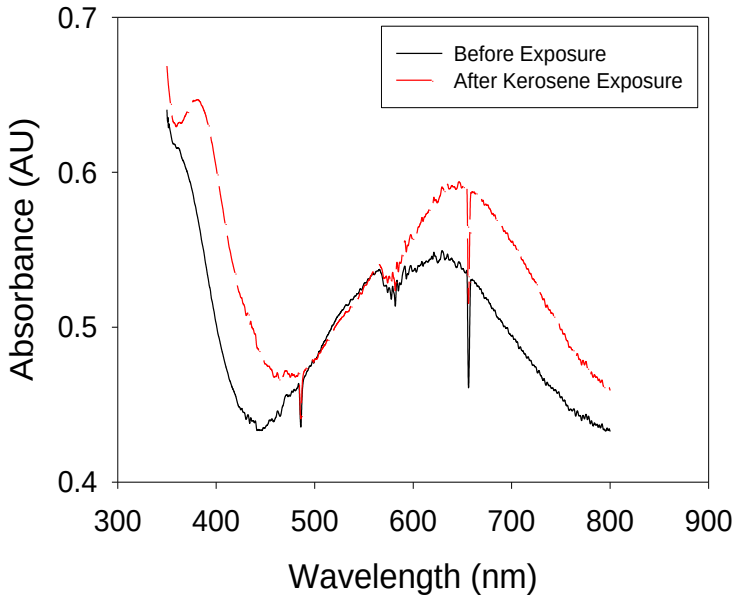

B

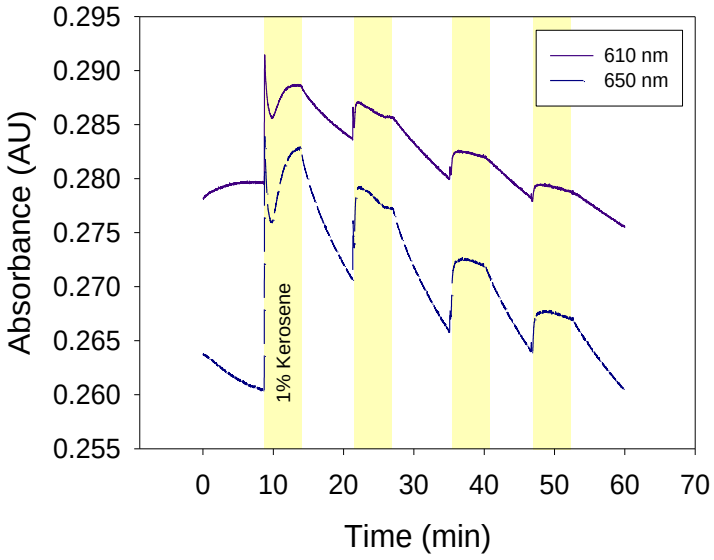

Figure 5.5. Modified sol gel recipe using Reichardt's dye exposed to kerosene in (A) the UV-Vis and (B) under a time based study.

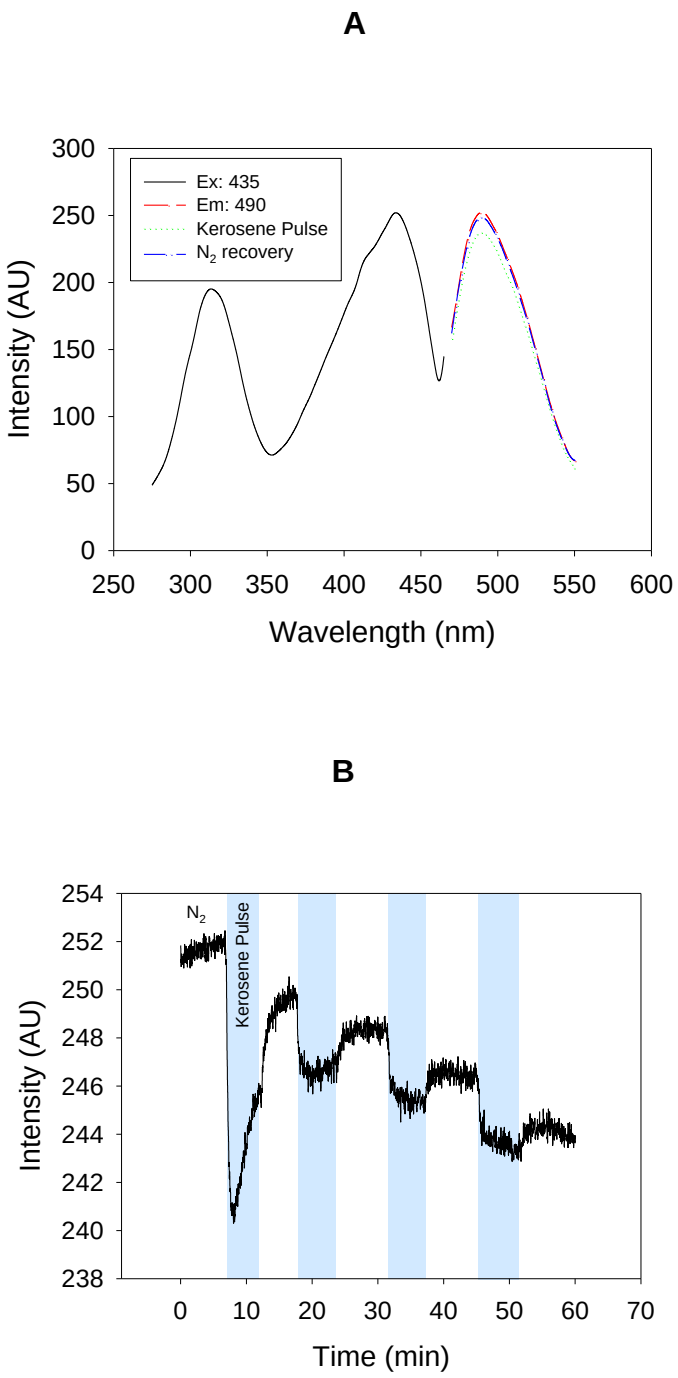

Figure 5.6. Response of the PVC-Reichardt's dye sensor exposed to kerosene vapor on (A) excitation and emission single scan measurements and (B) under time based measurements.

5.3.3. Coumarin 153 Indicator

Coumarin 153 (Figure 5.7) is another fluorescent dye that has been previously reported with solvatochromatic characteristics.[5] Coumarin has been used as a colorimetric chemosensor and selective fluorescence turn-on probe for a variety of different analytes.[6-8] To our knowledge, this dye has not been used for detection of kerosene in the gas phase. This dye was encapsulated into an optimized ethyl cellulose solution (2.5% w/w) and mixed thoroughly for 1 h. The solution was then spin coated onto glass substrates. Fluorescence studies show that the sensor has an emission peak at 530 nm and when exposed to kerosene vapor for 30 s there is a small quenching in fluorescence in response (Figure 5.8A). Time based fluorescence measurements were taken for Coumarin 153 when exposed to 1% kerosene (Figure 5.8B). The signal was allowed to stabilize for 15 minutes prior to testing. The sensor's response was then measured for pulses of kerosene and then flushed with N_2 gas and repeated. The signal shows a drop in intensity by approximately 30 units upon initial exposure to kerosene which corresponds to the single scans done previously. After flushing the sensor for N_2 gas the signal was not able to be fully recovered. Upon exposure to kerosene again the signal showed a smaller response and was not able to fully recover the signal again. However, Coumarin 153's response to kerosene makes it a potential candidate to use in a fingerprinting method.

5.3.4. Resorufin Indicator

Resorufin (Figure 5.9) is another potential dye that was suggested from our collaborators at InnoSense LLC for kerosene detection. Resorufin has been previously

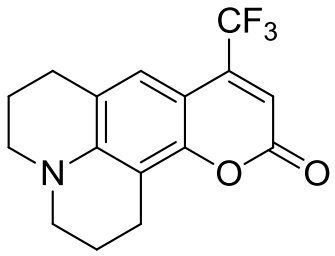

Figure 5.7. Structure of Coumarin 153 indicator dye.

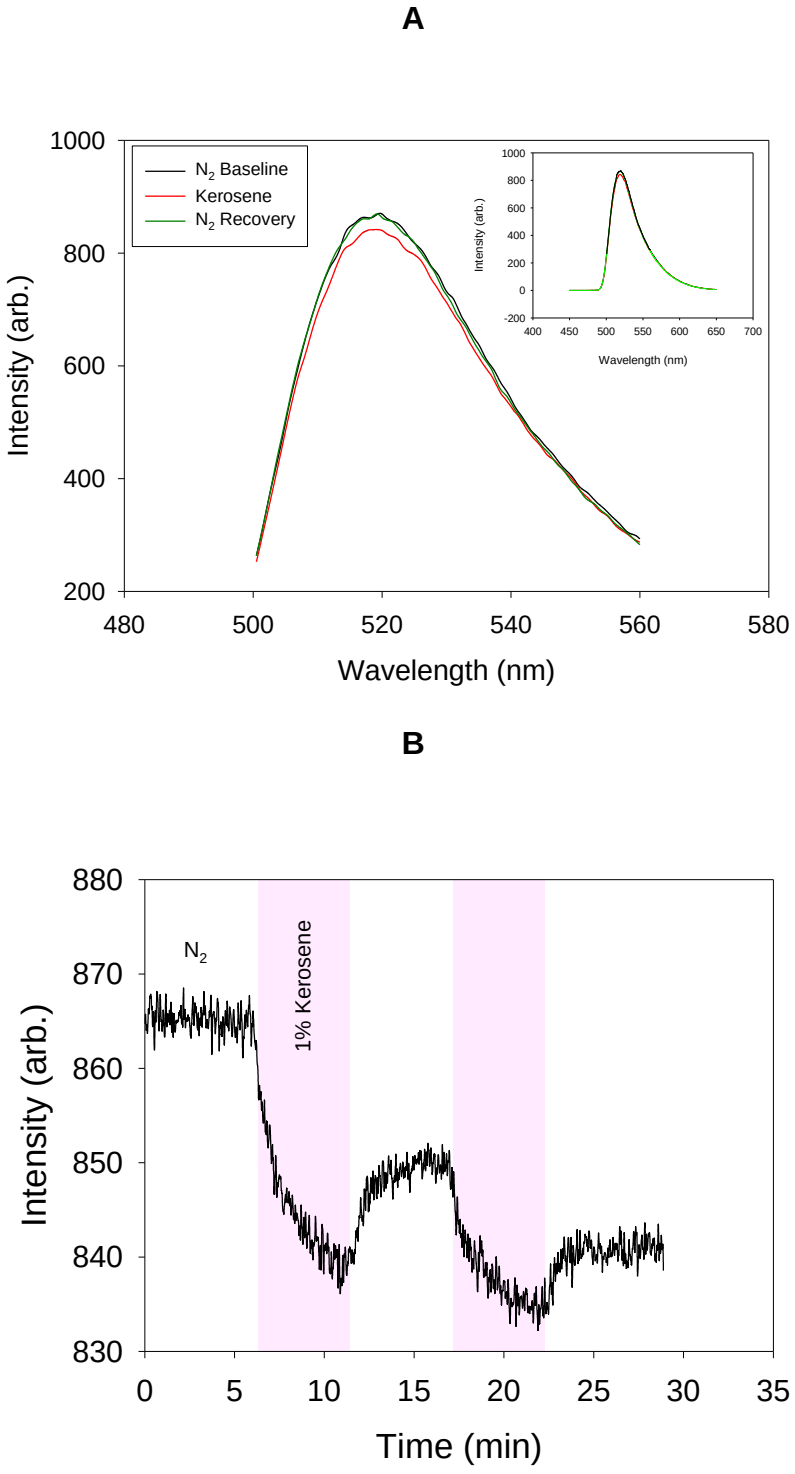

Figure 5.8. (A) Coumarin 153's fluorescence quenching response when exposed to 1% kerosene. Insert: Full view of emission spectra; (B) Time based measurement for

Coumarin 153.

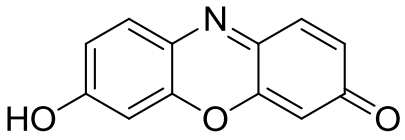

Figure 5.9. Chemical structure of Resorufin indicator dye.

used as a fluorescent probe for colorimetric applications.[9,10] This dye was encapsulated into a sol-gel matrix by mixing Resorufin dye (2 mg) with EtOH (1.5 mL), APTES (250 µL), GPTMS (250 µL), and TBAOH (25 µL). This solution was stirred for 1 h and then spin-coated onto glass slides, giving dark purple films (Figure 5.10). The films gave a distinct excitation peak at 590 nm and an emission peak at 625 nm (Figure 5.11). However, the sensor showed minimal response when exposed to kerosene vapor.

5.3.5. Multi-analyte Optical Sensor for Rocket Engine Testing

For the ultimate goal of this project, studies were conducted evaluating a miniaturized multi-channel sensing platform built to monitor various plume constituents in near real time. The device developed by InnoSense LLC for use with this project is termed a multi-analyte optical sensor for rocket engine testing (MOSRT). These studies use the second generation of the MOSRT device which contains a dual cube sensor with seven different channels with either a blue or amber LED light source. Each channel has a slot for a 500 nm or 600 nm longpass filter and data from these channels can be simultaneously obtained. Moreover, the device has a built-in temperature and humidity probe to monitor these factors during testing. The test unit is interfaced to a PC by a National Instruments USB controller and operated with LabView software.

Since Coumarin 153 in ORMOSIL and Resorufin and Reichardt's dyes in sol gel each have emission spectra past 600 nm, it was decided to use 600 nm longpass filters and to test these sensors in the amber LED to help optimize signal response. Therefore, channel A contained a sol-gel blank, Resorufin sensors were put in channels B and C, a sol-gel Reichardt's dye sensor was placed in channel E, and ORMOSIL

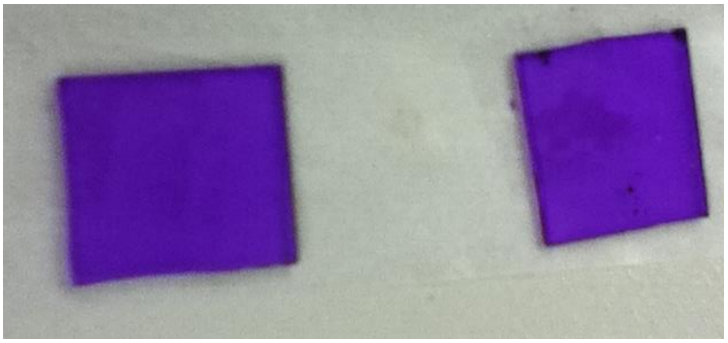

Figure 5.10. Glass slide spin-coated with Resorufin solution giving a dark purple color.

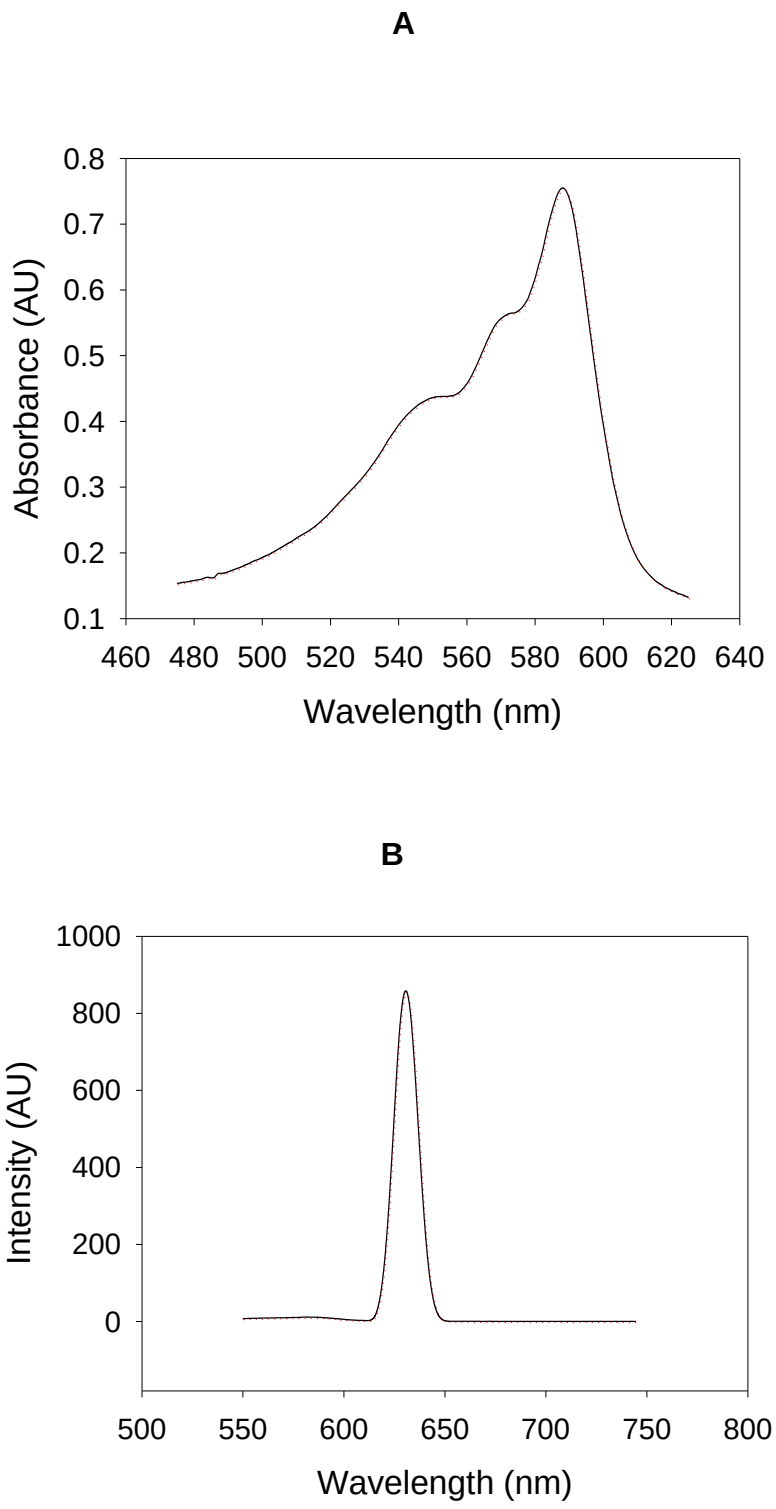

Figure 5.11. Resorufin sensor: (A) excitation peak and (B) emission spectra.

Coumarin 153 sensors were put in channels F and G. Figure 5.12 shows each sensor's response to 1% kerosene vapors. The data reveal that the Resorufin sensors have a slight response to kerosene by showing an increase in signal of 0.0005 V. However, the signal is very noisy and looks similar to channel A which contains a blank. Thus, deciphering a response is challenging. The sol-gel sensor containing Reichardt's dye demonstrated a somewhat reversible signal when exposed to kerosene vapor but exhibited an upward drift throughout the experiment. The ORMISIL matrix with Coumarin 153 displayed a response similar to that of the Resorufin sensors in channel B and C. The signal response was very noisy but a slight response can be interpreted from the data when the sensor is exposed to kerosene vapor. However, channel G does not show a similar noisy signal, but the response to kerosene is still difficult to detect.

After trying the amber LED cube, studies were done using the blue LED cube to compare each sensor's response to different LED light. Each sensor in the optoelectronic sensing device was placed in the blue LED cube with a 500 nm longpass filter. Channel A was treated as a blank channel and contained only a blank glass substrate with no film or indicator dyes, Channel B was placed with an EC sensor with Coumarin 153, and a PVC sensor containing Reichardt's dye was placed in channel C. An ORMISIL sol-gel sensor with Coumarin 153 was placed in channel E, a sol-gel sensor with Reichardt's dye was put in channel F, and channel G was left blank. The response of each channel is given in Figure 5.13. Channel F displayed a good initial response to kerosene by showing an increase in signal, but needed a much longer time to recover its original signal. ORMISIL and EC sensors containing Coumarin 153 each

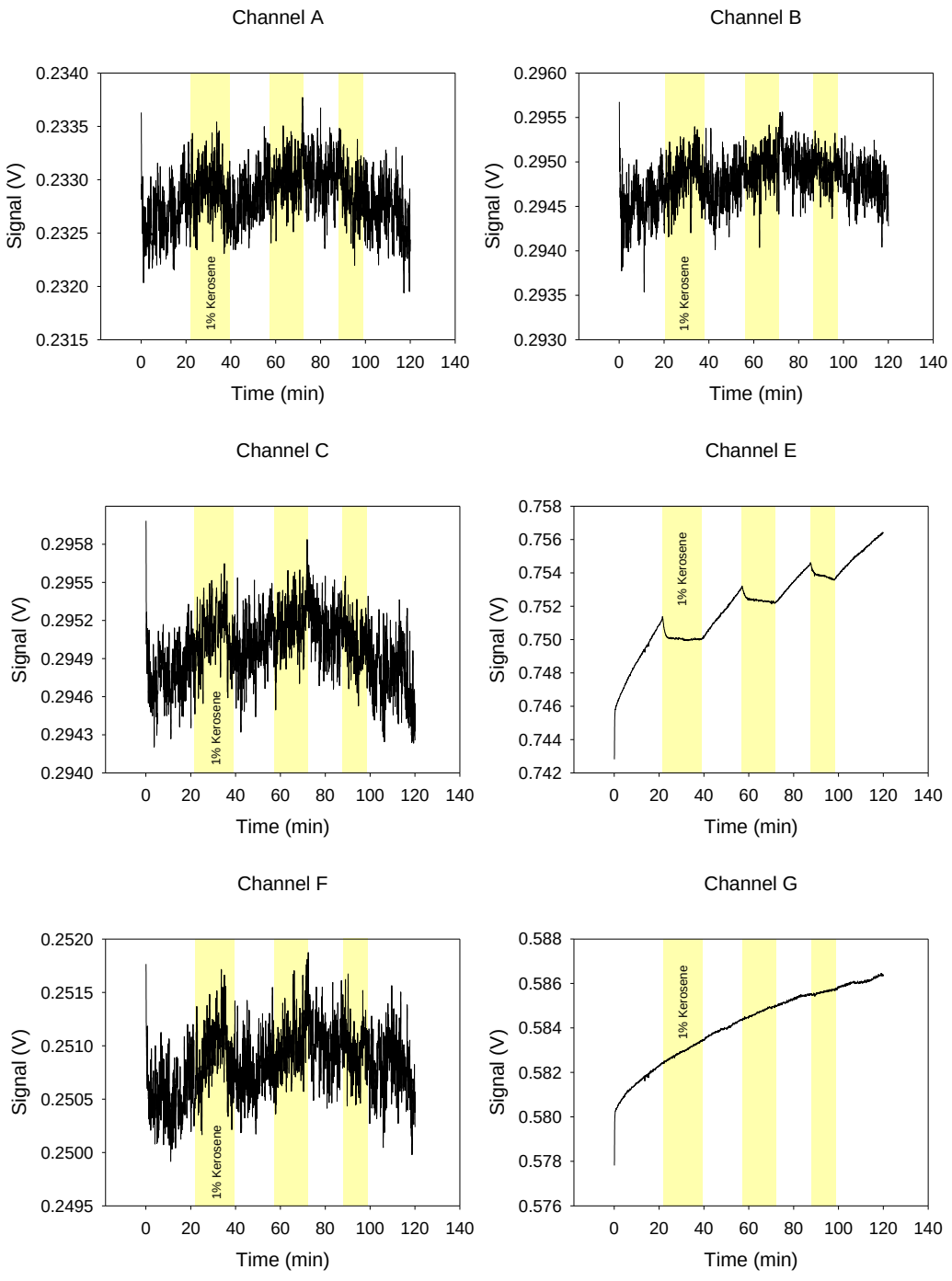

Figure 5.12. Evaluating the amber LED cube with a 600 nm filter and the response of sol-gel Resorufin sensors in channels B and C, sol-gel Reichardt's dye sensor in channel E, and ORMISIL Coumarin 153 sensors in channels F and G to kerosene.

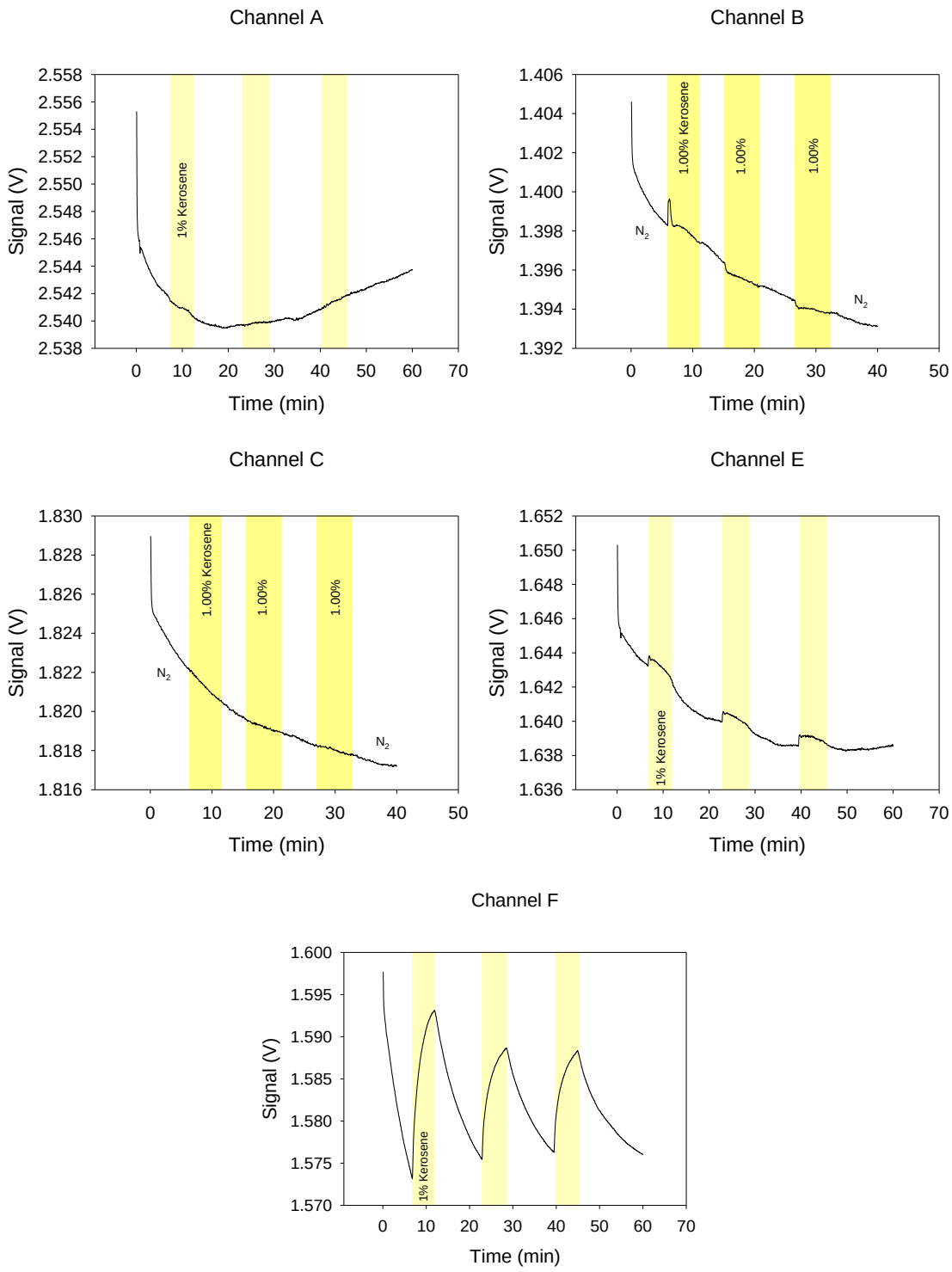

Figure 5.13. EC Coumarin 153 in channel B, PVC Reichardt's dye in channel C, ORMISIL-Coumarin in channel E, sol-gel Reichardt's dye in channel F exposure.

had similar responses to kerosene vapor, while channel F seemed to have no signal change at all when exposed to kerosene vapor. Since sol-gels containing Reichardt's dye provided some of the best results using the MOSRT, they were evaluated again along with sensors encapsulating Resorufin using the blue LED cube with a 500 nm longpass filter. Chanel A contained a sol-gel with no indicator dye to simulate a blank and channels B and C contained Resorufin sensors. Sol-gel sensors with Reichardt's dye were placed in channels E and F and the response of each sensor upon exposure to kerosene vapor was observed (Figure 5.14). There is a distinct increase in signal for the Resorufin and Reichardt's dye sensors when exposed to kerosene vapors. Also, after flushing the blue LED cube with N_2 each sensor roughly shows a reversible feature in signal.

5.4. Conclusions

After obtaining the results for these dye-doped sensors, the final recommendation for a fingerprinting method for kerosene detection using the MOSRT unit would be using sol-gels as the encapsulating matrix for Reichardt's dye, Resorufin, and Coumarin 153. Using sol-gels as the polymer helped to give the most unique response when exposed to kerosene and also displayed reversible traits for their respective signal as well. The blue LED cube gave the best signal response as well and perhaps a prototype box without the amber LED cube would help cut down on weight, bulk, and cost of the device. Preliminary tests using this fingerprinting method could be applied to test plumes to study the response to hydrocarbon constituents at SSC.

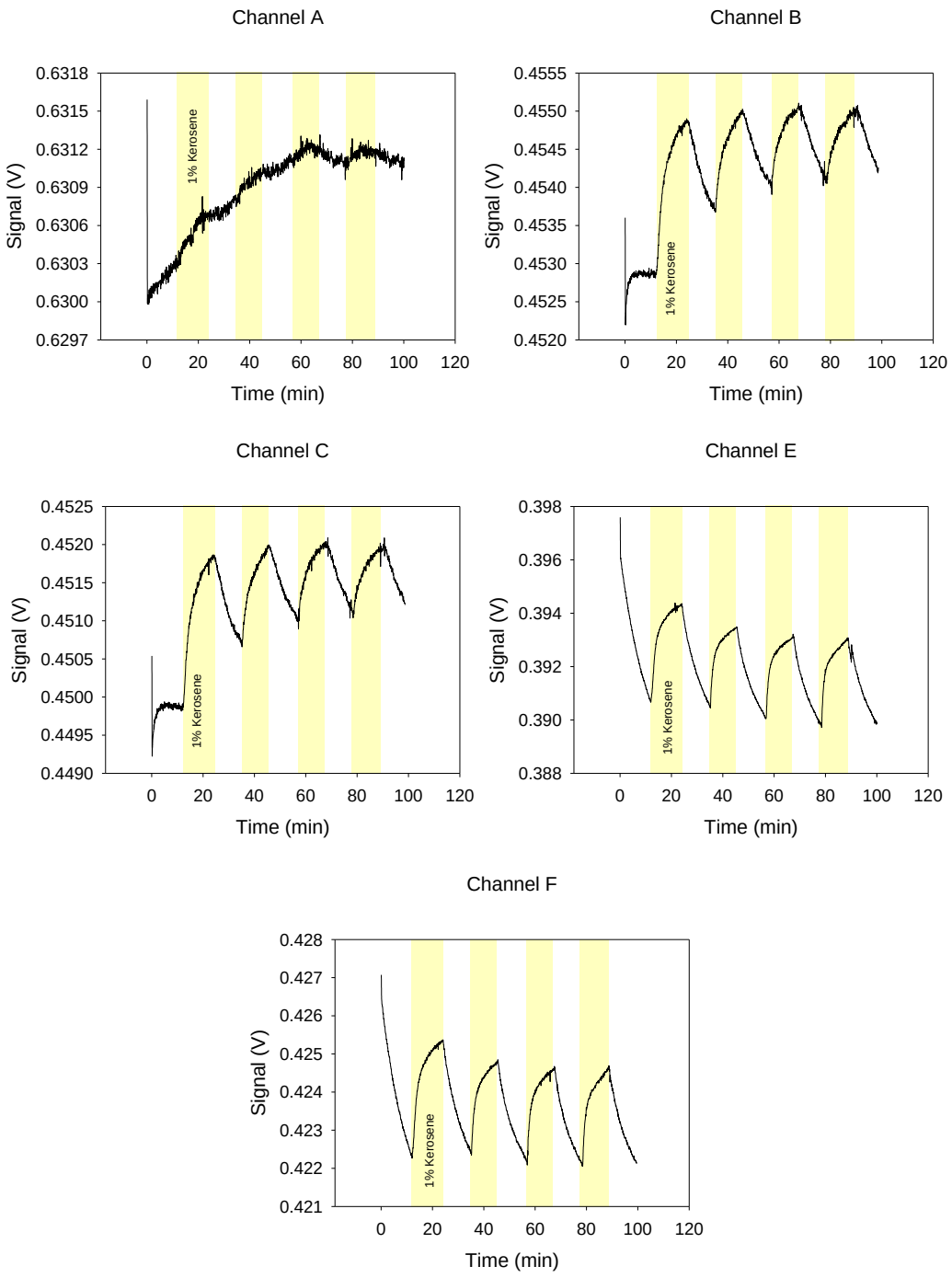

Figure 5.14. The response to kerosene in the blue LED cube with a 500 nm longpass filter of Resorufin sensors placed in channels B and C and Reichardt's dye sensors in channel E and F.

References

1. G. D. Tejwani; McVay, G. P.; Langford, L. A.; St. Cyr, W. W. *Hydrocarbon Fueled Rocket Engine Plume Diagnostics: Analytical Developments & Experimental Results*; 42nd AIAA/ASME/SAE/ASEE Joint Propulsion Conference & Exhibit; Sacramento, CA, 2006.
2. Tejwani, G. D.; McVay, G. P.; Langford, L. A.; St. Cyr, W. W. *Planning for Plume Diagnostics for Ground Testing J-2X Engines at the SSC*; NASA: Stennis Space Center, 2006.
3. Burt, M.C.; Dave, B.C. *Sens. Actuators, B: Chemical.* **2005**, *107*, 552–556.
4. Dickert, F. L.; Geiger, U.; Lieberzeit, P.; Reutner, U. *Sensor. Actuat. B-Chem.* **2000**, *70*, 263-269.
5. Fischer, K.; Prause, S.; Spange, S.; Cichos, F.; Borczyskowski, C.V. *J. Polym. Sci., Part B: Polym. Phys*. **2003**, *41*, 1210–1218.
6. Li, H.; Cai, L.; Li, J.; Hu, Y.; Zhou, P.; Zhang, J. *Dyes Pigments*. **2011**, *91*, 309–316.
7. Mahapatra, A.K.; Hazra, G.; Roy, J.; Sahoo, P. *J. Lumin.* **2011**, *131*, 1255–1259.
8. Sharma, V.K.; Mohan, D.; Sahare, P.D. *Spectrochim. Acta A.* **2007**, *66*, 111–113.
9. Bisson, A., Anslyn, E. *J Chem Soc Perk T 2*. **1999**, *2*, 1111–1114.
10. Golnabi, H.; Razani, M. *Sensor. Actuat. B-Chem*. **2007**, *122*, 109–117.

Part 6

Concluding Remarks

The majority of this work centered on the development of optical sensors for the detection of chemical analytes in the gas and liquid phase. The first portion of this dissertation, Part 2, illustrates a new approach in detecting biodiesel (FAME) in diesel. Having the ability to detect biodiesel at low and high concentrations would be immensely helpful for the aviation and diesel industries. Since FAME is a highly surface active material, it can potentially lead to cross contamination issues with jet fuel causing thermal stability problems and affecting the freezing point. This can lead to deposits in the fuel system or cause the fuel to gel which may cause jet engine operability problems and possible engine flameout. An optical sensor utilizing Nile Blue Chloride and its solvatochromatic properties has been developed to detect FAME in diesel. The dye dissolved in alcohol is made into a film where diesel does not displace the alcohol surrounding the dye keeping the sensor blue. Once the sensor is exposed to FAME, the FAME displaces the alcohol changing the sensor's color from blue to pink leading to the detection of biodiesel. The developed sensor is highly sensitive and is able to detect FAME from a range of 0.5–200,000 ppm (20% v/v). These sensors provide a viable alternative to compliment more sophisticated and expensive techniques currently being used to detect FAME in aviation fuels or used as a quick verification method to determine biodiesel concentrations (i.e., B5, B20) in diesel.

The next part describes the development of an optical sensor to detect chlorinated hydrocarbons in aqueous and non-aqueous solutions. The detection of chlorinated hydrocarbons is of intense interest for environmental and pharmaceutical applications. These optical sensors utilized a modified Fujiwara reaction, one of the only methods for detecting halogenated hydrocarbons in the visible spectrum, as its

sensing mechanism. 2,2'-Dipyridyl and tetra-n-butyl ammonium hydroxide were the modified Fujiwara reagents that were encapsulated into an EC film. Upon exposure to a CHC such as chloroform, a colored product would be produced within the film which could be analyzed spectroscopically. This technique yielded detection limits of 0.830 ppm (v/v) and a limit of quantification of 2.77 ppm. In aqueous solution of $HCCl_3$, a sol-gel sensor was developed which is able to be directly submerged in aqueous samples for detection. This sensor achieves a detection limit of 500 ppm. Each sensor is easy to fabricate and may be coupled to a portable spectroscopic instrument or fiber optic bundle for direct measurement studies in the field.

The remaining two parts of this dissertation focus on rocket engine ground testing. More specifically, evaluating NASA's J-2X rocket engine and its ability to start in vacuum conditions. In order to test this engine, an A-3 test stand was constructed capable of producing a vacuum environment through the use of chemical steam generators. These chemical steam generators produce ~2100 kg/s of steam through the combustion of Pr^iOH, LOX, and water. The combustion of these components may produce several combustion hydrocarbons such as methane, ethylene, acetylene, ethane, propylene, and propane. However, the production of these hydrocarbons may interfere with the line of sight and complicate the analysis of current optical emission/absorption measurements. Therefore, NASA has a need at space launch ground testing facilities for near real time detection of hydrocarbons as well as unburnt Pr^iOH in test plumes produced from chemical steam generators. Thus, developing sensors in order to monitor and detect gas plume constituents can be useful as a diagnostic tool for combustion efficiency and to ensure safe testing conditions. An

optical sensor doped with the fluorescent dye Chromoionophore IX has been developed for the detection of $Pr^{i}OH$. The sensing mechanism of this sensor utilizes the formation of a hemiacetal when exposed to alcohol vapor which quenches the fluorescence of the sensor. The developed optical sensor has detection limits of 9, 13, 21 ppm and quantification limits of 32, 43, and 70 ppm for MeOH, EtOH, and $Pr^{i}OH$, respectively.

Hydrocarbon detection is much harder to do because they have no functional groups to take advantage of in detection. Hydrocarbons are comprised mainly of saturated long carbon chains. Therefore, a fingerprinting method has been developed to detect kerosene/hydrocarbon vapors. Several indicator dyes, Reichardt's dye, Coumarin 153, and Resorufin, were used and encapsulated into a variety of polymer films and sol-gels. Their response to kerosene was then monitored using spectroscopy. Results showed that these indicator dyes gave the best response to kerosene vapor when encapsulated into a sol-gel. These sensors were then tested using a multichannel prototype test box developed by our collaborators at InnoSense LLC in order to evaluate the capability of the prototype for detecting kerosene vapor.

Vita

Jonathan Kelly Fong was born on February 11th, 1987 in Memphis, Tennessee. He was raised in nearby Germantown, Tennessee for much of his childhood and teenage years and graduated from Houston High School in May 2005. The following fall, Jonathan enrolled at the University of Tennessee, Knoxville. He graduated summa cum laude In May 2009 with a double major in chemistry and biochemistry and molecular biology.

Jonathan began his graduate studies in chemistry at the University of Tennessee, Knoxville in August 2009. He joined Dr. Zi-Ling Xue's research group in December 2009 with a primary focus on developing optical sensors for chemical detection of various analytes of interest. He completed the requirements for a Ph.D. in chemistry in the spring of 2014 with more to follow.